8128867

WHITE, HOWARD JAMES

THE STRATIGRAPHY OF THE SOUTHERN PAB RANGE, PAKISTAN

Iowa State University

PH.D. 1981

University
Microfilms
International 300 N. Zeeb Road, Ann Arbor, MI 48106

PLEASE NOTE:

In all cases this material has been filmed in the best possible way from the available copy. Problems encountered with this document have been identified here with a check mark __√__.

1. Glossy photographs or pages __√__
2. Colored illustrations, paper or print ______
3. Photographs with dark background __√__
4. Illustrations are poor copy ______
5. Pages with black marks, not original copy ______
6. Print shows through as there is text on both sides of page ______
7. Indistinct, broken or small print on several pages __√__
8. Print exceeds margin requirements ______
9. Tightly bound copy with print lost in spine ______
10. Computer printout pages with indistinct print ______
11. Page(s) ____________ lacking when material received, and not available from school or author.
12. Page(s) ____________ seem to be missing in numbering only as text follows.
13. Two pages numbered ____________. Text follows.
14. Curling and wrinkled pages ______
15. Other ____

The Stratigraphy of the southern Pab Range, Pakistan

by

Howard James White

A Dissertation Submitted to the

Graduate Faculty in Partial Fulfillment of the

Requirements for the Degree of

DOCTOR OF PHILOSOPHY

Department: Earth Sciences

Major: Geology

Approved:

In Charge of Major Work

For the Major Department

For the Graduate College

Iowa State University
Ames, Iowa

1981

TABLE OF CONTENTS

LIST OF FIGURES

LIST OF TABLES

INTRODUCTION

Objectives and Method of Study

The geodynamic evolution of Pakistan embodies an intricate history of Phanerozoic plate tectonics and sedimentation. The unravelling of this history is the objective of the Geodynamics of Pakistan program directed by Mr. Abul Farah, Geological Survey of Pakistan, and Dr. Kees A. DeJong, University of Cincinnati, USA. Numerous Pakistani and foreign participants have brought together many disciplines to study the structure, stratigraphy and ophiolites of Pakistan. Reports of the initial studies are published in the recent monograph edited by Farah and DeJong (1979).

Professor DeJong invited the writer to undertake a stratigraphic study of the southern Pab Range, Pakistan, as part of the NSF supported geodynamics project during the winter of 1978-79. The Jurassic through Paleocene strata exposed in extreme southeast Baluchistan Province record the pre-collision history of the northwestern margin of the Indo-Pakistani Subcontinent. The setting provides the opportunity to study the evolution of the Tethyan continental shelf prior to early Tertiary ophiolite emplacement and to evaluate the potential of the strata to serve not only as source but also as reservoir beds of economic hydrocarbon accumulations.

The study concentrates on the Cretaceous strata exposed

in the southern Pab Range and, in particular, the Upper Cretaceous which contain the first major influx of sand encroaching onto the continental shelf. It is the objective of this report to document the depositional environments of the Cretaceous stratigraphy and to reconstruct the depositional history of this active continental margin.

Field work involved detailed measurement and description of the Upper Cretaceous formations exposed along two major mountain passes traversing the Pab Range and reconnaissance surveys of the older Cretaceous strata in the study area. Political complications abbreviated the field season; however, two long sections through the Upper Cretaceous units were completed and chip samples were collected for thin sectioning and laboratory analysis. Mr. Jaffer Quershi of the Geological Survey of Pakistan provided assistance in the field.

Laboratory study of the sediment collected included thin section petrography, x-ray diffraction of whole rock and clay minerals, standard heavy mineral analysis with x-ray powder camera techniques, and scanning electron microscopy of microfauna and diagenetic features. Chemical analysis of the igneous sill in the lower part of the Goru Formation was accomplished by using standard wet chemical and atomic absorption procedures. The results of the petrographic and x-ray analyses are tabulated in the appendices of this report. Tallied results and interpretations occur

in appropriate sections of the text.

Location, Physiography and Climate

The area of study includes the eastern hills of the southern Mor Range, the isolated exposures of Kanraj Valley, and the prominent ridges of the southern Pab Range (figure 1a). The area lies east of the structurally complex Axial Belt region which contains the Bela Ophiolite. The Khude and Kirthar ranges rise to the east.

No major towns are situated within the study area. Uthal is 30 km to the west-northwest while Karachi is located approximately 100 km to the south. Roads in the region are primitive, undeveloped, jeep/lorry tracks largely confined to stream valleys. Travel is usually weather-dependent, camel caravans being the most reliable mode of transportation.

The physiography of the region is structurally controlled. A series of east-dipping cuestas comprise the Pab Range reaching elevations of 830 m. The prominent, west-facing scarp of the range is capped by the Parh Limestone. Kanraj Valley (figure 1b) averages 330 m. in elevation in the study area and is, in turn, flanked to the west by a fault scarp along the west-dipping hogbacks of the southern Mor Range (figure 1c). Obsequent drainage flowing west through the Pab Range reflects joint control on stream courses. South-flowing drainage in Kanraj Valley eventually

FIGURE 1. Photographs of the study area

a. View looking east toward the Pab and Khude ranges. The prominent sandstone in the lower Mughal Kot Formation is seen in the foreground.
b. View looking east across Kanraj Valley toward the southern Pab Range.
c. View looking north along the eastern ridge of the southern Mor Range; note the pencil cleavage superimposed on the Goru strata.

a

c

b

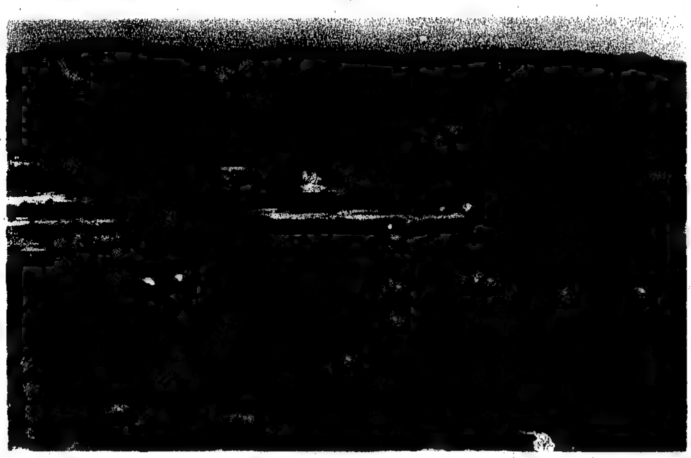

cuts westward through the west-dipping strata of the Mor Range. Thin alluvium veneers most of Kanraj Valley; erosion terraces demonstrate a succession of downcutting events lowering the floor of the valley.

Today the region is semiarid with infrequent heavy rains during the monsoon seasons. The main, perennial river, the Windar Nai (Nai=river) drains an extensive headlands to the north of the study area. Tributary ephemeral streams draining the study area head in the Pab Range and include the Langro, Drabber, Anero and Jakkher Dhoras (Dhora=small stream). Springs along the Mor Range also serve as local water supplies.

The limited rainfall sustains a sparse grass-acacia scrub flora in Kanraj Valley, suitable for camel and goat herding. Dense thorn scrub mantle ridges of the Pab Range and restrict the best exposures to the canyons of ephemeral streams. Jakkher and Drabber passes are examples which cut through the Pab Range exposing excellent profiles of the Cretaceous rocks.

STRUCTURAL GEOLOGY

The present structural configuration of Pakistan resulted from Middle Tertiary continent-continent collision between the north-advancing Indo-Pakistani Subcontinent and southern Eurasia. The Chaman and Ornach-Nal fault systems and the adjoining structural arcs and syntaxes across central Pakistan (figure 2) grossly outline the northwestern margin of the Subcontinent. The northern limit lies south of the Turan Block and Tarim Basin in the zone of the Himalayan thrust sheets. The Makran and Chagai arcs in western Baluchistan contain late Tertiary fold complexes stacked onto the southern edge of the Lut and Central Afghan blocks of eastern Iran and Afghanistan. Sinestral strike-slip movement along the Chaman and Ornach-Nal faults juxtaposed the Makranian and Subcontinent elements of Pakistan to its present configuration.

Structures formed on the northwest margin of the former Subcontinent during the Tertiary include, from north to south, the Sulaiman Range, the Mari Bugti Hills, the Quetta Syntaxis, the Khuzdar Knot, the Axial Belt, the Kirthar Range and the Karachi Arc. Each of these involves folded Mesozoic and Tertiary strata. The term "arc" is used here to describe gradual curvature in an orogenic belt as compared with "syntaxis" and "knot" referring to an abrupt bend in structural trend (Sarwar and DeJong, 1979). The topo-

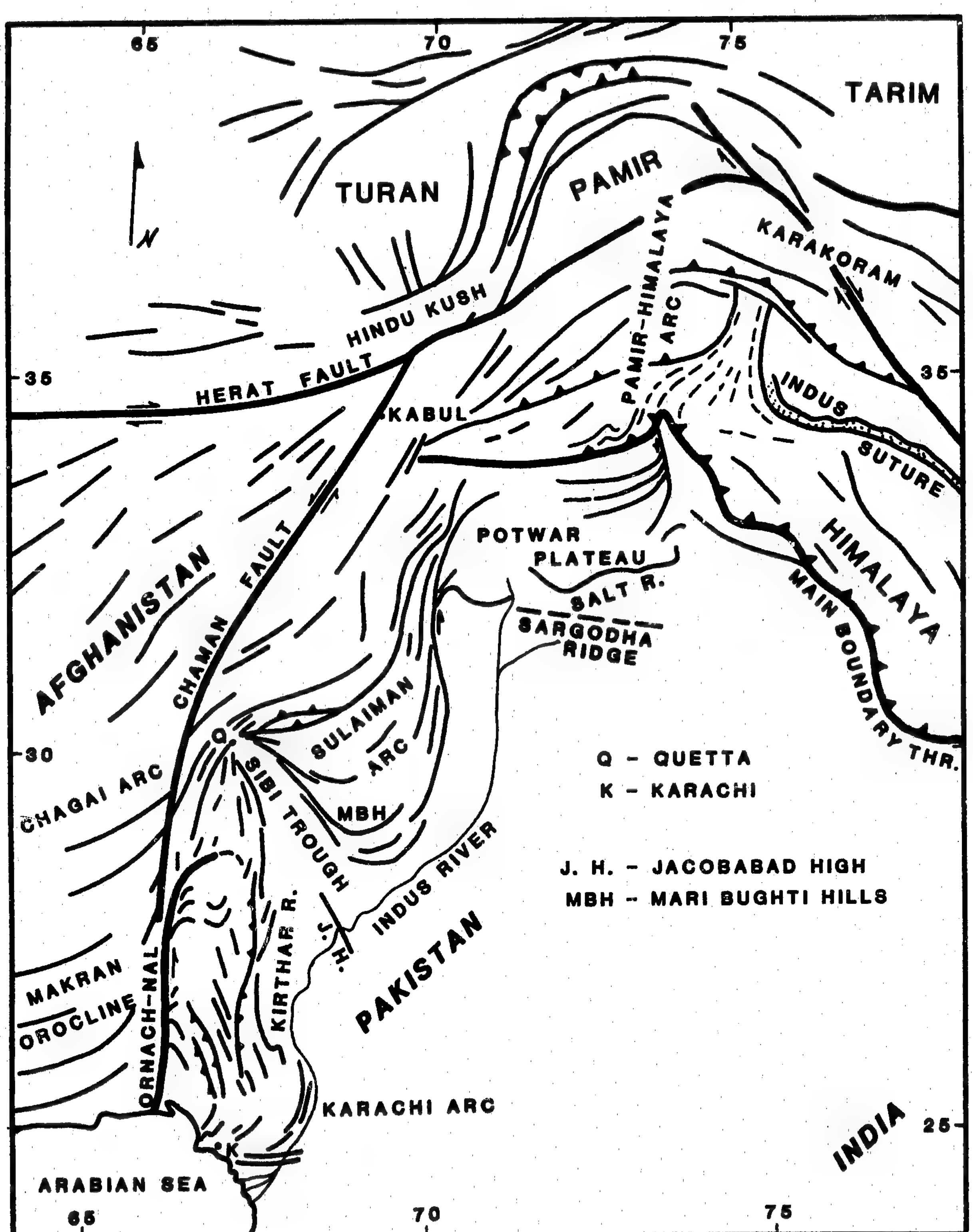

FIGURE 2. Structural elements of northwest India, Pakistan and Afghanistan

graphic relief of these ranges reflects uplift due to compressional folding, faulting or both. Large thrust sheets traceable for several kilometers are common in ophiolitic complexes in areas of intense deformation within the Axial Belt and Zhob Valley (DeJong and Subhani, 1979; Abbas and Ahmad, 1979).

The Sulaiman and Kirthar ranges display structural patterns and thrust faults that reflect block-rotation tectonics as compression intensified in the Neogene (Sarwar and DeJong, 1979). These blocks acted as "rigid" entities during deformation. Sarwar and DeJong further consider the Khuzdar Knot and the Karachi Arc to have acted as one block. Faults within the block show shallow thrust and/or strike-slip components. The authors conclude that the block has undergone counter-clockwise rotation accompanied by a general eastward displacement of the Karachi Arc. Kazmi (1979a) and Quittmeyer et al., (1979) present seismicity and lineament evidence of continued Holocene tectonic activity in Pakistan.

The study area of this report includes a part of the Axial Belt and the Karachi Arc in southeast Baluchistan (figure 3). The Pab Range borders the eastern limit of the southern Axial Belt. A diagrammatic, structural cross-section, east-west across the center of the study area (figure 4) depicts the Pab Range as a comparatively uniform eastward dipping upwarp situated on the eastern limits of the com-

plexly tectonized units of the Mor Range and the Axial Belt proper. Strata dip westward in the Mor Range with pencil cleavage intersecting bedding planes at high angles. The cleavage is attributed to compressional stress from the west during Paleocene ophiolite emplacement. The cross-section (figure 4) is modified after that of Gansser (1979, figure 33). The writer agrees with the configuration of the Mor and Pab ranges as shown by Gansser but envisions a much more complex structure for the poorly exposed strata in the Kanraj Valley. Additional detailed fieldwork is required to establish the correct relationships. Hunting Survey Corporation (1960) originally mapped Jurassic limestone along the axis of the Anero Anticline (so called because of its surface expression just north of Anero Dhora in the study area). Foraminifera from samples collected by the writer from these exposures have been tentatively assigned a Late Eocene to Early Miocene age (Dr. Bruce Masters, Amoco Production Research Company, personal communication). The cross-section in figure 4 attempts to account for Middle Tertiary strata outcropping within Kanraj Valley well-below the summit of the Pab Range. A major thrust is suggested here in light of the tectonic history of the southern part of the Axial Belt (DeJong and Subhani, 1979).

The prominent buttes in front of the Pab Range (figure 1a) are capped by the Parh Limestone. The tectonic cleavage in the Mor Range is exemplified by the pencil rock fragments

STRUCTURE MAP OF THE SOUTHERN AXIAL BELT

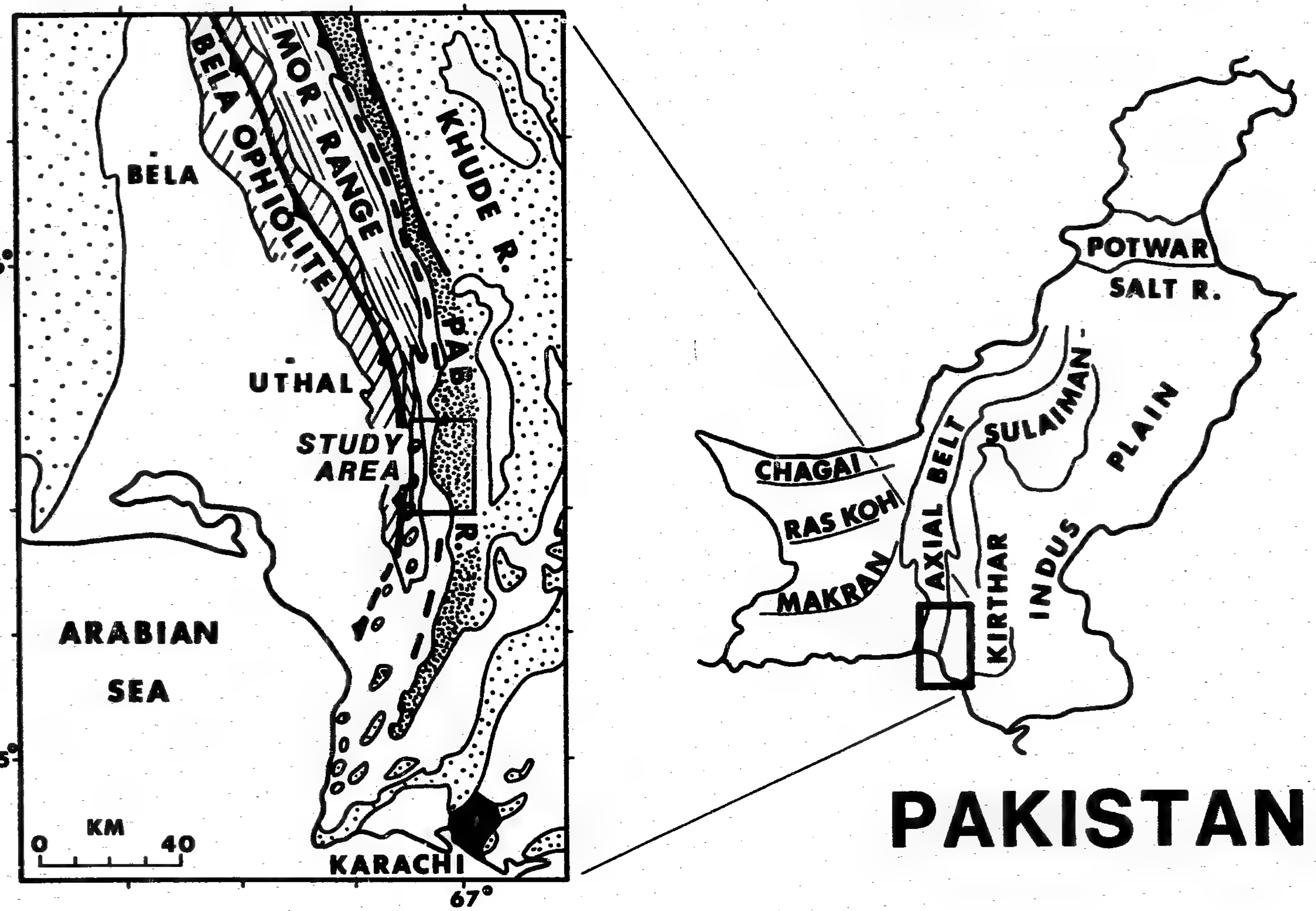

FIGURE 3. Structure map of the southern Axial Belt showing location of study area

strewn on the surface of the exposures (figure 1c). The extent and intensity of this pencil cleavage decreases dramatically to the east to a point halfway across Kanraj Valley beyond which it no longer occurs. The cleavage is believed restricted to the thrust sheet overlying western Kanraj Valley (figure 4). Numerous small scale folds and faults are extant in the western portion of the study area.

Strata of the Pab Range have not been subjected to intense compression. Small scale vertical faults transverse to the trend of the ridge, display a maximum stratigraphic throw of less than 10 m. The strata strike within N15°E to N15°W with an average dip of 20°E in Drabber Pass. The Jakkher Pass section is upturned (N72°E 60°S) in the lower Mughal Kot, changing to N15°E 22°S at the top of the Pab Sandstone. Subvertical joints trending N75°E in Drabber Pass, are filled with coarsely-crystalline calcite.

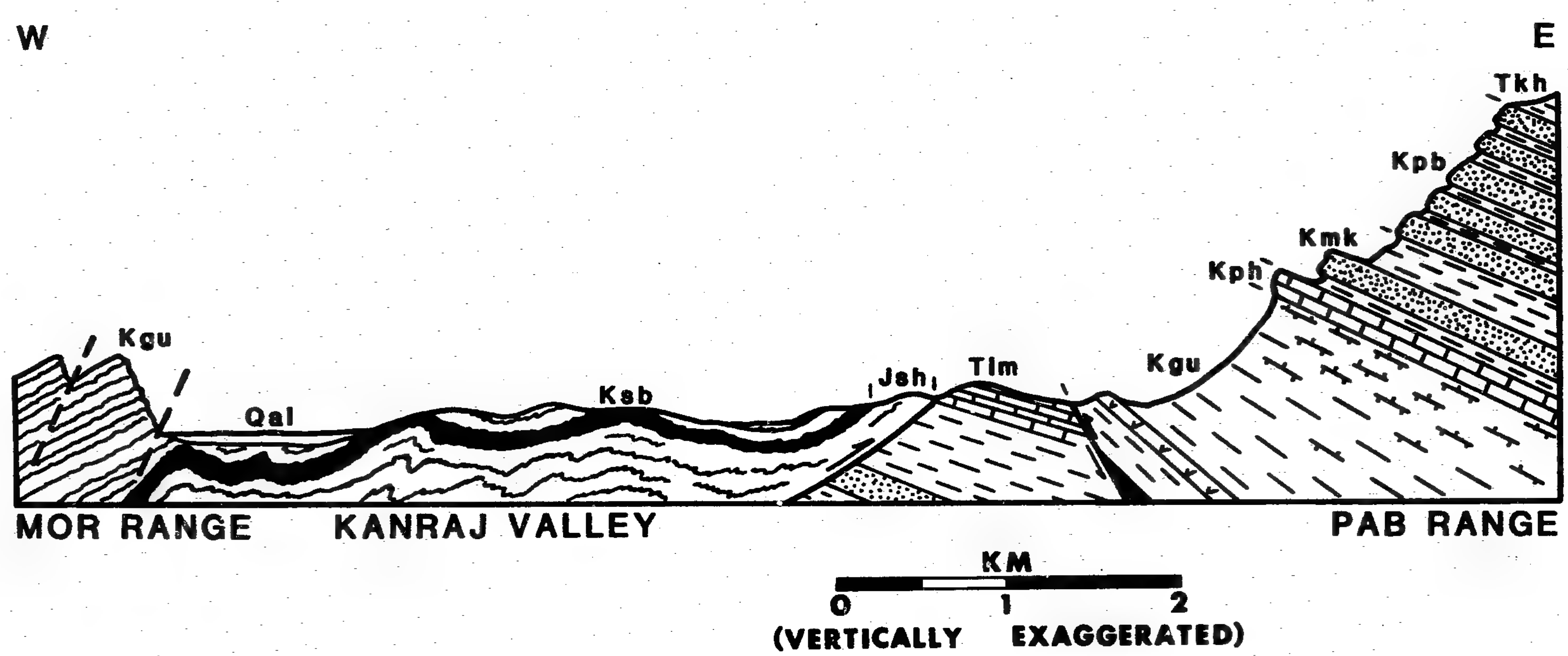

FIGURE 4. Generalized cross-section of the study area

GENERAL STRATIGRAPHY OF THE TETHYAN SHELF DEPOSITS

The geography of the Indo-Pakistani Subcontinent may be divided into three areas (peninsular India, extra-peninsular India and the Indo-Gangetic alluvial plain) (figure 5). Each is distinct in its stratigraphic and stuctural make-up. Extra-peninsular India includes northern India and parts of Pakistan, the mountainous Himalayan states, Bangladesh, and Burma -- that portion of the original Indo-Pakistani Subcontinent forming the northern Tethyan shelf. The continental shelf area in Pakistan has traditionally been referred to as the Indus Basin. The Indian Shield and the Axial Belt formed the eastern and western basin margins, respectively. Current understanding of the setting dictates abandoning the usage of "Indus Basin" for this former Tethyan continental shelf.

The foldbelts of the Karachi Arc, of particular interest to this report, consist of strata deposited on the continental shelf. The general stratigraphy has been known since the first geological survey expeditions traversed the region in the mid-nineteenth century. The Geological Survey of India at that time sent several of its British geologists into the mountain ranges west of the Indus River to assess the potential mineral resources present. Notable among these were W.T. Blanford and E.W. Vredenburg.

Blanford first published a report on the coal-bearing

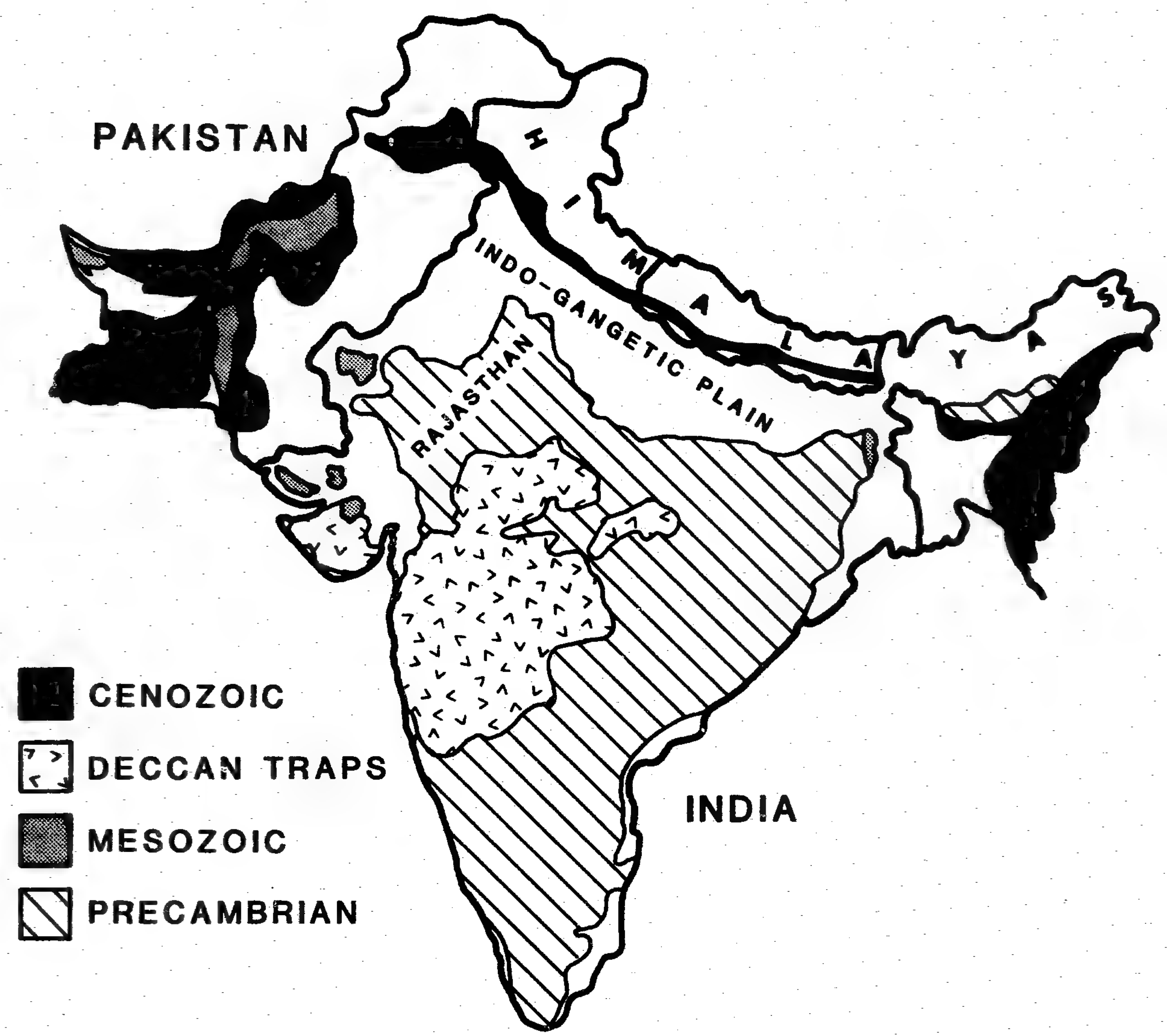

FIGURE 5. Simplified geologic map of the Indo-Pakistani Subcontinent and the surrounding region

strata exposed in the Laki Range in Sind in 1867. Subsequent notes on the geology of Sind were published in the Records of the Geological Survey of India in 1876, 1877, and 1878 culminating in Blanford's major memoir on the geology of western Sind in 1879. Within his memoir, Blanford recounted earlier literature describing geological features of Sind beginning with the journey of Captain N. Vicary through the eastern hills of the Kirthar Range (Vicary, 1847) and Vicary's traversal of the Mari-Bugti Hills north of Jacobabad (Vicary, 1846). Following Vicary's studies, Dr. H.J. Carter made extensive collections of the fossil invertebrates the Mesozoic and Tertiary and then subdivided the sequence on the basis of the faunal succession (e.g. Carter, 1853; 1854). The most extensive early paleontologic investigation was that of D'Archaic and Haime (1853).

E.W. Vredenburg also published extensively on regional geologic surveys of Sind as well as Baluchistan (Vredenburg, 1901; 1906; 1908; 1909a, 1909b). His report of the Axial Belt in Baluchistan is particularly important to the present study. From his traverses, Vredenburg observed two distinct geologic divisions which he described as follows: (Vredenburg, 1909b, p. 190)

> The area is divided into an eastern and a western region by an irregular north and south line roughly coinciding with longitude 66° 15'E. The western region is almost entirely occupied by a monotonous series of shales or clay-shales and sandstones known in the publications of the Geological Survey of India as Kojak or Mekran beds

> which correspond principally with the Oligocene 'flysch' of Europe. This western region may be spoken of as the 'flysch region'. The eastern region exhibits a far more varied geological sequence and consists of rocks ranging in age through a vast series of successive geological formations, all of which are remarkable for containing vast thicknesses of limestone. This area may be spoken of therefore as the 'calcareous region'.

By far the most comprehensive geologic survey undertaken in the area was that under the auspices of the Columbo Plan Cooperative Project which was financed by the Government of Canada and jointly conducted by the Geologic Survey of Pakistan and Hunting Survey Corporation, Ltd. of Canada. The report, published under the title of "Reconnaissance geology of part of West Pakistan" is referenced under the name of Hunting Survey Corporation (1960). The reconnaissance was conducted in the format of photogeologic surveys, field checked for accuracy. The publication includes 29 geologic sheets, each covering 15 minutes of longitude and 15 minutes of latitude, accompanied by a comprehensive 400 page report incorporating stratigraphy, structure, geologic history and economic resource evolutions. The study area in the southern Pab Range lies within Map No. 6, the Thano Bula Khan quadrangle.

Hunting Survey Corporation (1960) emphasized Vredenburg's distinction between the Arenaceous and Calcareous Zones, further differentiating the "Eruptive Zone" containing igneous and metamorphic rocks within the Axial Belt sep-

arating the Arenaceous and Calcareous Zones. Generally speaking, the Calcareous Zone is situated on the northwest margin (Tethyan shelf) of the Indo-Pakistani Subcontinent. The southern Axial Belt delimits the leading edge of the Indo-Pakistani Subcontinent.

Williams (1959) presented a useful descriptive report of the various formations outcropping in Sind and eastern Baluchistan provinces of Pakistan. His rock-stratigraphic nomenclature, equated with earlier and subsequent literature in the correlation chart of Table 1, illustrates the progressive complexity involved in stratigraphic nomenclature as more detailed studies are keyed into a regional framework. Recognition must also be given to the most recent publication indexing and interpreting the stratigraphy of Pakistan, namely that of the Geologic Survey of Pakistan (Shah, 1977).

The strata deposited on the Indo-Pakistani platform compile a thickness in excess of 11,000 m. Rocks of pre-Cretaceous age outcrop within the highly deformed fault blocks of the zone of tectonic melange to the west. Cretaceous and Paleogene strata outcrop in anticlinal ridges north of Karachi. The rocks display significantly less deformation. Neogene and molasse sediments interfinger with the youngest occurrences of shelf sedimentation.

Carbonate and shale dominate the lithologies of the Tethyan shelf deposits. Terrigenous sandstone is noticeably

TABLE 1. Stratigraphic nomenclature of the Indo-Pakistani continental shelf

AGE		VREDENBERG (1906)	HSC (1960)	WILLIAMS (1959)	SHAH (1977)
TERTIARY	PLIOCENE	SIWALIK FM	DADA CGL / MANCHAR FM	SIWALIK GP	SOAN FM / LEI CGL DHOK PATHAN FM CHINJI FM
	MIOCENE		GAJ FM	GAJ FM	MOMANI GP: GAJ FM
	OLIGOCENE	NARI FM	NARI FM	NARI FM	MOMANI GP: NARI FM NAL LM MBR
	EOCENE	KIRTHAR SERIES: UPPER KIRTHAR SERIES: LOWER LAKI SERIES	BRAHUI LM: GORAG MBR BRAHUI LM: KIRTHAR MBR GHAZIJ FM LAKI GP	KIRTHAR FM GHAZIJ FM DUNGAN FM	NISAI FM: KIRTHAR FM LAKI FM GHAZIJ FM DUNGAN LM
	PALEOCENE	CARDITA BEAUMONTI BEDS	RANIKOT GP JAKKHER GP	RANIKOT FM KHADRO FM	RANIKOT GP: LAKHRA FM BARA FM KHADRO FM
CRETACEOUS	UPPER	PAB SS HEMIPNEUSTES BEDS PARH LM	PAB SS HEMIPNEUSTES LM PARH LM	PAB SS FT MUNRO LM MUGHAL KOT FM PARH LM	PAB SS / MORO FM FT MUNRO FM MUGHAL KOT FM PARH LM
	LOWER	BELEMNITES BEDS	BELEMNITES SH	GORU FM SEMBAR FM	GORU FM SEMBAR FM
JURASSIC	UPPER		CHILTAN LM	TAKATU LM	MAZAR DRIK FM
	MIDDLE	POLYPHEMUS BEDS MASSIVE GRAY LM		ANJIRA FM	CHILTAN LM
	LOWER	DARK GRAY LM	LORALAI LM	LORALAI LM SPINGWAR FM	SHIRINAB FM: ANJIRA MBR LORALAI MBR SPINGWAR MBR
TRIASSIC			ALOZAI GP	WULGAI FM	WULGAI FM

subordinate except in certain Upper Cretaceous and Cenozoic units. A composite stratigraphic profile of the shelf succession is shown in figure 6. The brief formational descriptions, taken from Hunting Survey Corporation (1960), Williams (1959) and Shah (1977), grossly characterize lithologies and thicknesses of the strata.

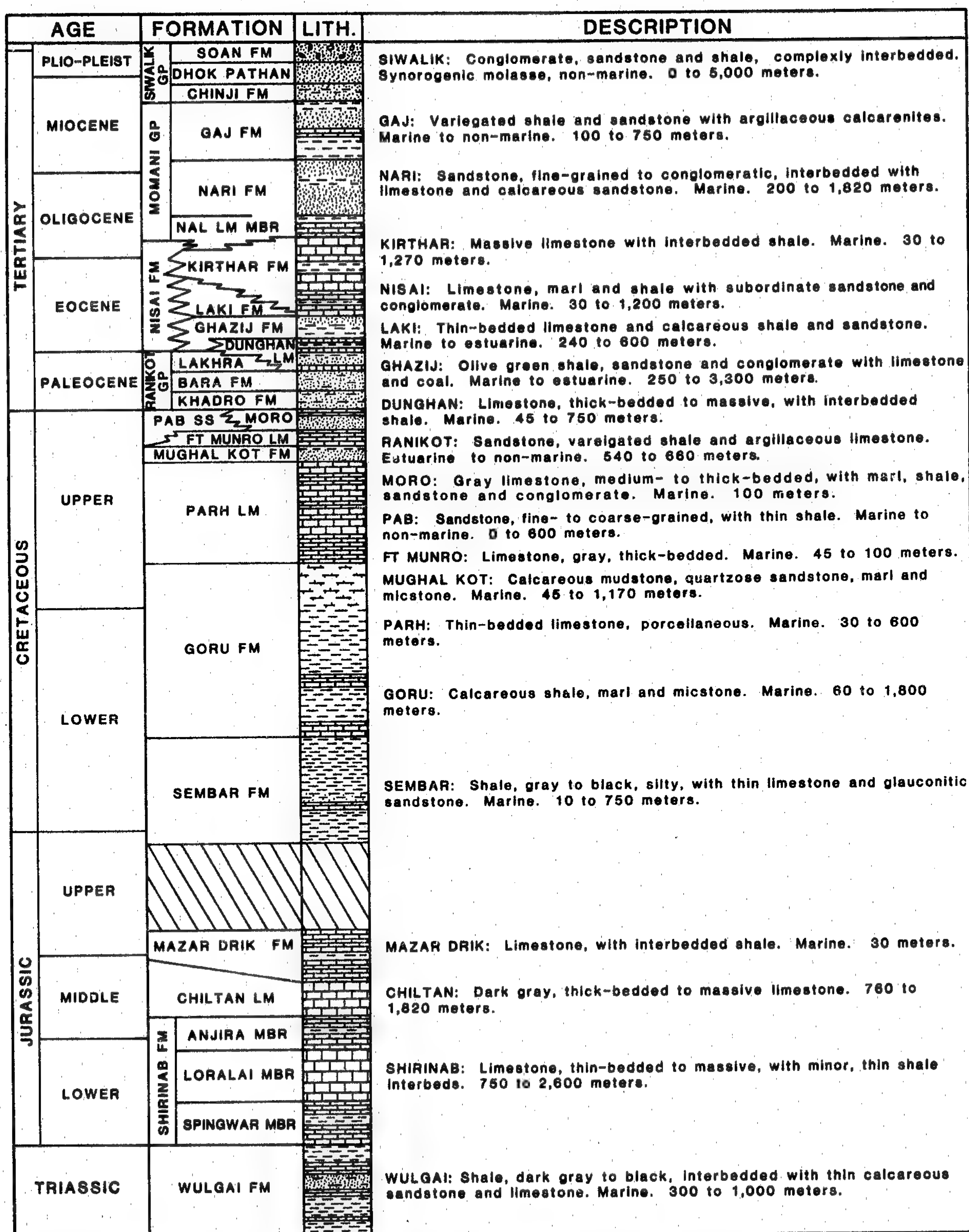

FIGURE 6. Stratigraphy of the Indo-Pakistani continental shelf (modified from Williams, 1959)

STRATIGRAPHY OF KANRAJ VALLEY AND SOUTHERN PAB RANGE

The study area, outlined in figure 3, incorporates portions of the extreme southern Mor Range on the west, the intervening Kanraj Valley, and the southern Pab Range. The area lies within portions of two 15-minute quadrangles (35-K-14 and 35-O-2) currently being mapped by officers of the Geological Survey of Pakistan. The Pab Range occurs just within the western limits of the former continental shelf on the northwest margin of the Indo-Pakistani Subcontinent.

The stratigraphic sequence consists of Cretaceous through Paleocene continental shelf and slope deposits. The composite section and general outcrop pattern are shown in figure 7. Fossiliferous samples collected from exposures mapped as the Jurassic Shirinab Limestone by the Hunting Survey Corporation (1960) were subsequently assigned a Tertiary age on the basis of the fossils present suggesting that Jurassic strata are not present in Kanraj Valley. Accordingly, a discussion of post-Jurassic stratigraphy is presented in this chapter.

The Sembar, Goru and Parh formations, successively, comprise the lower Cretaceous. Capping the Cretaceous and upholding the Pab Range are the Mughal Kot Formation and the Pab Sandstone. The youngest units included in this study are the Paleocene Khadro Formation and a Middle Tertiary

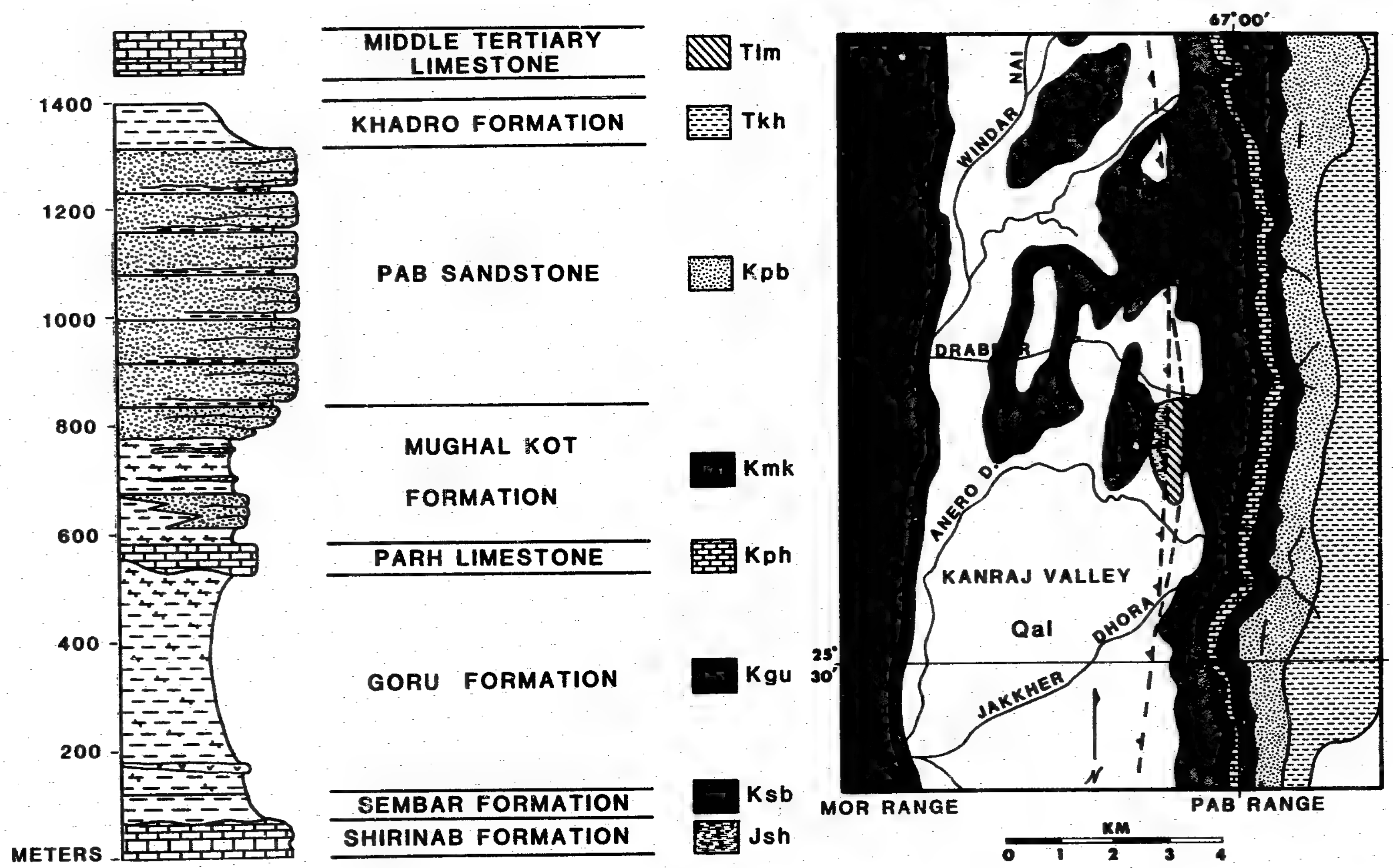

FIGURE 7. Composite stratigraphic section and geologic map of the study area

limestone.

The clastic sediments of the Mughal Kot Formation and Pab Sandstone, both Maestrichtian in age, comprise the principal focus of this study. Exposures along Jakkher and Drabber passes from the uppermost Parh Limestone through the basal Paleocene, 763 and 733 m, respectively, were measured, described and sampled in detail. Reconnaissance of the remaining formations was accomplished during the field season and included the general description and sampling of the units for comparison with published reports on correlative strata.

Sembar Formation

Definition, distribution and thickness

The Sembar Formation exposed in Kanraj Valley is similar in lithology to the black shales constituting the unit at its type locality in Sembar Pass, Mari Hills east of Quetta. The total thickness is estimated at less than 100 m though individual exposures of the Sembar are typically only 10 m or less thick. These outcrops are limited to cut banks along small streams and low weathered patches protruding through the thin alluvial cover on the floor of Kanraj Valley (figure 8a).

Lithology

The greenish black (5G2/1)[1] to grayish black (N2) shales of the Sembar lack interbeds of thin argillaceous limestone that occur in the thicker deposits of the type locality. The term shale often connotes different characteristics to different geologists. Accordingly, the terminology used in this report follows that outlined in Potter, Maynard and Pryor (1980). Shale is a fine-grained terrigenous rock consisting of more than 50% grains with a diameter less than 0.062 mm i.e., the sand-silt size cutoff. Characteristics of the Sembar clay-shales include (1) clay-size constituents which comprise more than 66% of the whole rock, (2) a moderate to high degree of induration usually associated with a superimposed tectonic cleavage which imparts a pencil-like cleavage fabric to most exposures in western Kanraj Valley, and (3) laminae. Because of the rock cleavage being near vertical in orientation, the shales typically do not break along stratification laminae or partings. The shale in thin section is 15 to 20% quartz silt, and 80% clay in parallel, horizontal stratification. Mechanical (pipette) analysis yields a mean grain size of 8.15 phi (3.8 microns) and a sorting value of 2.77 phi units (very poorly sorted). The textural parameters of this and

---

[1] For comparison, color references throughout this monograph will be those of the Geological Society of America Rock Color Chart.

other shale samples are listed in Appendix B. The largest quartz silt fragment observed in thin section is Ø.Ø5 mm diameter (figure 8b). X-ray analysis (Appendix E) confirms the dominance of quartz along with the clay minerals (kaolinite, chlorite and illite), feldspar, calcite and trace glauconite. The distinct black to very dark green color is attributable to these accessory minerals and to finely disseminated organic debris. The samples of Sembar analyzed for insoluble residue average 14% soluable carbonate by weight (Appendix G).

Facies and environments of deposition

The black clay-shale lithofacies of the Sembar do not display bedding features and primary structures indicative of a specific depositional environment. This situation is, in part, due to the lack of continuous exposure or undeformed strata in Kanraj Valley. Studies of the fauna collected from other localities suggest open, and possibly deep-water marine conditions. The association of Sembar with the overlying Goru and Parh has been interpreted to reflect deep water deposition on the outer shelf - upper slope position as part of a depositional continuum. This association was first recognized by Dr. Wayne A. Pryor, University of Cincinnati, (personal communication, 1979) for the same sequence in the Sulaiman Range. The depositional

setting will be developed in the following chapter.

Stratigraphic and structural relationships

Where best exposed along Windar Nai in western Kanraj Valley, the Sembar displays a prominent fracture cleavage which all but masks bedding and primary sedimentary structures. The bedding discerned is thin to more commonly laminated, generally dipping at a much lower angle than the high angle cleavage. The unit is not exposed along the eastern side of the valley, consequently the basal contact was not observed.

Age and correlation

Williams (1959) and Kureshy (1980b) consider the majority of the invertebrate faunae (belemnites and turbid (deep?) water foramifera) to be Neocomian (Early Cretaceous) in age. However, the range of the species present is from Late Jurassic (Tithonian) to Aptian. Identifiable faunae were not collected in the area studied; however, the similarity of lithostratigraphy to that of the Sembar type locality supports depositional continuity along the northwestern shelf of the Subcontinent. Williams (1959) extends this to include the Spiti black shales in northern Pakistan

which are equivalent Neocomian strata.

Goru Formation

Definition, distribution and thickness

The Goru Formation was named by Williams (1959) for exposures approximately 240 km north of the study area. The Formation outcrops extensively in the western Sulaiman and Kirthar provinces along the Axial Belt. The Goru is well exposed in the western scarps of the Pab Range (figure 8c), across the Kanraj Valley and the eastern ridges of the southern Mor Range. Its thickness is estimated to be at least 400 m, although the lowest portion of the sequence is not exposed in Kanraj Valley.

Lithology

Lithologically the pale olive (10Y6/2) to dusky yellow green (5GY5/2) strata consist dominantly of thin-bedded to laminated calcareous claystone in the lower two-thirds of the Goru. Occasional marl interbeds and at least one four meter interval of black carbonaceous mudstone/limestone occur in the upper part. Rhythmically interbedded marl and micstone with progressively fewer claystone interbeds comprise the upper third of the Goru. Micstones and marls are thin-bedded with few strata exceeding 10 cm in thickness. It is observed that an overall, though irregular, increase in carbonate content (claystone through marls to micstones)

is displayed from the Sembar Formation to the overlying Parh Limestone. Acid-insoluble residues from three samples representative of the lower, middle and upper portions of the Goru exposure corroborate this field observation by yielding a vertically decreasing percent insoluble residue of 61.28, 57.80 and 20.78 (Appendix F). Mechanical analysis of a lower Goru claystone gives a graphic mean grain size of 8.73 phi (2.5 microns) and a 4.00 phi sorting index (extremely poorly sorted) (Appendix A). Whole rock x-ray analysis similarly shows a progressive vertical increase in calcite and a corresponding decrease in quartz within the Goru (Appendix D). Kaolinite and illite clay minerals are trace constituents.

Thin-section description for three samples representing the typical lower, middle and upper thirds of the exposed Goru respectively are as follows:

Sample G-1. The silty claystone exhibits quartz silt to 20 microns in diameter. The claystone is faintly laminated and has a slight tendency to segregate between clay and silty clay bands. Occasional foram tests occur in the terrigenous framework.

Sample G-2. The marly claystone contains floating quartz grains up to 70 microns in diameter. Abundant coiled and uniserial foram tests up to 0.20 mm (200 micron) float in the matrix.

Sample G-3 (figure 8d). The sample is classified as a marly micstone with an occasional to rare quartz silt observed. Spherical radiolarian tests are abundant, some with preserved spines attached (tests up to 0.50 mm in diameter).

<u>Facies and environments of deposition</u>

Wilson's (1975) facies belt 2 in an open shelf position comprises the depositional setting proposed for the Goru Formation. The fine-grained detrital clastics and the increasing carbonate content vertically fit a regime of increasingly shallower water depths from the outer shelf to an inner shelf position. The angular silt-size quartz is considered windblown and may well have mixed with distal clayey muds. The planktonic foraminifera and radiolaria may represent a gradual shallowing and/or progradation of the Goru basinward over Sembar deep water deposits. Rahman (1963) proposes that the Goru strata in the western Kirthar Province are deeper water equivalents of the littoral sandstones of the Lumshiwal Formation of the Kohat-Potwar Province to the north of the Salt Range.

<u>Stratigraphic and structural relationships</u>

The basal contact of the Goru Formation with the Sembar is not exposed in the study area. Along the Windar Nai near Khamiso Hotel the two formations are closely juxtaposed but the relationship may be a fault contact defining the eastern ridge of the southern Mor Range. The contact to the north

changes from disconformity to conformity (Williams, 1959). At the type locality the Goru sequence consists of a shale interval positioned between two carbonate-dominated sequences. The basal carbonate section in eastern Kanraj Valley was not observed but may be present in the Mor Range to the west. The highly fractured character of the strata suggests the Mor Range (figure 1c) was subjected to much greater tectonism than the Pab Range just a few kilometers to the east.

Age and correlation

According to Williams (1959) and Shah (1977), the Goru fauna indicates an Albian to Cenomanian time range. Some species range from Neocomian to as young as Senonian in age. The Goru correlates with the terriginous Lumshiwal Formation several hundred kilometers to the north-northeast. Subsurface strata beneath the Indus Plain to the east contain a significant terriginous sand component apparently derived from the Indian Shield (Rahman, 1963).

Igneous intrusive in the lower Goru Formation

The Goru Formation along the eastern flank of the Kanraj Valley, contains a laterally extensive, 20 to 30 m sill of basaltic composition that interrupts what is otherwise a uniform lower Cretaceous succession. This unique occurrence conforms to the structural attitude of the Goru host according to Hunting Survey Corporation (1960) and is possibly

related to volcanism recorded in the Porali Volcanics to the west. Stratigraphic relations of the diabase sill are somewhat obscured by poor exposure in the study area. The intrusion is classified as a spilitic diabase based on its mineralogical composition.

The hand sample is dark gray (N3), porphyritic basalt. In thin section the rock contains approximately 5% phenocrysts, the largest of which are 2.0 by 5.0 mm. The plagioclase phenocrysts are laboradorites (An50 - An55) which are commonly oscillatorily zoned or show overgrowths in optical continuity with the parent crystal. The bulk of the diabase is a fine-grained matrix of microlitic laths of a more-sodic plagioclase, ranging in size from 0.01 mm by 0.04 mm to 0.07 mm by 0.25 mm. Other constituent minerals found in the groundmass are augite (up to 0.20 mm long), ilmenite and chlorite. Secondary veins of calcite and chalcedony are conspicuous both in hand specimen and thin section. The succession of vein mineral linings begin as chalcedony on the outside through fine-grained calcite to coarse-grained calcite in the center. At least one additional set of crosscutting veins suggests an active post-emplacement history of vein generation and filling. The alteration character of the diabase suggests intrusion of the magma into Goru sediments probably containing abundant marine connate waters.

Chemical analysis of two diabase sill samples and their

recalculations on a volatile-free basis are listed in Table 2. The analyses utilized standard atomic absorption and wet chemical techniques (Shapiro, 1975) following lithium metaborate fusions (Medlin, Suhr, and Bodkin, 1969). Normative mineralogy, based on volatile-free major oxides, indicates that the igneous rock may be classed as a quartz thoeliite. The origin of the intrusive is believed to be related to the initial outpourings of submarine lavas in the Axial Belt during the Late Cretaceous. Gansser (1979) correlates the sill with a similar occurrence west of the Mor Range. The significant percentages of volatile components underscore the influence of surrounding saturated Goru sediments.

Parh Limestone

Definition, distribution and thickness

The Parh Limestone caps the westernmost prominent ridge of the Pab Range. As with the underlying Sembar and Goru, the Parh outcrops extensively in the eastern Baluchistan Province. Field and thin section descriptions of the formation in the study area correlate closely with those of Shah (1977) and of the type locality (Williams, 1959). Along Drabber Dhora, the Parh reaches a thickness of 40 m, but the cliff-forming limestone thins locally along the Pab Range.

Lithology

Limestone, lithographic to porcellaneous with conchoi-

Table 2. Chemical analyses of the igneous sill in the lower Goru Formation

	with volatiles		volatile-free		CIPW Normative mineralogy		
	GV-1	GV-2	GV-1	GV-2		GV-1	GV-2
SiO_2	45.76	48.62	49.80	50.18	Q	4.86	5.42
Al_2O_3	13.60	13.30	14.80	13.73	Or	1.78	2.84
Fe_2O_3	2.13	3.04	2.32	3.14	Ab	23.49	21.55
FeO	11.39	10.52	12.40	10.85	An	27.04	24.62
MgO	3.00	4.93	3.27	5.07	Lc	---	---
CaO	8.99	9.30	9.79	9.60	Ne	---	---
Na_2O	2.55	2.46	2.78	2.55	Di	18.15	18.95
K_2O	0.28	0.47	0.30	0.48	Hy	13.12	14.17
TiO	3.97	4.04	4.32	4.17	Ol	---	---
MnO	0.20	0.23	0.22	0.23	Mt	3.36	4.56
CO_2	5.62	1.16	---	---	Il	8.21	7.92
H_2O	2.01	1.83	---	---			
Total	99.50	99.91	100.00	100.00		100.01	100.03
$Fe_2O_3(T)$	14.56	14.74			Tholeiite		
FeO(T)	13.10	13.26	14.49	13.68	(oversaturated)		

Trace element concentrations (ppm)

Ni	57	87
Cr	34	29
Rb	24	28
Sr	491	315

dal fracture, dominates the lithology. Colors vary from the characteristic light greenish gray (5GY8/1) to greenish gray (5G6/1) beneath the medium bluish gray (5B5/1) marly interbeds of the overlying Mughal Kot Formation at the formational contact. Within the Parh, bedding averages less than 30 cm, but occasional strata up to one meter thick are present (figure 8e). Few undulations are recognized in the uniform bedding. A grayish red purple (5RP4/2) micstone at the base of the Parh corresponds to the basal "maroon bed" described by Williams (1959). Rather than being restricted by bedding, the coloration occurs as discontinuous blotches cutting across bedding horizons. The significance of this banding may in fact be related to the local Parh - Goru contact rather than regional volcanic activity in the Axial Belt as suggested by the Hunting Survey Corporation (1960).

The limestone throughout the Formation consists of foraminiferal packstone and wackestones, with Globotruncana being the main component of the framework (figure 8f). The particle size ranges in thin section from 0.03 mm to 0.7 mm. A faint horizontal orientation of the tests is noted. X-ray analysis (Appendix D) reveals calcite as the principal mineral with minor to trace amounts of kaolinite, illite and quartz (windblown silt).

Facies and environment of deposition

The thin-bedded foraminiferal packstones display a very

FIGURE 8. Photographs of the Sembar, Goru and Parh formations

a. Weathered outcrops of the Sembar Formation in western Kanraj Valley.
b. Photomicrographs of Sembar shale. Bar scale is Ø.5 mm.
c. Prominent Parh Limestone capping thin-bedded marls of the Goru Formation.
d. Photomicrograph of a marl in the Goru Formation; note the radiolarian fauna with spines attached. Bar scale is Ø.5 mm.
e. Thin-bedded packstones of the Parh Limestone at entrance to Drabber Pass overlain by shales of the lower Mughal Kot Formation.
f. Packed Globotruncana tests of Parh Limestone. Bar scale is Ø.5 mm.

a

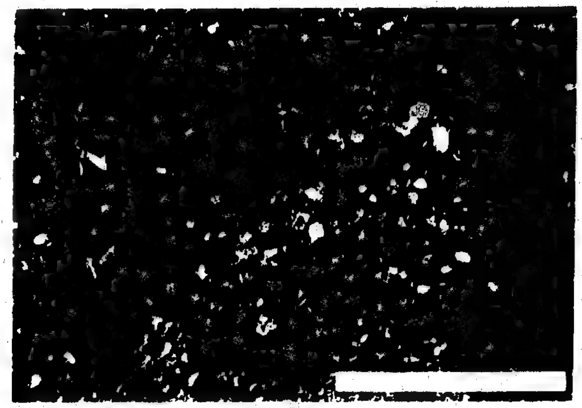

b

c

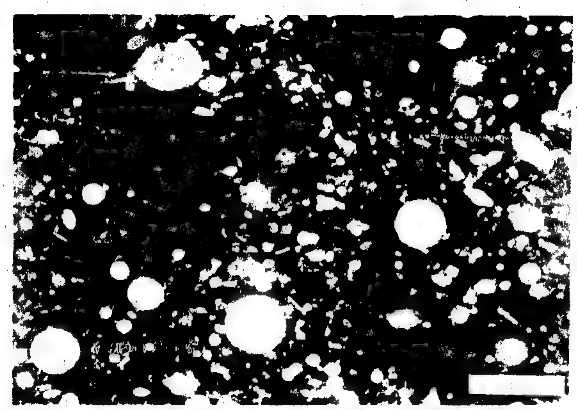

d

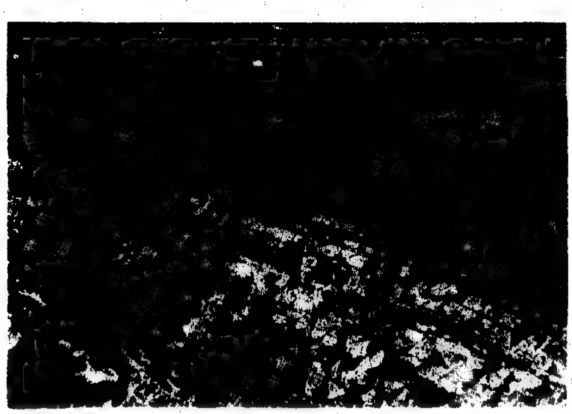

e

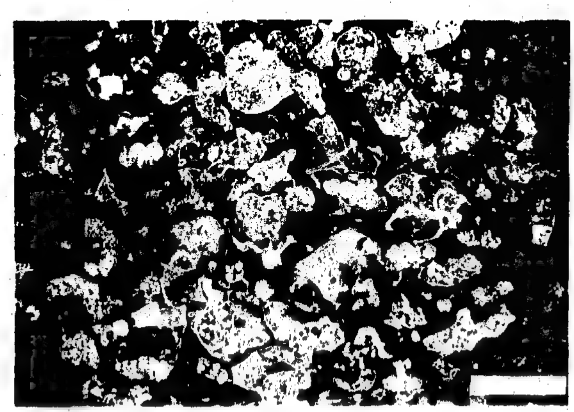

f

limited range of faunae in the study area. Globotruncana predominate at the expense of megafossils that should occur in a more open platform setting (Wilson, 1975). This suggests a shallow shelf regime not fully exposed to circulating currents of the open marine shelf. It is further inferred by Wilson (1975) that shallow restricted water must be warmer and of higher salinity than that of the open sea in order to inhibit a wide variety of fauna and flora. Such an environment may occur shoreward from a barrier reef on a shallow lagoonal shelf platform, perhaps similar to that described by Matthews (1966) off the coast of Belize.

Rahman (1963) attributes the Parh Limestone to a calcareous facies initiating on a westward high ground near the Axial Belt and building eastward. The Axial Belt flank in this setting would have had to have been an unusally uniform shelf. An alternative depositional setting envisions the Sembar, Goru and Parh formations acting as a sedimenatary wedge prograding westward over the outer continental shelf (Dr. Wayne Pryor, University of Cincinnati, personal communication, 1979). Even within this scheme, submarine ridges further west may have had a bounding effect on the migrating environments.

Stratigraphy and structural relationships

The contact with the underlying Goru is defined (Williams, 1959) as the top of the stratigraphically highest shale interbed. The contact at the entrance to Drabber Pass is conformable. The cliff-forming Parh thins considerably to the south but does not pinch out completely. It becomes prominent again only a few kilometers to the south at Jakkher Pass. From the field reconnaissance it is inferred that the basal surface has several meters of relief. Early Parh deposition may have been restricted to local depressions within back-reef lagoons.

The Parh Limestone caps the prominent hogback along the west flank of the Pab Range. Two prominent joint sets trend across the strata which otherwise exhibit a conchoidal fracture. The strike of the Parh along Drabber Dhora is N9°W, roughly parallel to its depostional strike. The dip is 29°E.

Age and correlation

An abundant foraminiferan fauna (Globotruncana) has been identified by Williams (1959) and Gigon (1962) as Senonian in age. The prominent geomorphic expression is easily recognized throughout the region. The uniformity and great lateral extent of the Parh typify the Cretaceous formations

on the continental shelf.

Mughal Kot Formation

Definition, distribution and thickness

Williams (1959) recognized the Mughal Kot Formation as a widely occurring unit positioned between the Parh Limestone and Pab Sandstone. At its type locality in the northern Sulaiman Range, the Formation consists of interbedded quartzose sandstone, calcareous mudstone and marl capped by a thick-bedded limestone, the Fort Munro Limestone Member. The Fort Munro was raised to formational status by the Geological Survey of Pakistan (Shah, 1977) as was the Kahan Conglomerate, a thick boulder and cobble conglomerate of volcanic porphyry and basalt debris locally underlying the Fort Munro at Kahan on the Kach-Zariat road east of Quetta. Kazmi (1979b) includes the conglomerate as part of his Bibai Formation.

In the southern Pab Range, lithologies similar to that of the type locality comprise the stratigraphic interval between the Parh and Pab and is here formally given the name, Mughal Kot. Further, the Formation exposed in Drabber Pass is suggested as a stratigraphic reference section for comparison with the type locality. The stratigraphic thick-

ness of the Mughal Kot in these exposures is 255 m.

Lithology

The Mughal Kot Formation at Drabber Pass (figure 9) is divisible into four subunits which are easily recognized elsewhere. The lowest subunit rests conformably on the Parh (figure 8e). It consists of thin beds (up to 0.5 m) of alternating dark gray (N3) to greenish gray (5G6/1) calcareous mudstone, marl and micstone near the base. This grades upward into a very thin-bedded to laminated, dark greenish gray (5GY4/1) mudstone. Yellowish gray (5Y7/2) bedded siltstone caps the sequence. The subunit has a total thickness of 30 m. It is nonresistent; consequently it forms slopes which are largely rubble-covered.

The succeeding and most prominent interval of the Mughal Kot is a light gray (N7) to yellowish gray (5Y8/1) quartzarenite. The well-indurated sandstone displays indistinct, small to large scale trough crossbeds which generally indicate westward paleocurrent directions. These occur in lenticular beds up to 3 m thick (figure 10a). Occasional low angle planar cross sets exhibit a reversed, eastward dip. Scattered through this subunit are several lenses of thin (less than 20 cm thick) mudclast conglomerate. The basal contact with the underlying siltstone is sharp and irregular with elongated, bulbous loadcasts protruding downward 0.3 m (figure 10b). Individual elongated load casts

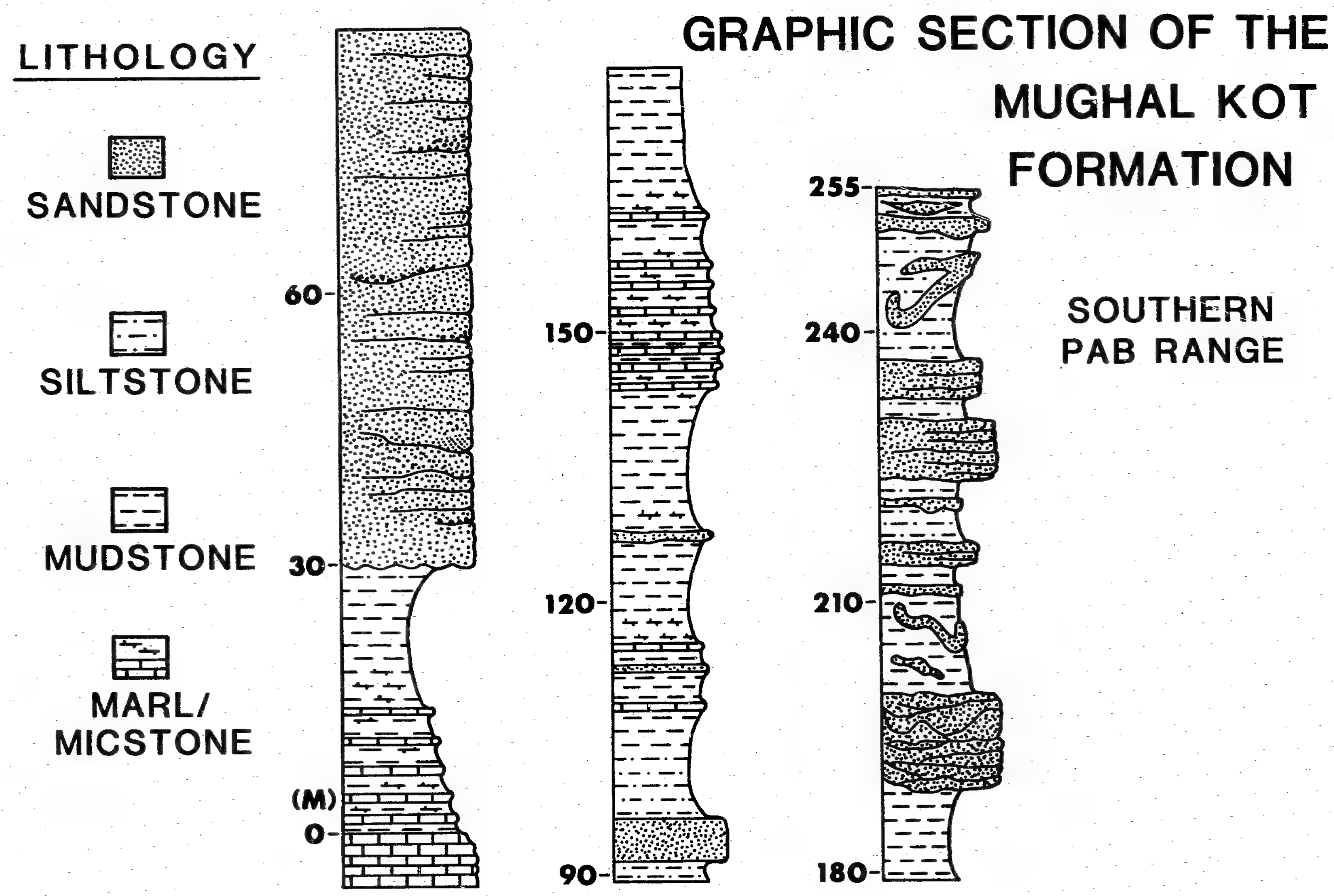

FIGURE 9. Graphic section of the Mughal Kot Formation exposed along Drabber Pass

thicken in a westerly orientation (S76°W). The subunit attains a thickness of 60 m along Drabber Dhora.

Overlying this the Mughal Kot consists of a shale-dominated subunit beginning with arenaceous mudstone, grading upwards through calcareous claystone, marl and micstone repetitions, and ending with marly mudstone (figure 10c). The arenaceous mudstone is pale olive (10Y6/2) to olive gray (5Y4/1) and thin-bedded to laminated. Thin interbedded sandstones in the lower half of the subunit consist of dominantly medium light gray (N6) to light olive gray (5Y6/1), very fine- to medium-grained quartzarenites. Grazing/crawling trace fossils (figure 10d) are abundant along the sharp basal and upper contacts of the thin sandstones. The trace fossil assemblage is largely horizontal with indications of bioturbation within the sands. Parallel and ripple lamination are infrequently preserved. The sandstone interbeds are typically less than 20 cm thick, but occur up to one m. thick. Overlying the lower part are calcareous claystone, marl and micstone repetitions similar to those described below the thick sandstone. The marly mudstones capping this middle interval are light olive gray (5Y5/2) to grayish olive (10Y4/2) and very thin-bedded to laminated. The shales become less calcareous beneath the succeeding Mughal Kot interval. Overall thickness of this subunit is 100 m.

The uppermost subunit of the Mughal Kot is an interbedded sandstone - mudstone complex (figure 10e). The very

poorly sorted sandstone is a medium light gray (N5-N6) sublitharenite to litharenite which weathers dusky brown (5YR2/2). Volcanic rock fragments comprise up to 30% of the framework with quartz and a trace of feldspar grains constituting the remainder. Individual sandstone beds are up to 1.5 m thick and display indistinct horizontal lamination. Several sandstone beds are contorted into chaotic slump overfolds (figure 10f) which are incorporated in a very poorly sorted, sandy, calcareous mudstone matrix. Rounded micstone clasts up to 30 cm long are also incorporated into the chaotic slumps. The mudstone is light olive gray (5Y5/2) weathering to dark gray (N4) and contains finely disseminated black (N1), carbonaceous plant debris throughout. The mudstone is similarly fractured and folded within the slump overfold intervals. The thickness of the subunit is 60 meters.

The stratigraphy of the Mughal Kot Formation to the south at Jakkher Pass is similar with the exception of minor variations within each of the subunits. The lower thick quartzarenite breaks up to the south (figure 11a) and is represented by thinner sandstones interfingering with interbedded calcareous mudstone to micstone. Rare wood impressions (figure 11b) occur in the sands. The distinctive sandstone cliff thins to the north but can be traced for several kilometers along the Pab escarpment. The fine-grained middle interval displays low angle faulting of lim-

FIGURE 10. Photographs of the Mughal Kot Formation in Drabber Pass

a. Lenticular beds in the prominent sandstone in the lower Mughal Kot.
b. Ball and pillow deformational structures at the base of the sandstone in photo(a).
c. Central, fine-grained interval of the Mughal Kot Formation.
d. Scolicia and chevron trail trace fossils of central Mughal Kot interval.
e. Interval of chaotically-slumped sandstones in the upper Mughal Kot Formation.
f. Individual slump-overfolded sandstone. Jacob's staff is 1.25 m long.

a

b

c

d

e

f

ited (less than 10 m) stratigraphic throw (figure 11c). Field observations suggest that the displacement may have been, in part, penecontemporaneous soft-sediment deformation. The chaotic subunit to the south involves sandstone thicknesses up to 10 m (figures 11d, e and f).

Mughal Kot shales (Appendix A) possess an average grain size in the coarse clay grade (8.42 phi, 2.9 microns) and are very poorly sorted (2.86 phi). Average skewness and normalized kurtosis for the shales are near-symmetrical and platykurtic. Numerical values for sorting, skewness and kurtosis are listed in Appendix A.

Coarser sediments (bedded siltstones) occur just beneath the prominent sandstone in the lower Mughal Kot of Drabber Pass. Shales range from mudstone to claystone above the sandstone in the middle Mughal Kot interval and become coarser again in the uppermost chaotic interval.

The trend in acid-insoluble residue of selected Mughal Kot shales (Appendix F) parallels that of grain size in that marl and micstone beds usually contain a finer clastic component. Percentage of carbonate removed by 5% HCl range from 19.28% in the chaotic mudstone to 75.86% in the middle subunit.

Appendix B lists several sieve-corrected textural analyses of thin sections of selected Mughal Kot sandstones. Quartz grains of the prominent lower Mughal Kot sandstone possess an average diameter of 1.29 phi (0.41 mm medium-

FIGURE 11. Photographs of the Mughal Kot Formation in Jakkher Pass

a. Interfingering of the lower Mughal Kot sandstone with calcareous shale and micstone.
b. Wood impression in lower Mughal Kot sandstone.
c. Penecontemporaneous slumping and post-depositional faulting in central Mughal Kot interval.
d. Interbedded micstone, shale and thin-bedded sandstone of the central interval.
e. Stacking of chaotically-slumped sandstones in the upper Mughal Kot.
f. Rotated sandstone block in chaotic body.

a

b

d

c

e

f

grained) and an average sorting index of 0.92 phi (moderately sorted). Fossil fragments in the quartzarenite also have an average grain diameter of 1.29 phi (0.41 mm). Thin-bedded sandstones within the middle fine-grained interval are fine-grained and moderately sorted. Sandstones within the chaotic slumps are fine- to medium-grained and poorly sorted.

The thin section petrography of 30 Mughal Kot sandstones is given in Appendix C. The clastic detritus in the thick sandstone in the lower Mughal Kot consists of quartz grains which are mostly monocrystalline with planar to strongly undulose extinction. Compositionally these sandstones are quartzarenites (Folk, Andrews and Lewis, 1970). The most conspicuous components after quartz grains are the fossil fragments consisting of algae "heads" (Bathurst, 1975) (figure 12a and b). As seen in the photomicrographs, longitudinal views show an elongated pattern while the transverse cross-sectional views reveal a polygonal cellular structure within the calcareous fragments. Calcite cements the well-indurated sandstone.

The thin-bedded sandstones within the middle, fine-grained subunit are quartzarenites, as below, with the exception of an occasional litharenite containing greater than 25% lithic sedimentary clasts (sedarenite). Calcite and clay minerals comprise the cementing material. Fewer and less generally well-preserved fragments of the same fos-

sil algae are found.

The chaotically slumped sandstones differ in composition from the quartzarenites in that they record the first and greatest influx of volcanic detritus onto the western continental shelf. The percent computed from thin section analysis varies up to 45% of the total framework. Quartz dominates the rest, with highly altered feldspar typically constituting less than 1%. Chert is also present in trace though persistent amounts. The volcanic fragments are generally much better rounded than quartz and slightly larger in grain size. Smaller volcanic grains are often replaced by iron oxide and calcite but larger grains are less affected leaving the microlite feldspars with an unaltered pilotaxitic (flow) texture (figure 12c and d). Plagioclase content (computed by the Michelle-Levy technique) grossly averages An40 though a wide variation exists. The inference derived from microlite composition is that the volcanics were weathered from a nearby andesite/basalt terrain and not the distant basalt flows of the Deccan Trap in western India (White and Vondra 1980). The implications will be discussed more fully in a later section of this report. For the present it is sufficient to document the volcanic presence in the upper Mughal Kot. The volcanic admixture is noted in varying proportions throughout the overlying Pab Sandstone. Calcite, chlorite, illite and analcime fill the intergranular pore space.

Whole rock x-ray diffraction analysis (Appendix D) of Mughal Kot sediments confirms the presence of quartz, calcite (no dolomite detected), clay minerals (kaolinite, chlorite and illite), and feldspar (oligoclase to bytownite). Feldspar content increases dramatically in sediments containing volcanic debris.

The heavy mineral suite was identified using x-ray powder camera. Zircon (Z), tourmaline (T) and rutile (R), occur throughout the Formation. Significant magnetite is present in the thick sandstone of the Lower Mughal Kot (Appendix E). The composite ZTR index for six samples averages 58:36:6, indicating a resistant, ultramature mineralogical suite.

Facies and environments of deposition

Lithofacies of marine shelf to near shore sedimentation comprise the four stratigraphic intervals of the Mughal Kot. The stratification, bed geometries, primary structures and fossils present are considered within a process - response model (Weimer, 1975) that is indicative of a specific depositional environment.

The lower 30 m of the Mughal Kot represent the first influx of detritus on the shelf following carbonate deposition (Parh Limestone). The thin-bedded to laminated nature of these shales suggests low-energy, possibly within an offshore marine - prodeltaic setting. The presence of marls

and micstones higher in this interval to the south suggests that the deposits at Drabber Pass were more proximal to the point of influx of terrigenous material into the area.

The overlying 60 m thick quartzarenite at Drabber Pass confirms the proximity of deltaic input. Ball and pillow load casts on the sole of this thick sandstone indicates rapid loading over saturated mud and subsequent syndepositional deformation. The lenticular stratification and large scale trough crossbedding persist vertically through the sequence at Drabber Pass. The sandstone thins and interfingers with low energy, inner shelf sediments to the south. The sandstone body displays features attributable to distributary channel - delta front sands. The presence of wood impressions further supports this marginal marine interpretation.

Shelf sedimentation resumes above the lower sandstone interval of the Mughal Kot. Bedding features visible in the thin sandstones and calcareous shales demonstrate limited ocean bottom currents. Horizontal trace fossils (*Scolicia*, chevron trails, etc.) characterize nearly all sand beds and are noted similarly to be abundant within shallow-water offshore facies by Howard (1972). The presence of marl and micstone interbeds are allied to shallow platform carbonate facies (Wilson, 1975). The uppermost portion of this middle interval becomes progressively less calcareous and slightly coarser-grained beneath the capping chaotic sandstone inter-

val again suggesting prodelta conditions with disseminated organic debris.

The chaotic nature of the uppermost Mughal Kot could have formed from subaqueous, soft-sediment slumping on a deep water submarine fan or on an oversteepened delta front. The presence of marginal marine sediments above and below the chaotic interval supports the latter slump origin. Estimates based on the examination of slumped sandstone beds point to west dipping (N75°W) paleoslope nearly perpendicular to present-day structural strike. Individual overfolded sands are typically detached, telescoping bodies exhibiting several convolutions within a disturbed shale matrix (see figure 10 and 11).

Stratigraphic and structural relationships

The Mughal Kot Formation conformably overlies the Parh Limestone in the study area. The Formation is uniform in its total thickness within this portion of the southern Pab Range although the subunits comprising the Mughal Kot change considerably laterally along the depositional strike.

Age and correlation

Williams (1959) stated that the entire Mughal Kot Formation appears to be of Maestrichtian age. Foraminifera observed by Williams belong to the genera, *Omphalocyclus* and *Orbitoides*. Thin section and scanning electron photomicrographs of some fossil tests present are illustrated in fig-

ure 12 (e and f).

Williams (1959) included the Fort Munro Limestone as a member of upper Mughal Kot. Although it does not occur in the Formation here, the middle marl-micstone units may be time-stratigraphic equivalents.

Pab Sandstone

Definition, distribution and thickness

The stratigraphy of the Pab Sandstone is the principal objective of this study. The unit is named for extensive exposures in the Pab Range of southeast Baluchistan. The type locality (Williams, 1959) is located along Drabber Dhora within the study area (topographic map series of Pakistan No. 35-O-2, Lat. 25°31'12" North, Long. 67°00'19" East). General descriptions of the Sandstone from the Laki Range date back to the early reconnaissances of Blanford during the late 1800s. Vredenburg (1906) was the first to formally apply the formational name.

The distribution and thickness of the Pab Sandstone along the Pab Range vary considerably. The Pab maintains a narrow outcrop belt from Naka Pabni in the south to Khuzdar though numerous faults disrupt the unit in the north. It thickens slightly just to the north then thins further north until it disappears south of Khuzdar. The writer measured a total thickness of 478 m for the Pab Sandstone at its type locality (figure 13), however Williams (1959) quoted thick-

FIGURE 12. Photomicrographs of Mughal Kot petrography and faunae

a. Lower Mughal Kot quartzarenite; note the algal fragment present. Bar scale is Ø.5 mm.
b. Scanning electron microscope (SEM) photo of algal fragment from the lower sandstone. Bar scale is 13Ø microns.
c and d. Crossed- and plane-polarized photomicrographs of volcanic rock fragment; the feldspar microlites exhibit pilotaxitic flow fabric. Scale is Ø.5 cm.
e. Scattered foraminiferan faunae of Mughal Kot Formation. Scale is Ø.5 cm.
f. SEM photo of globigerinid test. Bar scale is 7Ø microns.

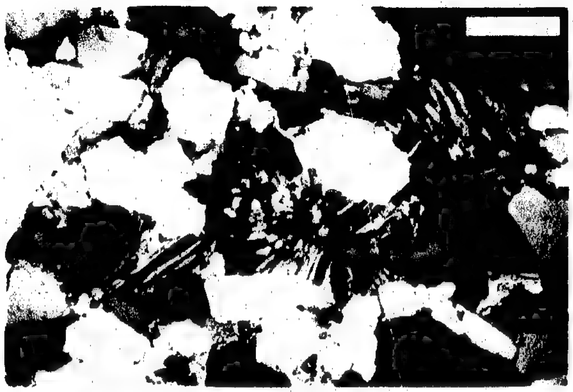

a

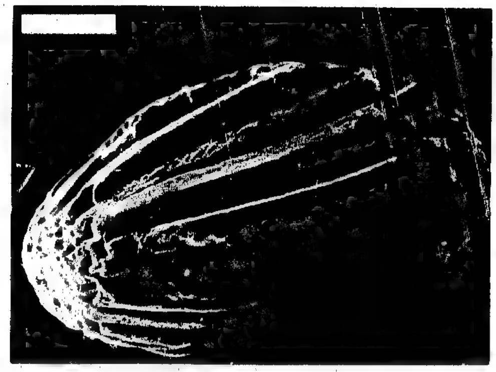

b

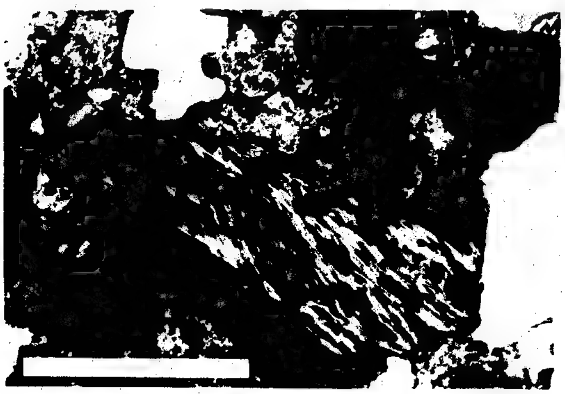

c

d

e

f

ness of 490 m. The difference may be attributed to possible errors in measurement due to a changing dip at the type locality and/or to the choice of the formational contacts. The unit thickens slightly to 498 m at Jakkher Pass 5 km south of the type locality, it thins, and finally pinches out near Naka Pabni 30 km to the south. Thin outcrops of the Pab occur at Haji Lakar and Ispaia between Naka Pabni and Karachi. The stratigraphy and structural settings of these exposures are unknown.

Lithology

The Pab Sandstone conformably overlies the chaotic slump overfolds of the Mughal Kot with up to 25 m of thin- to thick-bedded, coarse- to very coarse-grained sandstone interbedded with calcareous shale. Sandstone composition ranges from sublitharenite to litharenite. The admixture of volcanic fragments exceeds 30% in some beds. The light greenish gray (5GY6/1) sandstones display low angle planar and large scale trough cross-sets that are frequently obscured by bioturbation. Plate-shaped shale clasts up to 10 cm diameter are common on top of and in the sandstones. The shale clasts are similar in lithology to the interbedded mudstone.

The strata overlying the basal Pab sequence occur in cycles of interbedded sandstone and shale. The typical cycle consists of a basal shale interbedded with thin, hori-

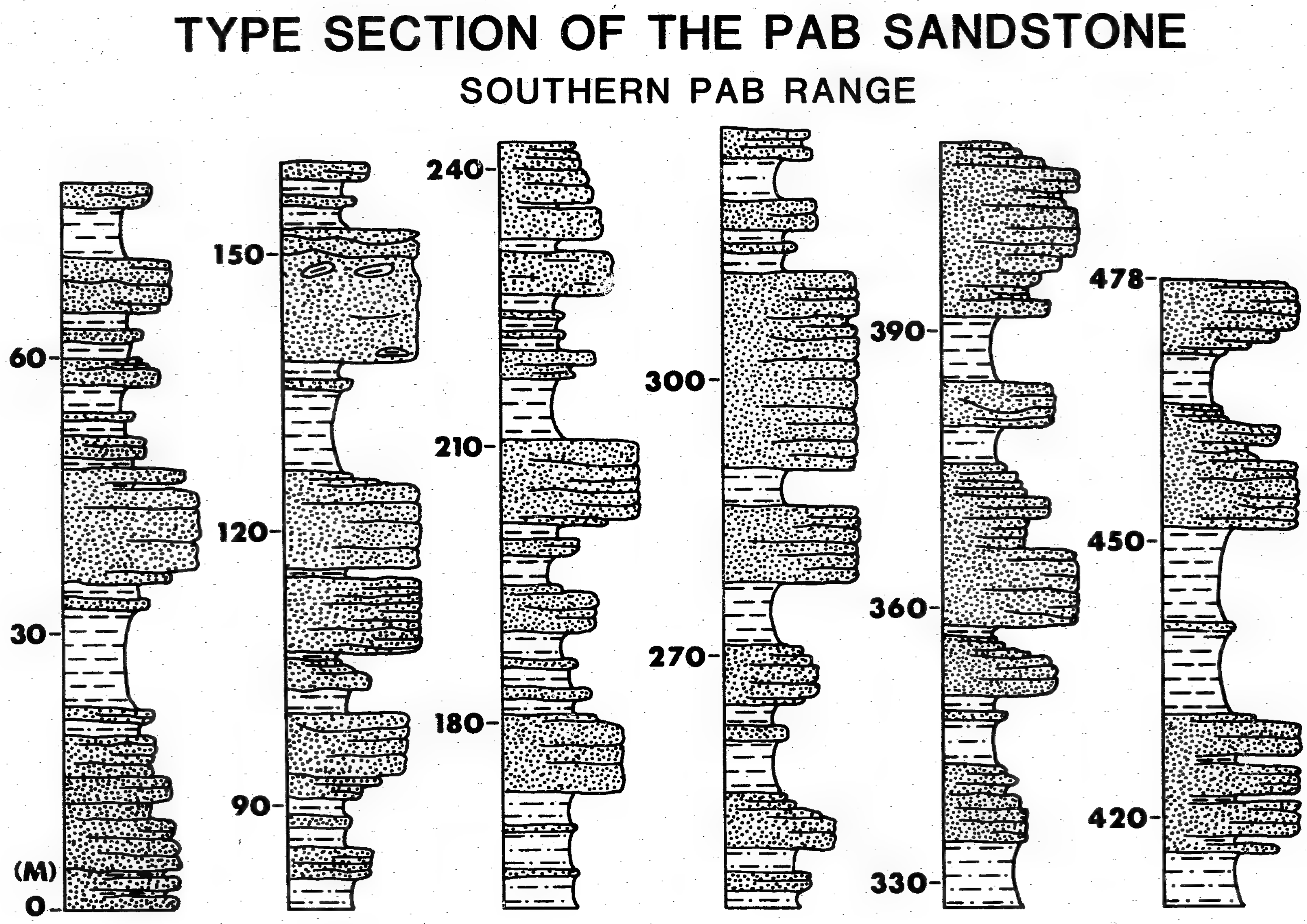

FIGURE 13. Type section of the Pab Sandstone

zontal- to ripple-laminated sandstones, followed by a sequence of sandstones which increase in thickness and grain size upward to a capping of thick-bedded to massive sandstone which exhibits faint large-scale trough crossbedding. Bed contacts within these stacked units are not gradational but nevertheless are interpreted by the writer to represent a genetic, depositional continuum. Thickness of these cycles ranges from 5 to 45 m, the average thickness being 20 to 25 m. The number of cycles recognized within each of the Drabber and Jakkher Pass sections is 20.

A composite section of the ideal Pab cycle (figure 14) begins with light olive gray (5Y6/1) to grayish olive (10Y4/2) claystone which abruptly overlies the preceding cycle. The indistinctly laminated to bioturbated beds contain occasional marl intercalations up to 10 cm thick and several meters long. Claystone thickness varies up to 15 m. Fine-grained sublitharenite interbeds can exceed 0.5 m but average less than 30 cm. The sandstones display sharp upper and lower surfaces, abundant trace fossils, horizontal lamination and shale clasts to 5 cm long. Trace fossils in the form of horizontal burrows and trails are common on the tops of sandstone interbeds and occasionally along their bases. Rare plant(?) debris also is found on the tops of thin sands.

The sandstone interbeds typically thicken vertically and dominate the middle of the unit. Silty to sandy mud-

COMPOSITE GRAPHIC SECTION OF PAB SEDIMENTATION UNIT

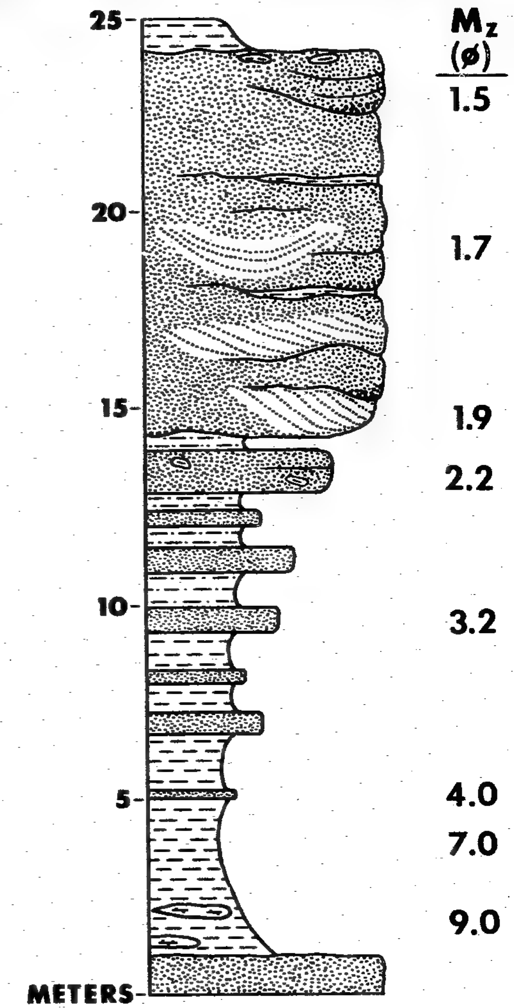

THICK BEDDED SUBLITHARENITES AND VOLCANIC ARENITES; MEDIUM GRAINED; FAINT LARGE SCALE TROUGH CROSSBEDDING; OCCASIONAL THIN SILTSTONE BREAKS; LEDGE FORMER.

THIN BEDDED SUBLITHARENITES, BECOMING THICKER AND COARSER GRAINED VERTICALLY; MUDSTONE INTERVALS COARSEN AND THIN; TRACE FOSSILS ON BASAL AND UPPER SURFACES OF SANDSTONES; MARLY INTERBEDS IN BASAL CLAYSTONE.

FIGURE 14. Composite section of cyclical Pab sedimentation sequence

stone occurs as thin (20 cm), often lensatic, intercalations. Coarse-grained sublitharenites commonly contain granular conglomeratic lenses up to 30 cm thick. Horizontal lamination is common but trough-crossbedded sandstones are observed. Again trace fossils occur on upper and lower sandstone surfaces.

Thick-bedded sandstones cap the ideal Pab cycle. The sandstones comprise the prominent ledges observed in the Pab Range. Colorwise the beds range from yellowish gray (5Y7/2) and pale olive (10Y6/2) to their distinctive weathered hues of light olive brown (5Y5/6) and moderate brown (5YR3/4). The sands exhibit only indistinct large-scale trough crossbedding in beds that frequently exceed 2 m in thickness. Bedded siltstones are intercalated within the sandstones. The beds are extremely persistent laterally with only local lenticular character. Rare abraded fauna and poorly preserved trace fossils are observed within the sandstones but cementation and weathering have all but obscured these plus bedding features. The geomorphic expression of the cliff-forming sandstones is quite pronounced compared to the underlying interbedded sandstones and shales of the Pab cycles. The interbeds typically form rubble-covered slopes.

The lithostratigraphy of one individual cycle has been studied in detail for comparison with the ideal, composite section. The cycle is 12 m thick and begins 180 m above the base of the Pab Sandstone in Drabber Pass. The graphic sec-

tion of the profile showing lithologies and compositional data is given in figure 15.

The interval (figure 16a) begins as shale interbedded with thin-bedded sandstones. The grayish olive (10Y4/2) to light olive gray (5Y5/2) claystone is bioturbated to indistinctly laminated. Similarly sandstones in this lowest interval range from less than 5 cm to 25 cm in thickness (figure 16b). The sandstones show horizontal to ripple lamination and display two features characteristic of the sands below the thick capping sand, namely, locally abundant shale clast accumulations and a horizontal trace fossil assemblage along upper and lower surfaces. The rip-up clasts are well-rounded disc and plate shapes, up to 10 cm long and 2-4 cm thick (figure 16c), but show no preferred orientation in outcrop. The trace fossils are mostly branching feeding trails (figure 16d). A reed-like plant impression (figure 16e) was also observed.

The middle part of the cycle consists of lenticular sandstones to 0.5 m thick and subordinate mudstone interbeds. The grayish olive (10Y4/2) sandstones horizontally laminated coalesce laterally over a distance of 15 m. Larger mudclasts up to 20 cm long and 5 cm thick occur in the sandstones and usually display soft-sediment deformation. The shale interbeds which occur up to 30 cm thick include two thin (less than 5 cm) marl bands containing a Late Cretaceous foram fauna.

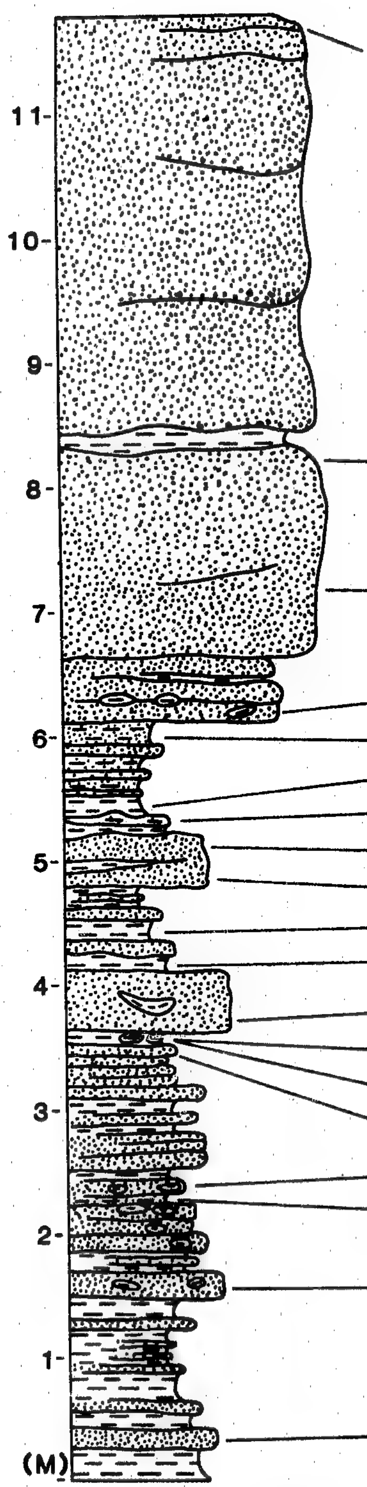

SAMPLE	COMPOSITION	MEAN (Ø)
Pb-DP-39-8d	Sublitharenite	1.71
Pb-DP-39-8c	Sublitharenite	1.94
Pb-DP-39-8b	Sublitharenite	1.91
Pb-DP-39-8a	Sublitharenite	2.75
Pb-DP-38-7h	Mudstone	7.85
Pb-DP-38-7g	Claystone	8.60
Pb-DP-38-7f	Micstone	
Pb-DP-38-7e	Sublitharenite	2.06
Pb-DP-38-7d	Sublitharenite	2.29
Pb-DP-38-7c	Claystone	8.33
Pb-DP-38-7b	Claystone	8.30
Pb-DP-38-7a	Sublitharenite	1.80
Pb-DP-38-6f	Sublitharenite	2.71
Pb-DP-38-6e	Volcanic Arenite	4.27
Pb-DP-38-6d	Sublitharenite	3.64
Pb-DP-38-6c	Sublitharenite	2.06
Pb-DP-38-6b	Volcanic Arenite	2.75
Pb-DP-38-6a	Sublitharenite	1.83
Pb-DP-37-5	Sublitharenite	2.18

FIGURE 15. Characteristics of a single Pab cycle studied in detail

The basal surface of capping, thick-bedded sandstone demonstrates only 5 to 1Ø cm of local relief overlying the middle portion of this cycle. The first half meter of sandstone comprises three sand beds, the lowest of which contains abundant shale rip-up clasts. The remaining 7 m is divided into two thick-bedded sandstones by a poorly bedded siltstone less than 2Ø cm thick (figure 16f). The yellowish gray (5Y7/2) to pale olive (1ØY6/2) sandstones weather light olive brown (5Y5/6) to light olive gray (5Y5/2). Indistinct broad low-angle trough crossbedding can be discerned on weathered outcrop of the capping sandstones. Estimates of trough-axis orientations trend in a westerly direction. Significant variations of the axes to the north and south however suggest frequently shifting current directions.

Textural parameters of nineteen Pab sandstones are listed in Appendix B, all but a few belonging within the cycle just described. Sieve-connected data from grain-size measurements in thin section follow the nomograph of Friedman (1958) for statistical comparison with mechanical analyses of shale samples. The scattering of sandstone samples, representing each interval of the ideal Pab profile, average 2.36 phi (Ø.19 mm) mean grain size with a sorting index of Ø.78 phi (moderately sorted). All but one sample contained sufficient volcanic rock fragments to statistically compare mean grain size and sorting indices between quartz and volcanic detritus:

FIGURE 16. Photographs of the Pab cycle studied in detail

a. View of cycle in Drabber Pass.
b. Lower shale-dominated portion of cycle. Scale is 30 cm long.
c. Thin- to medium-bedded sandstones with rip-up shale clasts in central part of cycle.
d. Trace fossil feeding trails along upper and lower sandstone surfaces.
e. Reed-like plant fragment on upper surface of thin-bedded sandstone.
f. Thick-bedded sandstone capping this Pab cycle.

a

b

c

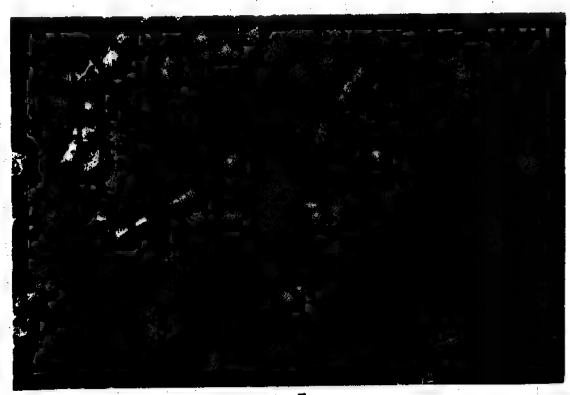

d

e

f

	Mean		Sorting
	Phi	(mm)	Phi
Quartz	2.29	(Ø.2Ø)	Ø.84
Volcanics	2.18	(Ø.22)	Ø.59

The volcanic admixture is consistently slightly larger in grain size and better sorted than the dominant quartz population sampled. Sphericity and roundness parameters are also higher in the rock fragments; an observation attributable to the more easily abraded volcanics during aqueous transport. The provenance for the rock fragment is inferred to have been comparatively close as suggested by the larger grain size.

Textural parameters of shale samples are given in Appendix B. Very poorly sorted claystones characterize all but one of the Pab samples. Grain size distribution of the shales is near-symmetrical to coarsely-skewed and platykurtic. As demonstrated by the textural data listed for the profile in figure 15, the Pab cycle coarsens upward.

Thin section petrography for selected Pab sandstones is cataloged in Appendix D. The quartz (Q) - feldspar (F) - rock fragment (R) average calculated is 83:1:16. Thus, the sandstones may be classed as sublitharenite (Folk et al., 197Ø). When considering total thin section petrography, the Pab sandstones average 66% detrital grains in a framework cemented dominantly by calcite with clay minerals. Only one

sample was cemented by silica.

Quartz grains dominate the detrital mineralogy (figure 17a). The fragments are largely single crystals with planar to strongly undulose extinction. Polycrystalline and composite grains are observed from trace to minor amounts and exhibit the same moderate to high sphericity and roundness. Rutile needles and vacuole trains are common inclusions within quartz particles.

Feldspar components continue to be trace constituents in the Pab Sandstone above the upper Mughal Kot. Sand-sized grains observed in thin section show alteration sufficient to render the grain nearly unrecognizable. Calcite and clay minerals occur within and around the feldspar. Twinned plagioclase grains are noted more often than orthoclase or microline. The presence of detrital feldspar is noted in direct correlation with abundant volcanic rock fragments. Quartzarenites of the lower Mughal Kot do not contain the trace feldspar component suggesting possible kindred source terrains with the volcanic rock fragments.

The volcanic rock fragment fraction persists throughout the Pab Sandstone comprising up to 28% of the thin sections analyzed. Textural and mineralogical features (figure 17b) are similar to the greater accumulation in the upper Mughal Kot. Though measured microlite composition suggests a possible andesitic terrain, several fragments display a recognizable flow structure with the alignment of microlites

attributable to flow as trachyte basalt (Dr. Basil Booth, University of London, Birkbeck College, personal communication, 1980) (figure 17c and 17d). Generally the volcanic rock fragments are well-preserved but occasionally show clay mineral/iron oxide alteration or grain coating especially when the fragments are fine sand to silt sized. The origin of this component will be more fully discussed in a later section. Chert rock fragments (figure 17f) occur in trace amounts. The microcrystalline grains are interpreted to be chert though the possibility remains that they may be fragments of rhyolitic volcanics.

The heavy mineral assemblage listed in Appendix F is similar to that of the Mughal Kot with zircon, tourmaline, and rutile plus trace amounts of magnetite. Varieties superficially matching optical properties of sphene were subsequently identified by x-ray powder camera to be zircon. Hematite- and leucoxene-coated grains are abundant in the heavy mineral separates. The averge ZTR index is 67:28:5, indicating a slightly more mature sediment than the suite extracted from the Mughal Kot. Zircon grains generally display high sphericity and roundness. Tourmaline fragments, on the other hand, show characteristic hexagonal cross-sections. Dravite is the only tourmaline variety identified in diffraction patterns. Elongated rutile grains show abrasive rounding and traces of cleavage on grain facets.

Matrix materials, identified in thin section and/or

x-ray diffraction, include calcite, clay minerals and occasionally alacime. Calcite crystals occur from very fine-grained size to optically continuous mosaics surrounding many quartz/volcanic grains. A carbonate staining technique (Dickson, 1965) incorporating alizarin red and potassium ferricyanide creates a reddish blue stain suggesting the calcite cement to be ferroan. No dolomite rhombs in thin section or identifiable x-ray diffraction peaks from whole rock analysis were found. Analcime infrequently occurs in minor but recognizable amounts in the matrix of sandstones containing a large admixture of volcanic rock fragments and are inferred to be genetically related.

Clay minerals identified by x-ray analysis from the sandstone matrix as well as shale interbeds of the Pab include kaolinite, chlorite and illite. Silica overgrowths were observed in only one sample, Pb-JP-94c (figure 17f). Appendix E lists mineralized components recognized from x-ray diffraction patterns of pulverized whole-rock samples. Qualitatively, chlorite dominates in strata containing high amounts of volcanic rock fragments while illite and kaolinite are pervasive and locally significant. The greenish hue of the Pab Sandstone in outcrop is probably due to chlorite. An x-ray peak at approximately 23 to 24 angstroms suggests that portions of the chlorite and kaolinite minerals may occur interlayered rather than in a more common random mix. Trace components identified in thin section include glauco-

FIGURE 17. Photomicrographs of Pab Sandstone petrography

a. Quartz granule exhibiting composite crystallinity and undulose extinction. Bar scale is Ø.5 cm.

b. Shale clast and volcanic rock fragment in very poorly sorted framework; note reaction halo surrounding sedimentary clast. Scale is Ø.5 cm.

c and d. Crossed- and plane-polarized photos of a large, well-preserved volcanic fragment. Scale is Ø.5 cm.

e. Quartz volcanic rock fragments and chert in a calcite-dominated matrix. Scale is Ø.5 cm.

f. Quartz overgrowths filling pore space; note dust rims outlining original detrital grains. Bar scale is Ø.5 cm.

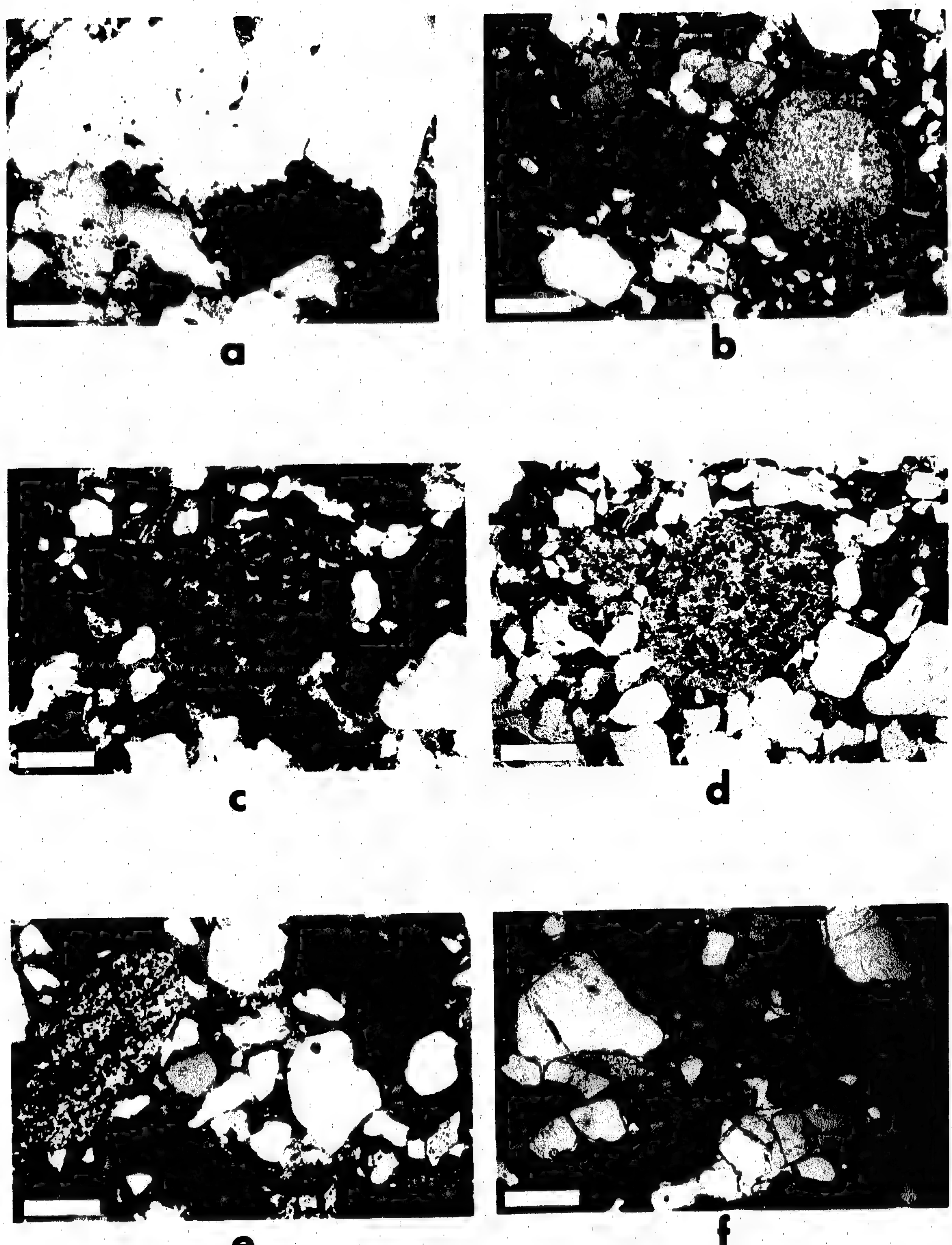
a
b
c
d
e
f

nite grains and occasional fossil fragments, possibly foraminifera or gastropod mollucs.

Facies and environments of deposition

The Pab Sandstone in the southern Pab Range consists of repetitive intervals of shale and thin- to thick-bedded sandstone. The unit is cyclic in origin; and, as such, its type locality is divisible into at least twenty cycles. Each cycle begins as a shale-dominated unit and is capped by a geomorphically-prominent sandstone (figure 14). Three lithofacies are recognized within each cyclothem of the Pab Sandstone. These and their corresponding depositional environments are:

1) Olive gray shale lithofacies: lower offshore marine shelf deposition,

2) Interbedded bioturbated siltstone and thin-bedded sandstone lithofacies: upper offshore - lower shoreface transition zone, and

3) Thick-bedded, trough cross-stratified sandstone lithofacies: shoreface environment.

Figure 18 graphically illustrates this sequence of environments within the ideal Pab cyclothem.

The initial lithofacies of the coarsening upward pro-

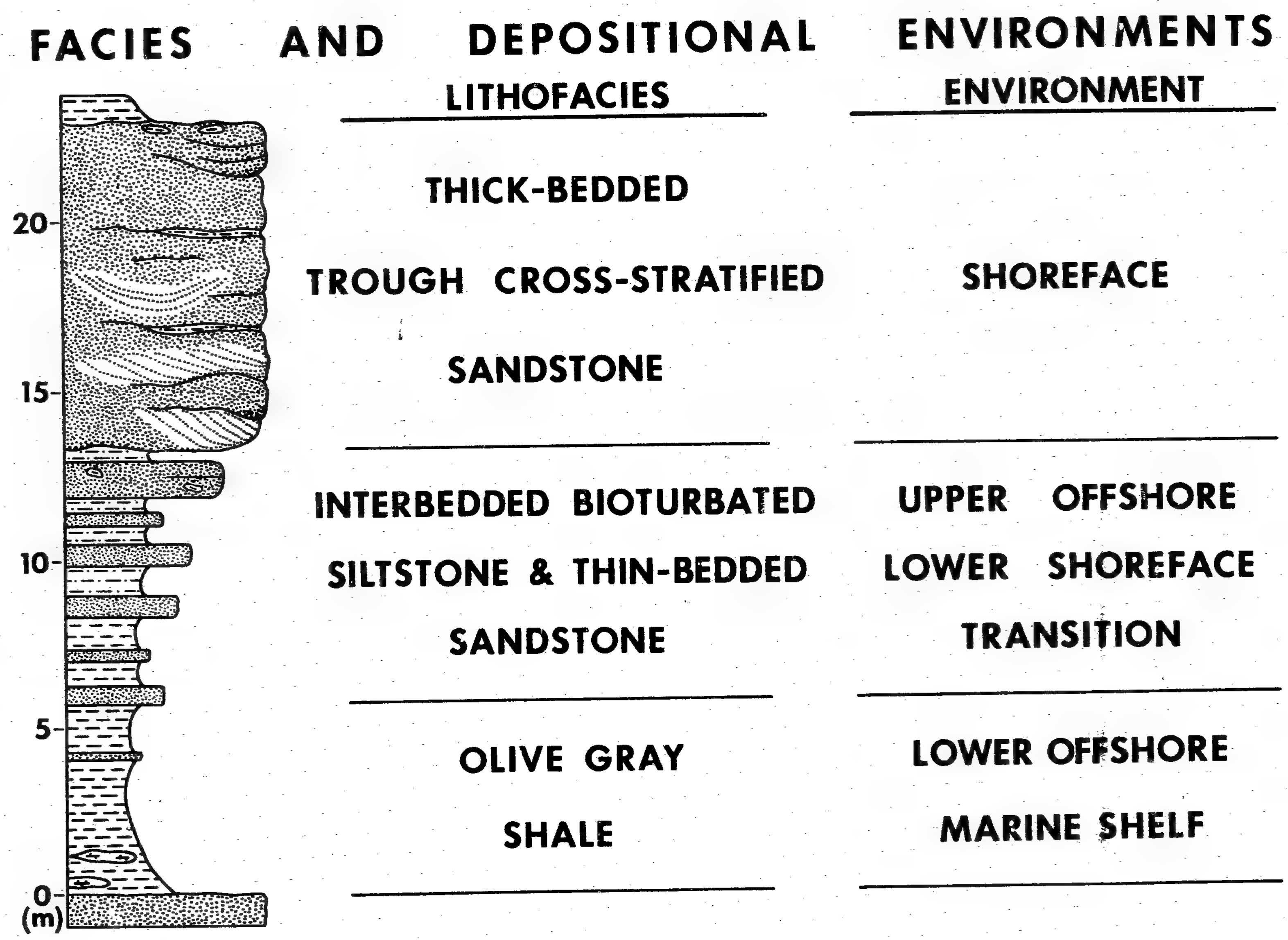

FIGURE 18. Pab lithofacies and depositional environments

file is an olive gray shale containing infrequent thin sandstone interbeds and marly lenses. The gray shale, often deeply weathered and rubble-covered, is up to 7 m thick (figure 19a). Claystone dominates the lithology and may grade to silty mudstone interbedded with thin sandstones. The sandstones are bioturbated and contain occasional trace fossil feeding trails along sharp upper and lower surfaces.

Ryer (1977) attributes the above characteristics of the olive gray shale lithofacies to deposition on a lower offshore marine shelf. The physical characteristics of the shale require only a comparatively low energy environment which would be found offshore of shoaling breaker waves approaching the shoreline. The granular fracture of the shales may be a response to thorough bioturbation which destroys laminations and other primary sedimentary structures as suggested by Byers (1974). The sandstones present represent the occasional influx of coarser detritus due to storm activity or transition to the higher energy regime of the overlying environment. Depths in this offshore setting are sufficient to be below normal wave base while sedimentation rates are slow enough for extensive organic activity (figure 19b). Fossil remains are rare in the shale. Their scarcity may be attributable to inhospitable bottom conditions and/or to lack of adequate exposure for representative sampling.

The olive gray shale lithofacies grades into the over-

lying interbedded bioturbated siltstone and thin-bedded sandstone lithofacies. The interbedded silts and sands range in thickness up to 1Ø m though complexes of 5 m are typical. The frequent occurrence of sandstone and coarser shale fraction contrast with the underlying claystone indicating an increased energy regime closer to the source. The shales are generally coarser however variations from claystone to sandy siltstone occur. Bioturbation is prevalent but, as below, faunal remains are rarely observed. The marly micstone lens, described from the profile in the previous section, contains a globigerinid foram population but no macro-invertebrates.

Thin- to medium-bedded sandstones, up to 5Ø cm thick are common in this lithofacies. Basal contacts are sharp as are generally upper surfaces though evidence of bioturbation in the upper few centimeters is common. Trace fossils occur along upper and lower surfaces. Planar lamination, interrupted occasionally by trough cross-sets, is the primary sedimentary structure. Abundant shale rip-up clasts to 1Ø cm long commonly pack these sandstones. The clasts display no imbrication but occasionally, as in figure 19c, clast deformation is observed which is attributable to deformation of the soft sediment either during erosion, transport and/or deposition.

An upper offshore - lower shoreface transition zone is the depositional environment suggested for this lithofacies.

The environment is one of shallower water depths and greater proximity to breaking waves further shoreward. Physical characteristics observed here match those of recent sediments in an upper offshore transiton position of the Georgia coastline studied by Howard and Reineck (1972).

The sandstones within this transition zone are due to storms which result in the transportation of sand offshore into the shallow marine environment. Parallel lamination is the most commonly observed primary sedimentary structure. No hummocky cross-stratification as described by Harms, et al., (1975) was observed. Ryer (1977) mentions the presence of mudclasts in similar sandstones and attributes their origin to have been cohesive lagoonal muds which were eroded and transported by laterally-migrating tidal creeks, as originally proposed by Howard and Reineck (1972). Goldring and Bridges (1973) have also noted lenticular sands resulting from storm tides bringing sand offshore via rip currents. In Ryer's study, these sandstones were assigned to a subfacies of the offshore - shoreface transition interfingering with the bioturbated siltstone and sandstone lithofacies. Such a distinction is not warranted here; therefore the beds are incorporated into one transition zone.

The capping lithofacies in the Pab cyclic sequences is the thick-bedded trough cross-stratified sandstone lithofacies representing deposition within a high energy shoreface environment. The facies overlies the interbedded profile

with sharp, slightly irregular, although conformable contact. Relief on this surface rarely exceeds one meter and no major erosional ravinements (Ryer, 1977) into the underlying lithofacies occur in the sections measured. Thicknesses of these prominent sands vary from less than 5 m to a stacked sequence of over 35 m probably representing two or more shoreface episodes. The shoreface environment is the highest energy zone of shoreline sedimentation. Large scale trough cross-bedded sets occur in beds to 3 m thick (figure 19d) though the crossbedding is generally poorly displayed. Indications of Ophiomorpha-like ichno-fossils are also present as are occasional lenses of granule-sized gastropod fragments. Abundant truncation surfaces within the sandstone attest to a rapidly shifting current pattern in the environment (figure 19e).

Ryer (1977) compares his observations in ancient shoreline profiles with those of Clifton, Hunter and Phillips (1971) on recent beach and nearshore processes active along the high energy Oregon coastline. Clifton et al., (1971) recognize an "upper surf zone, inner rough facies" with the same shoreface characteristics as described for the Pab. Water depths of only Ø.5 to 1.5 m are encountered in this modern analog. Apparently only high energy coastlines produce sufficient wave-dominated surf zones to produce large scale trough crossbedding (i.e. compared to ripple drift lamination produced by the much lower wave energy of the

Georgia coastline, Howard and Reineck, 1972). Accordingly, the dynamics of Pab deposition may also have been very energetic (figure 19f).

The sequence of depositional environments represented by the cyclic Pab Sandstone records coarsening-upward sedimentation in an increasing energy regime from offshore through surf zone marine environments. In the following section, a depositional model for the shoreface cycles will be discussed in context of an overall depositional history during Late Cretaceous time on this portion of the Tethyan shelf.

Stratigraphic and structural relationships

The Pab Sandstone conformably and transitionally overlies the Mughal Kot Formation in the southern Pab Range. Because the name Mughal Kot had not been officially extended into the Kirthar Province, the basal contact of the Pab in the type locality is here defined as the base of the first prominent sandstone package above the chaotically slumped sandstone/shale interval of the upper Mughal kot. This contact is similarly recognized in the Jakkher Pass section to the south though the transitional continuity of the two formations does not allow easy differentiation on aerial photographs.

Structurally, the strata of the Pab strike generally north-south and dip 20° east though significant local varia-

FIGURE 19. Photographs of Pab lithofacies

a. Cyclic Pab Sandstone exposed in type locality.
b. Trace fossil trails on surfaces of thin-bedded sandstones.
c. Deformed rip-up clasts in medium-bedded sandstone.
d. Trough crossbedding in thick-bedded sandstone.
e. Truncation surfaces in thick-bedded shoreface sandstones.
f. Thick development of capping shoreface sandstone.

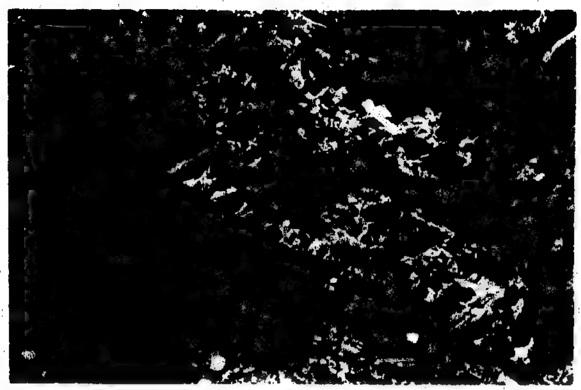

a

b

c

d

e

f

tion has been noted. Two subvertical joint sets control drainage across the range, namely N23°E and N67°W changing in the upper Pab Sandstone to N5°E and N85°W (the latter being the dominant direction). From the geometry of the Pab shoreface cycles and interpreted paleogeographic setting, the present strike of the Pab Sandstone roughly parallels the depositional strike of the ancient Tethyan shoreline.

Age and correlation

Fauna is conspicuously absent from the Pab Sandstone. Unidentifiable gastropod fragments are present in coarse-grained lenses within the trough cross-bedded sands. Globigerinid forams observed in thin section can only provide a general date of Late Cretaceous. The fauna present is too sparse to be more specific (Dr. Bruce Masters, Amoco Research, personal communication, 1981). Invertebrate faunal assemblages both below and above the Pab help to bracket the Pab as being mostly, if not wholly, Maestrichtian in age.

Field studies by Pryor et al., (1979) suggest that the Pab Sandstone in the Sulaiman Range is composed of a series of stacked shoreface cycles. The age of the Pab in the Sulaiman Range is also Maestrichtian. Equivalent marls and thin-bedded limestone in the lower part of the Moro Formation occur between the principal exposures of the Pab Sand-

stone.

Khadro Formation

Name, distribution and thickness

The Hunting Survey Corporation (1960) introduced the name Jakkher for a predominantly shale sequence overlying the Pab Sandstone in the southern Pab Range. Subsequent redefinition by Williams (1959) and the Geological Survey of Pakistan (Shah, 1977) has assigned the name Khadro Formation to the lower Jakkher sediments. The Khadro is the basal unit of the Ranikot Group that outcrops extensively in the Sind Province. Only a few meters of the basal Khadro overlying the Pab Sandstone were studied in detail in order to characterize the contact with the Pab and the change in depositional environment.

Lithology

The lower 20 m of Khadro consist dominantly of shale (figure 20a). The shale is light olive gray (5Y5/2) to grayish olive (10Y4/2) claystone which weathers dusky yellowish green (5GY5/2). The claystone fractures into minute granules and shows no fissility, suggesting extensive bioturbation (Byers, 1974). Mineral components determined by x-ray analysis (Appendix E) include quartz, varying amounts of calcite (with some beds of marl being present), minor to trace amounts of feldspar, major to trace amounts of kaolin-

ite, chlorite and illite.

Interbedded sandstones vary from 1 cm to 1 m in thickness however they are usually less than 10 cm. The grayish brown (5YR3/2), fine-grained sandstones occur from 15 to 30 cm apart throughout this basal sequence. Ripple to horizontal lamination (figure 20b), abundant horizontal trace fossils, and sand- to granule-sized shale clasts characterize the sandstones. A one meter thick lenticular sandstone along Jakkher Dhora contains a fragmented molluscan assemblage (figure 20c). Compositionally the sandstones are sublitharenites similar to the Pab with the same persistent volcanic admixture (Appendix D). A single heavy mineral separation is predominantly zircon with trace tourmaline and rutile (Appendix F).

One interesting feature of the Khadro is the presence of concretionary bodies which increase vertically in diameter (figure 20d). The composition is dominantly silt-sized quartz in calcite with minor amounts of feldspar and a trace of clay minerals. The concretions display finely disseminated organic plant(?) fragments and isolated biserial forams in thin section. The origin of the features remains unclear.

Lithofacies and depositional environments

Low energy, quiet water deposition is suggested for the shale-dominated lower Khadro. The extent of bioturbation in

the shale supports the inference that the depositional environment was a shallow marine inner shelf (offshore marine) which received a periodic influx of sand. Except for the thicker, coarser sandstones, containing abraded mollusc fragments, the sandstones were deposited under low, low flow regime conditions (ripple to horizontal lamination). The thicker lenticular, sandstones may be storm sheet sandstones similar to those discussed by Goldring and Bridges (1973) and which were brought offshore by rip currents and were subsequently burrowed during quieter interludes. The character of the remaining Khadro does not contain sandstone interbeds and is not bioturbated suggesting increasingly deeper water conditions.

Stratigraphic and structural relationships

Williams (1959) states that the contact between the Pab Sandstone and Khadro Formation is unconformable at the type locality to the east in the northern Laki Range. However the Pab and Khadro are conformable in the Pab Range. Local folding occurs in the lower portion of the Khadro because of the abundance of incompetent shales.

Age and correlation

Blanford (1878) first named the strata equivalent to the Khadro, the *Cardita beaumonti* beds, because of the rich molluscan fauna present and the dominance of *C. beaumonti*. The molluscan and associated microfauna indicate a Danian

age (Paleocene) for the Khadro. The abraded gastropod tests concentrated in the sandstone of the lower Khadro probably are part of Blanford's molluscan assemblage.

Hunting Survey Corporation (1960) defined the Jakkher Group (now Khadro Formation) as the strata between the Pab Sandstone and Nari Formation south of latitude 25#50' in the southern Pab Range. The proportion of limestone increases to the south. There the upper and lower contacts of the Khadro are reported to be conformable. Two basalt flows are interbedded in the basal Khadro at its type locality in the Laki Range (Shah, 1977) while conglomeratic equivalents at Thar in the northern Pab Range include volcanic, plutonic and sedimentary clasts including jasper.

Middle Tertiary Limestone

Definition, distribution and thickness

Limestone, outcropping in "Anero Anticline", was originally believed to be Middle to Late Jurassic in age (Hunting Survey Corporation, 1960). Two isolated hills of this limestone were visited by the writer for sample collecting. Thin section analysis of the samples reveals a diverse foraminiferal assemblage. The faunae were subsequently identified by Dr. Bruce Masters (Amoco Production Research Company, personal communication, 1981) to be Late Eocene to possibly Miocene in age. Consequently, the strata are described here under the heading of Middle Tertiary. Less

than 1ØØ m of this limestone is present in the isolated outcrops.

Lithology

The light yellowish gray (5Y8/1) limestones are horizontally laminated to thin-bedded with few beds exceeding 2Ø cm in thickness (figure 2Øe). They consist of moderately well-indurated packstone to grainstone. Foram tests vary from 5ØØ microns to less than 5Ø microns in diameter. Detrital, silt-sized quartz is a trace constituent. Microgranular calcite cement fills intergrain pore space as do local patches of detrital lime mud. Carbonate staining indicates part of the calcite cement to be ferroan. Skeletal fragments stain red (calite). Detrital lime mud also fills occasional foram tests.

Interbedded with the foraminiferal grainstones are thicker beds of micstone consisting of lime mud, fine silt-sized organic debris and occasional forams. The limestone is chalky and friable in hand specimens. X-ray analysis reveals minor to trace quartz, illite and kaolinite.

Facies and environment of deposition

The grainstones and packstones more frequently appear as mixed species of forams and other skeletal fragments, but occasional beds of predominantly one foram type, e.g. globerinid are common. No megafossils were observed in outcrop or thin section. The tests identified by Dr. Masters

include the large Eocene benthonic forams (<u>Discocyclina</u> and <u>Nummulites</u>) and Middle Tertiary (Miocene?) planktonic forams (primarily globigerinids and unkeeled and occasional keeled globorotalids) (figure 20f). The fragmented bentonic tests suggest rapid, vigorous transport possibly into deeper water and where they were mixed with the associated planktonics. A clearer picture of the depositional environment must await firmer age control and a re-interpretation of the strata's structural setting.

Stratigraphic and structural setting

The gently inclined strata are interpreted to be faulted against lower Cretaceous strata in Kanraj Valley (figure 4). Given a Late Eocene or Miocene age, the strata should have been involved in Late Neogene orogenic uplift and folding. It is conceivable that an arm of the retreating Miocene sea occupied the valley but is seems equally fortuitous that this outcrop is the only one remaining today. Rather the writer suggests that the Middle Tertiary limestone is situated on a tilted fault block rotated by Himalayan thrust faulting that reactivated thrusts initiated during Paleocene ophiolite obduction.

Age and correlation

The Late Eocene to Miocene age of the strata is tentative. Formations containing similar limestones of this age include the Khude Limestone, described locally as a foramin-

FIGURE 2Ø. Photographs of the Khadro Formation and the Middle Tertiary limestone

a. Exposures of the Khadro Formation at the head of Jakkher Pass; reef carbonates of the Eocene Kirthar Formation overlie the Khadro to the east.
b. Parallel and ripple lamination in thin-bedded Khadro sandstones.
c. Abraded gastropod concentrate in the Khadro sandstone.
d. Vertical concretionary bodies in the basal Khadro Formation.
e. Thin-bedded carbonates of the Middle Tertiary Limestone in Kanraj Valley.
f. Photomicrograph of the foraminiferal packstones of the Limestone. Bar scale is Ø.5 cm.

a


b


d



c


e


f

iferal grainstone (Hunting Survey Corporation, 1960). The Khude Limestone has been renamed the Nisai Formation by the Geological Survey of Pakistan (Shah, 1977).

DEPOSITIONAL HISTORY OF THE NORTHWESTERN SHELF OF THE INDO-PAKISTANI SUBCONTINENT

The stratigraphy of the southern Pab Range records the progressive shallowing of the Indo-Pakistani continental shelf. The discussion of the depositional history which follows combines the regional stratigraphic summaries of Hunting Survey Corporation (1960), Rahman (1963) and Shah (1977) with the environmental interpretations of the previous section of this report.

Jurassic

The Jurassic was a time of widespread sedimentation on the continental shelf. Facies grade from thin, fluvial and shoreline clastic deposits in the region of Cutch (the Umia and Catrol formations described by Pascoe, 1950), through interbedded clastic shelf deposits buried beneath the Indus Plain, to carbonate facies on the outer continental shelf. Early Jurassic carbonates in the Mor Range comprise the Springwar Member of the Shirinab Formation (figure 6). Geologists of the Hunting Survey Corporation (1960) interpret the limestone to have been deposited on a platform created by initial uplift of the Axial Belt. The uplift on the continental margin may be related to Cretaceous volcanic arc development. Middle Jurassic, deep water radiolarian limestone formed to the east of the platform (Lorali and Anjira

members of the Shirinab). Equivalent oolitic and biohermal limestone comprise the lowest strata of the Chiltan Limestone further to the east.

A major regression during the Callovian resulted in the emergence of the Indo-Pakistani shelf. The regression may have been in response to Gondwanaland fragmentation. Transgression occurred again in the Late Jurassic initiating another episode of marine shelf sedimentation. The Hyderabad and Sanjawi arches may have been initiated in the Jurassic but did not significantly influence sedimentation.

Cretaceous

Lower Cretaceous shales of the Sembar and Goru formations accumulated on the continental slope and outer shelf. The marls and micstones in the overlying portion of the Goru attest to the progressive shallowing of the shelf sea during Aptian time.

The Parh Limestone forms a prominent carbonate facies of Albian age. Hunting Survey Corporation (1960) suggested that the Parh initially developed as shallow-marine deposits on the eastern flank of the aforementioned volcanic arc and subsequently built eastward toward the Indian shoreline. The thin-bedded foraminiferal packstones comprising the Parh in the study area have been interpreted to constitute a restricted back-reef carbonate facies. The basal relief previously noted on the Parh-Goru contact may represent ini-

tial infilling on the shallow depositional surface.

A different depositional scheme has been inferred for a similar Sembar - Goru - Parh sequence in the Sulaiman Range to the north (Dr. Wayne A. Pryor, University of Cincinnati, personal communication, 1979). The formations comprise a depositional succession from continental slope facies (Sembar) through upper slope - outer shelf facies (Goru) to inner shelf facies (Parh). The sequence records deep to shallow water sedimentation gradually building westward over the continental shelf. The Sembar - Goru - Parh strata of the study area support a similar deep to shallow depositional scheme. Hunting Survey Corporation (1960) noted lateral stratigraphic thickening of the Cretaceous Parh Series away from the Axial Belt. This bounding effect may have acted to pond sediments which further promoted shallow marine environments. Noted also was a maroon coloration in the basal Parh Limestone of the study area. The colors were attributed to the proximal volcanic activity of the Axial Belt resulting in "ferriginous-enriched" marine waters penecontemporaneous with deposition. However, the maroon color in the Parh is only locally pervasive, and cuts across bedding planes; therefore, it is concluded to be secondary.

Upper Cretaceous strata are dominated by two clastic successions, namely, the Mughal Kot and Pab formations. The depositional histories of these units are of primary concern to this report as they represent the first major influx of

terrigenous sand to have prograded across the Tethyan continental shelf and to reach its western limits. This voluminous influx of sand suggests uplift in the Indian Shield source area. Hunting Survey Corporation (1960 p. 65), which included the Mughal Kot in the Pab Sandstone, recognized the significance of this clastic influx.

> The Pab Sandstone in the Late Cretaceous marked the first great invasion of the geosyncline by clastic sediments and signalled a progressively greater direct influence of the land margins on the sedimentation. Prior to the Pab, such influences were practically confined to the geosynclinal margins as in the regions of Jaisalmer and Cutch where the whole Cretaceous assemblage is relatively thin and of estuarine, deltaic, and fluviatile origins.

The first sandstones occur in the distributary channel complex in the lower Mughal Kot Formation. Ball and pillow structures at the base and bedding truncation surfaces within the sandstone body indicate rapid deposition by shifting sand bars. Measurements of trough crossbedding axes indicate a westerly flow in the channel. Other similarly-positioned sandstones occur in the lower Mughal Kot to the north and south of the study area and may have been part of a much more extensive stream network. Subsurface information on equivalent strata to the east is not available, however it is conceivable that the streams flowed across a wide alluvial plain. The coastline was positioned much farther west than previously in the Cretaceous.

Shale-dominated sediments overlying the sandstone mark

a return to open marine shelf deposition. The shale sequence is interrupted by thin beds of sand which were flushed into the area possibly during severe storms. Micstone beds attest to the comparatively low energy deposition of this middle interval.

The upper Mughal Kot displays a second episode of deltaic sedimentation in the study area. Unique to this interval are chaotically slumped sandstones in a disturbed shale matrix. The slumps are inferred to have formed on oversteepened delta front slopes.

Gravity slumping occurs within a continuum of deposits formed by mass-gravity transport processes; the deposits range from olistostromes to turbidites (Rupke, 1978). Most literature on slump deposits describes features from submarine canyon - continental slope settings (e.g. Helwig, 1970; Kleist, 1974). Submarine slumps are known to occur on marine delta slopes (Roberts, 1972; Weimer, 1973) but Holocene examples have been several orders of magnitude larger than the slump folds in the upper Mughal Kot. Small-scale features characteristic of soft-sediment folds are generally restricted to a particular stratigraphic interval and include pinch and swell (figure 21a), pull-apart terminations (figure 21b), and boudins with rounded terminations (figure 21c and d) (Kleist, 1974). Shales commonly show shearing (figure 21e). Exotic blocks may also be incorporated such as the rounded micstone cobble in figure 21f.

Woodcock (1976; 1979) stresses the importance of tight, isoclinally folded sandstone lenses as paleoslope indicators. The fold axes are consistently perpendicular to paleoslope with axial surfaces of the folds oppositely inclined to the paleoslope (see figures 10f and 21f). Westerly paleoslopes are inferred from field observations of slump direction in the upper Mughal Kot Formation.

In addition to this unique occurrence, the upper Mughal Kot also contains the initial and highest volcanic admixture into otherwise quartzose sandstones. The composition of these rock fragments range from andesitic to basaltic. Pilotaxitic to felty flow structures denoted within several grains in thin section suggest trachyte basalt as the volcanic precurser to the fragments.

The simultaneous occurrence of chaotically slumped sandstones and the first influx of volcanic debris onto the continental shelf suggests a common factor. This factor may have been the uplift of a volcanic arc off the shelf. The existence of such an arc with associated submarine volcanism has been postulated by DeJong and Subhani (1979). Uplift of the arc, causing erosion of the volcanics, may have been accompanied by local earthquake activity triggering depositional slope instability along the continental shelf coastline. Hunting Survey Corporation (1960) also suggests that tectonically-induced slumping occurred on the flanks of the Axial Belt. The constraints on the depositional basin

FIGURE 21. Photographs of Mughal Kot syndepositional, gravity-slump features

a. Pinch and swell features and rounded sandstone terminations.
b. Pull-apart terminations in chaotic interval.
c and d. Boudins with rounded terminations; note hammer in center for scale.
e. Shearing in shales encasing individual slumped sandstones.
f. Slump overfold with lens of light-colored micstone in lower fold.

a

b

c

d

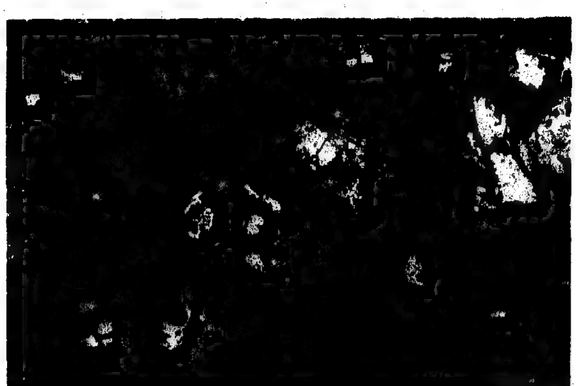

e

f

inducing the mixing of volcanic and terrestrial detritus are considered in the following section.

The Pab Sandstone overlies the Mughal Kot Formation with a transitional contact. The initial sandstone package of the Pab consists of delta front sheet sands which prograded westward over the top of the chaotically slumped interval of the upper Mughal Kot. The transition in the study area displays two chaotic intervals sandwiched between the delta front sandstones. Individual sandstones within this zone thicken and thin over several 10s to 100s of meters along depositional strike. The coalesced sandstones demonstrate lateral migration of the distributary channels entering the shelf.

The Pab above the delta front sandstone consists of a successive stacking of shoreface cycles (figure 13). Approximately twenty coarsening-upward cycles are present. A composite cyclothem (figure 14) closely resembles the shoreface profiles in Cretaceous strata of the western United States (e.g. Asquith, 1970, 1974; Weimer and Land, 1975; Kauffman, 1977; Ryer, 1977; Weimer and Tillman, 1980). The Pab cycles are abbreviated in that they lack foreshore through coastal fluvial facies. The lithofacies present (figure 18) document the repetition of marine shelf to shoreline sedimentation. The Pab has been eroded from the ranges to the west thus the original extent of the cycles is uncertain. The abnormally thick sequence does however sug-

gest a restricted, possibly rapidly subsiding shelf proximal to the volcanic arc. The setting is similar to the depositional "trough" envisioned by Hunting Survey Corporation (1960). It is difficult to account for such rapid yet restricted marine sedimentation without shelf-margin subsidence keeping pace with, and possibly initiating, the deposition of each successive shoreline profile (Ryer, 1977).

The sedimentation pattern proposed is a prolonged history of repeated asymmetric regressive progradations (illustrated in figure 22). A barrier island model of sedimentation has been used most often to depict shoreface development (Weimer and Land, 1975; Ryer, 1977; Flores, 1978). Utilizing such a model, an ideal profile containing offshore through coastal fluvial environments could be repeated via brief marine transgressions (the transgression leaving little, or usually, no trace of sedimentation) followed by regressive progradation. The Pab cycles may have resulted, alternatively, from (1) non-barrier - beach coastline shoreface development (supplied by longshore drift and aggraded to the coastline) or (2) from the lateral migration of marine delta front complexes along the margin of the tectonically active shelf. Any model proposed must account for the lateral continuity of the thick-bedded sandstones as well as the other characteristics of the cycles outlined in the previous section and figure 22. Abundant sand supply via longshore drift proximal to a marine delta are condi-

tions conducive to rapid shoreface development (Weimer and Tillman, 1980). Current directions determined from trough crossbedding axes vary from north to south but show a dominantly westward transport direction.

Ryer (1977) discussed several conditions favorable to cyclic shoreline sedimentation, namely, (1) rapid subsidence adjacent to structural uplift, (2) the rate of change in relative sea level, and (3) the high rate of sediment input, all of which help to promote regressive prograding asymmetric cycles. Transgression abruptly ends these regressive profiles when the rate of sediment supply can no longer overcome the relative rise in sea level. Rapid transgression leaves little or no stratigraphic record and may even be erosive. However, little deposition or erosion can be attributed to transgressive events in the Pab cycles. Relative sea level may be locally controlled via tectonics and subsidence (Jeletzky, 1974) or globally controlled from eustatic sea level change (Kauffman, 1973). Ryer (1977) concludes that a rapid pulsation of the rate of sea level change does not require eustatic control. The remaining factor affecting development of asymmetric cycles may be a variation in sediment supply due to tectonism in the source area, in which case the lengthy duration of tectonic uplift and sediment erosion may greatly exceed that required for a single shoreface event (approximately 30,000 years/cycle estimated by Ryer, 1977). Nontectonic controls such as

DEVELOPMENT OF PAB CYCLIC SEDIMENTATION

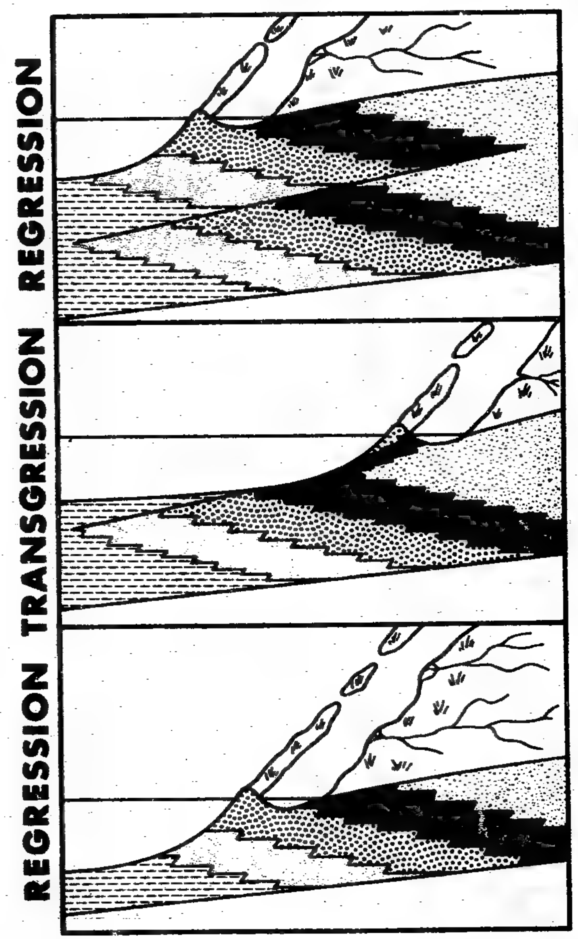

- FLUVIAL COASTAL PLAIN
- MARGINAL MARINE
- SHOREFACE (BARRIER ISLAND)
- OFFSHORE-SHOREFACE TRANSITION
- OFFSHORE SHALLOW SHELF

CHARACTERISTICS OF PAB CYCLES

ONLY OFFSHORE THROUGH SHOREFACE ENVIRONMENTS OBSERVED

PROGRADATIONAL ASYMMETRIC CYCLES WITH NO TRANSGRESSIVE SEDIMENTS PRESERVED

FIGURE 22. Development of Pab cyclic sedimentation

directional change in ocean-current patterns or shifting of distributaries may also contribute to asymmetric development. A rapidly subsiding narrow shelf satisfies, at least partly, the Pab depositional regime in the study area. Subsidence was a much more influential factor governing cyclic shoreline sedimentation on the Indo-Pakistani continental shelf than was rapid fluctuation in sediment supply due to tectonism within the Indian Shield.

The Pab Sandstone and equivalent strata in the Sulaiman Range are also composed of numerous shoreface cycles (Pryor, 1978; Pryor et al., 1979). These profiles are more complete however in containing estuarine-tidal and fluvial facies. A uniform rate of shelf subsidence (interrupted by episodic transgressions) and progradation (controlled by sediment supply) are responsible for the continuous cyclic sedimentation in the Mughal Kot, Pab and Khadro formations (Pryor et al., 1979). The Pab Sandstone which outcrops near Amri Kot in the Laki Range approximately 100 km east of the Pab Range is partly fluvial in origin (Hunting Survey Corporation, 1960). The inference here is that several large channel systems must have developed across the continental shelf to supply sand to the Late Cretaceous shoreline.

A depositional couplet, similar to that of the Sembar - Goru - Parh, is proposed for the Mughal Kot - Pab strata. The two formations comprise a second Cretaceous sedimentation "cycle" prograding across the Tethyan shelf. The prin-

cipal change noted is the lack of deep-water slope lithofacies in the Mughal Kot Formation as compared with the Sembar Formation. The proximity of the volcanic arc during the Maestrichtian may have been responsible for maintaining shelf conditions following Parh deposition.

Tertiary

The Paleocene Khadro Formation reflects an abrupt decrease in sand supply to the shelf area and a return to open marine shelf conditions. No estuarine or fluvial environments are present. Deeper water facies gradually replace shelf sediments in the overlying Khadro strata. The Hyderabad Arch was emergent to the east at the end of the Paleocene. Erosion removed beds of the Ranikot Group and a laterite soil developed locally. Erosion on the Sanjawi Arch to the northeast precluded extensive lower Paleocene sedimentation in the southern Sulaiman area.

The sedimentation pattern and tectonics of the Indo-Pakistani continental shelf changed dramatically during the Eocene and the later Tertiary. The Lower Eocene Ghazij Shale contains terrigenous material thought to be derived from the Laurasian continents (Hunting Survey Corporation, 1960). This signalled continent-continent collision resulting in the closing of the Tethyan Ocean. The middle Eocene Kirthar Limestone is best developed to the south of the initial collision. Shah (1977) reviews the depositional his-

tory of the many, varied Tertiary formations.

The first severe orogenic compression between the Indo-Pakistani Subcontinent and the Eurasian blocks began during the Late Eocene to Early Oligocene. The sea had retreated southward from most of the shelf area by Middle Oligocene time except for the Karachi Embayment. Marine strata become progressively younger towards the south marking the final retreat of the sea.

Intense uplift along the Himalayan front in the Early Miocene created synorogenic molasse basins which were filled longitudinally with Siwalik conglomerates and sandstones. The Himalayan Orogeny continued into the Pleistocene and remains active today.

REGIONAL TECTONOSTRATIGRAPHIC SYNTHESIS OF POST-GONDWANA PLATE TECTONICS

Gondwana reconstruction originally based on continental bathymetric, geologic and paleontologic similarities are continuing to be refined via terrestrial and marine paleomagnetic data and radiometric dating. The position of India with respect to Africa, Arabia and Madagascar is of particular interest to this report. A recently revised fit has been proposed by Powell et al., (1980) and elaborated upon in Powell (1979) and Embleton et al., (1980) (see figure 23). Madagascar is positioned between Kenya and Tanzania on the west and the northern portion of the western margin of India to the east. The Smith and Hallam (1970) reconstruction placed Madagascar opposite the southern portion of India's western coastline. The northern position of Madagascar permits wrapping the Antarctic Peninsula around the Pacific margin of South America providing space for the submerged continental crust of the Falkland Plateau (Barker et al., 1974) and the submarine Madagascar Ridge (Darracott, 1974). The Australia-Antarctica fragment borders what Veevers et al., (1975) termed "Greater India", an attempt to extrapolate India's original north and east continental margins before collision.

Either fit is feasible given the available paleomagnetic data. Klootwijk (1979) and Embleton et al., (1980)

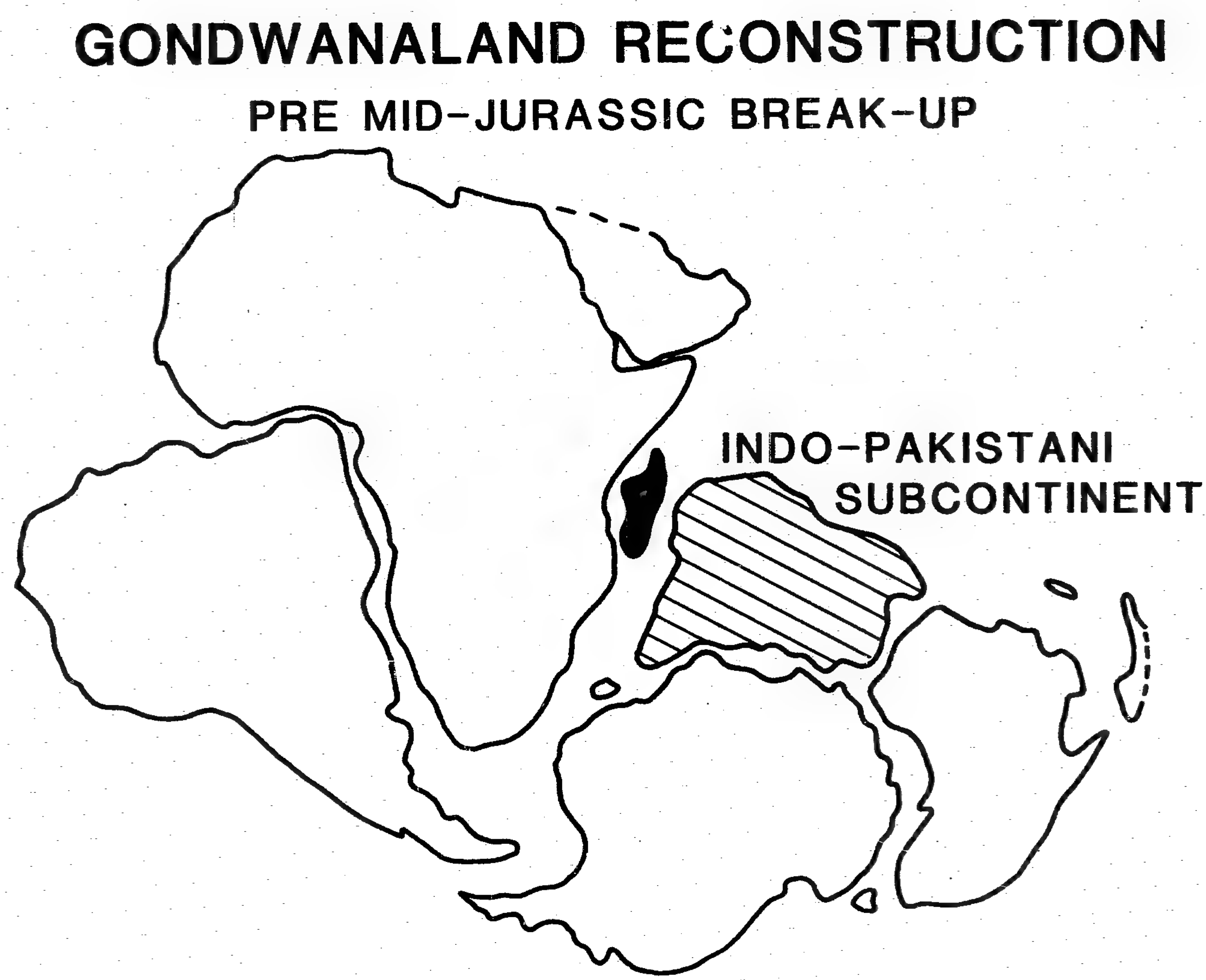

FIGURE 23. Gondwanaland reconstruction (after Powell, et al., 198Ø)

believe that except for the Permo-Triassic fit of Powell et al., (1980), Smith and Hallam (1970) propose an overall better fit (less dispersion of paleomagnetic data). The fit of Powell et al., (1980) however juxtaposes Madagascar near northwest Indo-Pakistani margin. Coeval volcanic terrains on Madagascar and the volcanic arc off the Indo-Pakistani shelf may also have been in close geographic proximity.

Initial separation of East and West Gondwana has been variously dated as Middle Triassic (Dietz and Holden, 1970) to Early Jurassic (Dingle and Scurtton, 1974) to Late Jurassic (150 m.y. ago. Powell et al., 1980). The record of sea floor spreading creating Indian Ocean crust in the wake of India's northward movement is manifested in the preserved marine magnetic anomaly pattern. The oldest anomaly, no. 33 (dated at 80 my BP), is found along the Mauritius Fracture Zone east of Madagascar and also west of the Ninetyeast Ridge. The several orientations of anomaly patterns and fracture zones have been interpreted by various authors in the evolution of the Indian Ocean (e.g. McKenzie and Sclater, 1971; Sclater and Fisher, 1974; Markl, 1974; Schlich, 1975; Johnson et al., 1976; Larson, 1977; Pierce, 1978). Considerably more work has been conducted in the eastern Indian Ocean. Reviewing the literature, Powell (1979) proposes three principal stages of separation between India, Australia and Antarctica, as follows:

(1) 13Ø to 8Ø my BP: India moved north to the equator while the coupled Antarctica/Australia fragment moved south at 3-5 cm/yr.

(2) 8Ø to 53 my BP: India moved rapidly north across the equator with respect to Australia/Antarctica, 2Ø cm/yr; the fastest rate in its history.

(3) 53 mya to present: At first all three fragments moved independently then the Indian and Australian plates moved as one; India slowed to a 4-6 cm/yr northward advance and began its 2Ø degree counter-clockwise rotation with respect to the geomagnetic pole.

The northward migration of the Indo-Pakistani Subcontinent (figure 24), causing closure of the Tethys Ocean, represents the last of three episodes of continental accretion to Laurasia since the Late Paleozoic (Boulin, 1981; Tapponnier et al., 1981). The Mesozoic and Cenozoic plate movements have been quite active; the Indo-Pakistani Subcontinent has moved the farthest of all the Gondwana fragments. Those regions affected by Indian Plate movement include the structural zones of the Oman and Zagros mountains, the Makran of Pakistan and Iran, and the Axial Belt of Pakistan (figure 25). It is informative to chronologically equate the various stratigraphic and tectonic events of these provinces with the depositional history of the northwest Indo-Pakistani shelf (summarized in Table 3).

Stoneley (1974) condenses the plate collision history of the Tethyan region to a passive south-Tethyan continental margin approaching and finally colliding with Eurasia during the Neogene. Subduction took place along the north-Tethyan

PALEOLATITUDINAL POSITION OF THE INDO-PAKISTANI SUBCONTINENT

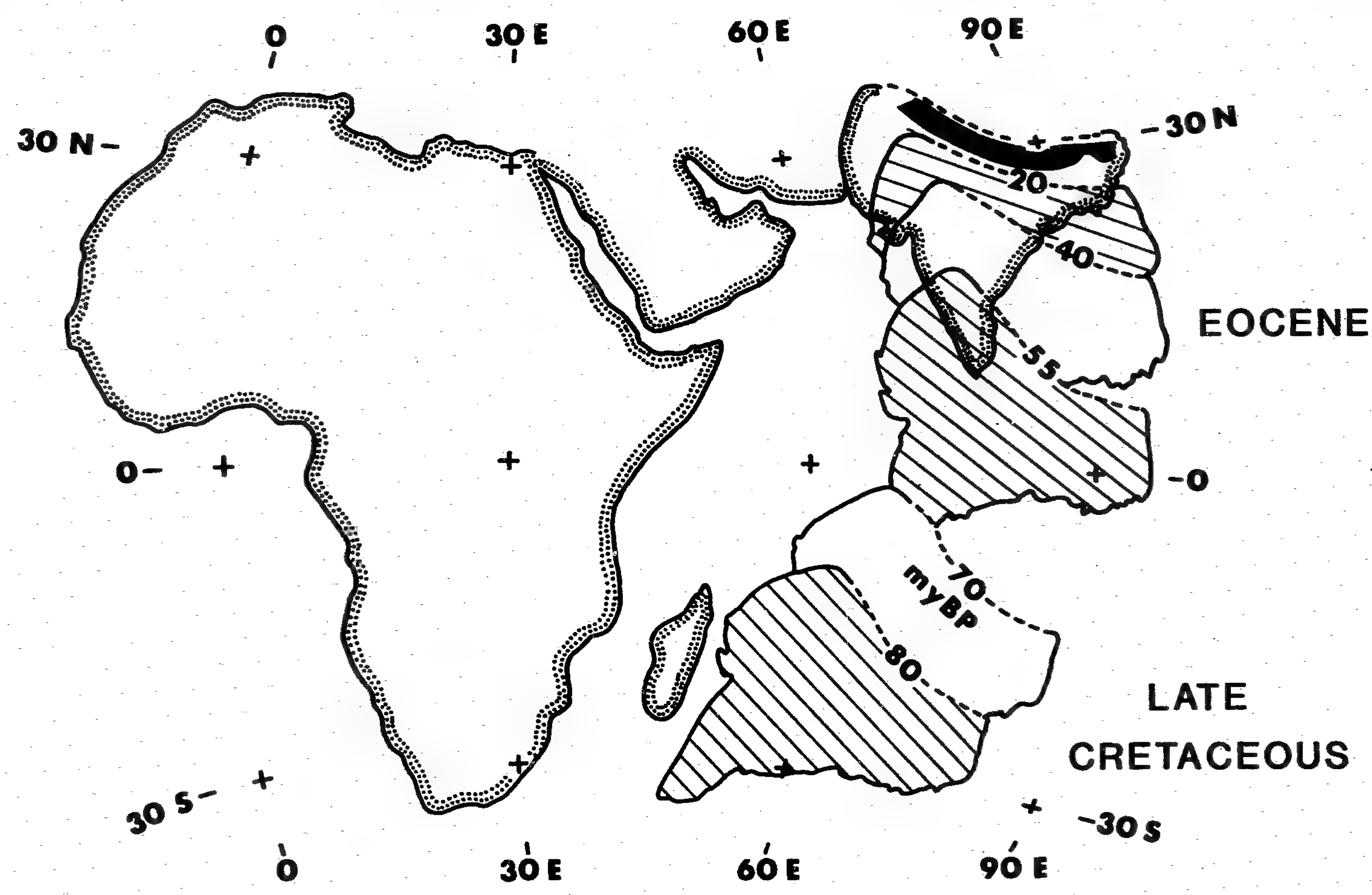

FIGURE 24. Paleolatitudinal position of the Indo-Pakistani Subcontinent (modified after Powell, 1979)

margin. The ensuing discussion incorporates the depositional and tectonic events of the areas abstracted in Table 3, into a series of time-lapse plate reconstructions proposed by Powell (1979).

Prior to the Late Cretaceous, microcontinent fragments in Iran and Afghanistan (e.g. the Lut Block) detached themselves from northern Gondwana. The blocks subsequently moved northwards via a spreading center off the Arabian block and subduction south of the Turan Block (Eurasia) during the Permian. This represented the initial closing of the "paleo-Tethys" in the wake of the small continental fragments (Stocklin, 1974; Boulin, 1981; Tapponnier et al., 1981). The Early Mesozoic Alborz-Hindu Kush-Kun Lun suture (Iran-India-Tibet) signaled final closing of the paleo-Tethys.

The most intense Jurassic to Early Cretaceous tectonism is displayed west of the Djaz Murian Depression in the Iranian Makran on the southern margin of the Lut Block. The colored melange (Falcon, 1974b) represents a thick interval of syndepositional slumping of sedimentary strata down the paleocontinental slope (of the Lut Block) and intermingling with abyssal submarine lava flows in chaotic olistostromes. Subsequent compressional thrusting created a tectonic melange. Other occurrences of colored melange are known from the eastern margin of the Lut Microcontinent but are Late Cretaceous in age (Stocklin, 1974).

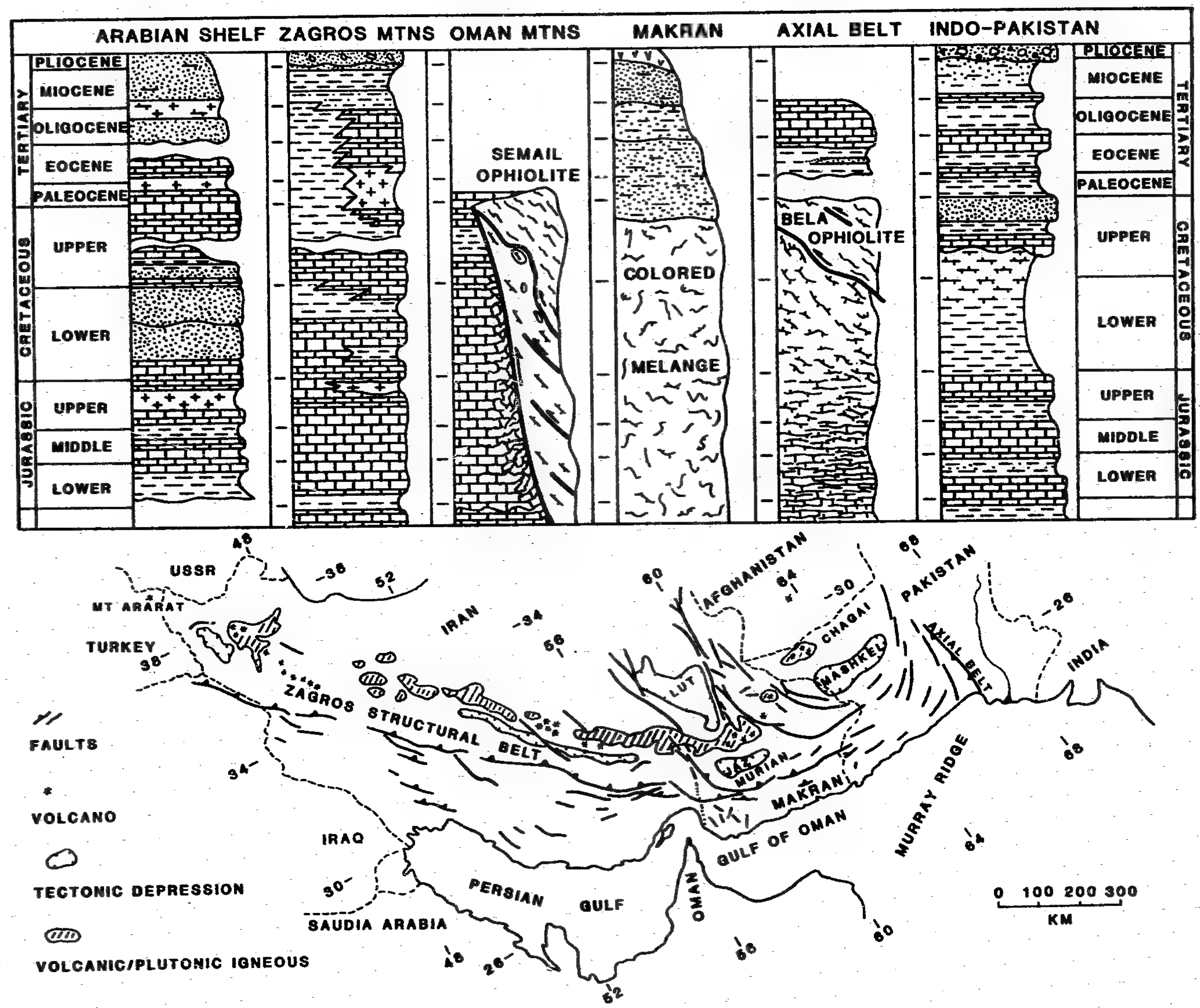

FIGURE 25. Tectonostratigraphic setting of the Arabian, Eurasian and Indian plates

Elsewhere just prior to the Senonian the initial tectonic melanges of the Hawasina Group heralded the evolution of the Oman Mountains (Gealey, 1977). Gealey attribptes the development to north-south collision of the passive Afro-Arabian margin with an island arc similar to that proposed by Welland and Mitchell (1977). The Semail Ophiolite in this setting would have been the former forearc limb of the island arc couple obducted via continental underthrusting. Glennie et al., (1973) concludes that obduction resulted from the collision of the Proto-Owen Fracture Zone and the Iran-Afghan blocks. Compression ceased before the Maestrichtian. Alternatively, Stoneley (1974) and others do not agree that ophiolites necessarily invoke continental underthrusting and the ensuing tectonic response. Instead, the Oman example as well as other Late Cretaceous ophiolites in Iran and around the Indo-Pakistani Subcontinent simply represent gravity sliding and nappe formation following geoanticlinal uplift along the continental margins. Evidence sited by Gealey (1977), Welland and Mitchell (1977), and DeJong and Subhani (1979) strongly favor tectonic emplacement. Smaller but similar Late Cretaceous ophiolite complexes occur within the Zagros Mountains indicating closure of the Permian rift between central Iran and Arabia (Pamic et al., 1979). It is also conceivable that the Senomanian Sinjrani Volcanic Group along the southern Central Afghan Block is an andesitic remnant of this island arc

TABLE 3. Summary sheet of regional tectonostratigraphic events

SUMMARY SHEET OF REGIONAL TECTONOSTRATIGRAPHIC EVENTS

Period	Epoch / Stage	MY	Arabian Shelf	Zagros Belt	Oman Mountains	Makran Shelf	Axial Belt	Indo-Pakistan
Tertiary	Pliocene		Shelf folding	Magmatic arc volcanism; Synorogenic molasse	Pelagic sediments	Arc volcanism	Syn- and post-orogenic molasse (Siwalik) from Himalayan uplift	
Tertiary	Miocene	10–20	Shallow-shelf sandstone and evaporite (Sabkha)	Zagros island arc development; Shelf clastics and evaporite	Flysch (Gulf of Oman)	Emergence of forearc basins; Granitic intrusions; Thrusting of accretional, trench-forearc wedge	Flysch	Shelf carbonate & flysch basins; Reefs and slope deposits
Tertiary	Oligocene	30	Erosional unconformity related to Zagros?	Shelf & slope deposits	Flysch	Flysch; Compressional thrusting and folding	Shelf carbonate; Marine transgsession	
Tertiary	Eocene	40–50	Shelf limestone and evaporite	Slope sediments and submarine volcanism; Begin migration of depositional-trough axis to south (trench-forearc)		Flysch; Imbricate folding		Reef limestone; Shelf deposits
Tertiary	Paleocene	60	Shelf carbonate		Flysch basins with ophiolite debris	Flysch basins and deformation; Beginning of subduction zone	Bela ophiolite obduction; Kunno melange	Shelf & slope sediments
Cretaceous, Upper, Senonian	Maestrich.	70	Regional unconformity	Slope-basin flysch and thin limestone	Undisturbed carbonate	Shelf limestone	Porali agglomerate; Porali volcanic arc	Tethyan shoreline sandstone
Cretaceous, Upper, Senonian	Campanian			Ophiolite emplacement	Semial ophiolite obduction	Igneous intrusions	Tectonic uplift	
Cretaceous, Upper, Senonian	Santonian	80	Shelf carbonate	Submarine volcanism		Submarine andesitic volcanism		
Cretaceous, Upper, Senonian	Coniacian			Basin radiolarian chert and andesite	Imbricate thrusting of Hawasina melange	Widespread tectonism	Shallow-platform carbonate	
Cretaceous, Upper	Turonian	90	Shelf(?) sandstone		Slope-basin flysch			
Cretaceous, Upper	Cenomanian	100		Shelf-basin carbonate and clastics	Shelf carbonate			
Cretaceous, Lower	Albian		Shelf carbonate			Deformation of colored melange		
Cretaceous, Lower	Aptian	110				Submarine volcanism	Shelf to slope shale	
Cretaceous, Lower	Barremian				Shelf carbonate	Shelf-slope clastics		
Cretaceous, Lower	Neocomian	120–140		Regional uplift			Slope deposits	
Jurassic		150	Shallow-shelf carbonate, calcarenite and evaporite; Shelf subsidence	Slope-basin carbonate and marl; Rifting of Iran from Arabia	Shelf carbonate	Shelf-slope deposits	Gondwanaland fragmentation	

(Arthurton et al., 1979).

Cretaceous deposition on the outer continental margin of the Indo-Pakistani Subcontinent began with slope deposits of the Sembar Formation. The Subcontinent had begun its isolated northward movement by this time. The Cretaceous strata reflect broad, stable shelf conditions characteristic of a passive continental margin. The Sembar, Goru and Parh formations comprise the initial sediment wedge prograding across the continental shelf. The development of the Porali Volcanic arc apparently affected only the youngest phases of the sedimentation.

The Maestrichtian epoch (figure 26) exhibits the most widespread tectonism prior to the Neogene Alpine-Himalayan Orogeny. This is necessarily coupled with the fastest spreading rates (15-20 cm/yr) recorded in the marine magnetic anomaly patterns of the Indian Ocean (Johnson et al., 1976; Powell, 1979). The evolution of the Indian Ocean and northward movement of the Indian Plate forced subduction of the Tethyan oceanic crust along the Eurasian continental margin. The southern Tethyan continental margin off northwest India moved northward relative to Madagascar. Basaltic volcanoes erupted on Madagascar and are belived related to rifting (Klootwijk, 1979; McElhinny et al., 1976). Maestrichtian volcanism was extensive in Madagascar and Afghanistan; the distribution of related volcanogenic sediments in the northwestern Indian Ocean has been surveyed by Vallier

and Kidd (1977). Davies and Kidd (1977) dredged abyssal plain clays of Maestrichtian(?) age from the ocean floor between Madagascar and India. Verma (1980) also advocates a Late Cretaceous separation of India and Madagascar.

The Maestrichtian depositional setting of the study area is of primary concern to this report. The Mughal Kot and Pab clastics were deposited near the edge of the continental shelf yet within near-shore marine environments. It is inferred that volcanism from submarine seamounts (on oceanic crust) and the Porali Volcanic Arc (on continental crust) created the structural barrier that played a key role in controlling sedimentation patterns (figure 26). Uplift and erosion of the Porali Volcanics supplied the volcanic admixture that occurs in the upper Mughal Kot Formation and persists throughout the Pab Sandstone. The tectonostratigraphic setting envisioned is that of a back-arc basin (figpre 27). The narrow north-south continental shelf in this setting promoted the mixing of the dominant terrigenous quartz with the volcanic debris brought shoreward. The proposed setting hinges on the provenance of the volcanic rock fragments being offshore. The Porali Volcanics defined by DeJong and Subhani (1979) represent the most likely source, but, alternatively, a very remote possibility suggests that the proximity of volcanism on Madagascar may have been closely associated. None of the published palinspastic reconstructions for the Maestrichtian place Madagascar near

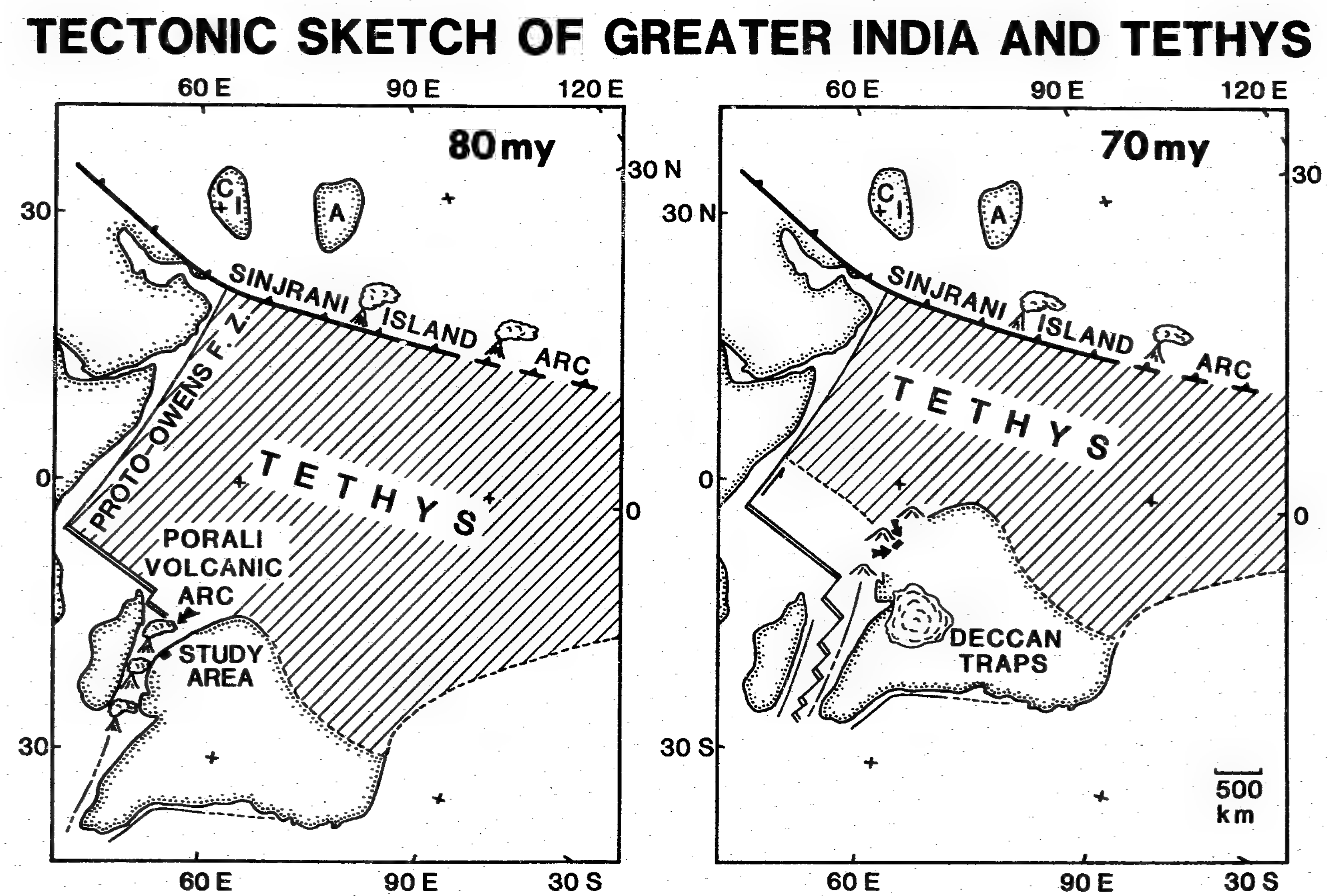

FIGURE 26. Tectonic sketches of the Tethyan Ocean and surrounding elements during the Late Cretaceous

the northwestern part of the Indo-Pakistani Subcontinent and is considered here to be an unlikely source terrain. Reasons contrary to a Deccan Trap source in western India are (1) the first occurrence of volcanic fragments in the upper Mughal Kot predates the 65-60 my BP age range of Trap extrusion (Powell, 1979), (2) basalt flows in the Laki Range attributed to the Deccan event, occur within Paleocene strata overlying the Pab Sandstone, (3) the basaltic trap in the upper Pab Sandstone exposed in the Hyderabad Arch, originally believed to be a subaerial flow (Blanford, 1879), was later interpreted as a hypabyssal sill associated with the subaerial traps of the overlying Khadro (Hunting Survey Corporation, 1960), and (4) the fresh volcanic grains of the Mughal Kot and Pab in the study area are consistently larger than quartz which suggests limited distance of transport.

At 55 my BP (Paleocene/Eocene boundary, figure 28a), the northern-most continental extension of Greater India intersected the Chitral island arc zone. This initial continent-continent collision greatly slowed the rate of northward movement. The tectonic emplacement of the Bela Ophiolite eastward onto the continental shelf occurred during the Paleocene (based on faunal studies by Allemann, 1979). Between 70 and 55 my BP, Powell (1979) estimates approximately 500 km of convergence, however, none of the new Indian Ocean crust had as yet been subducted in the Makran region west of India. Paleomagnetic evidence from the Dec-

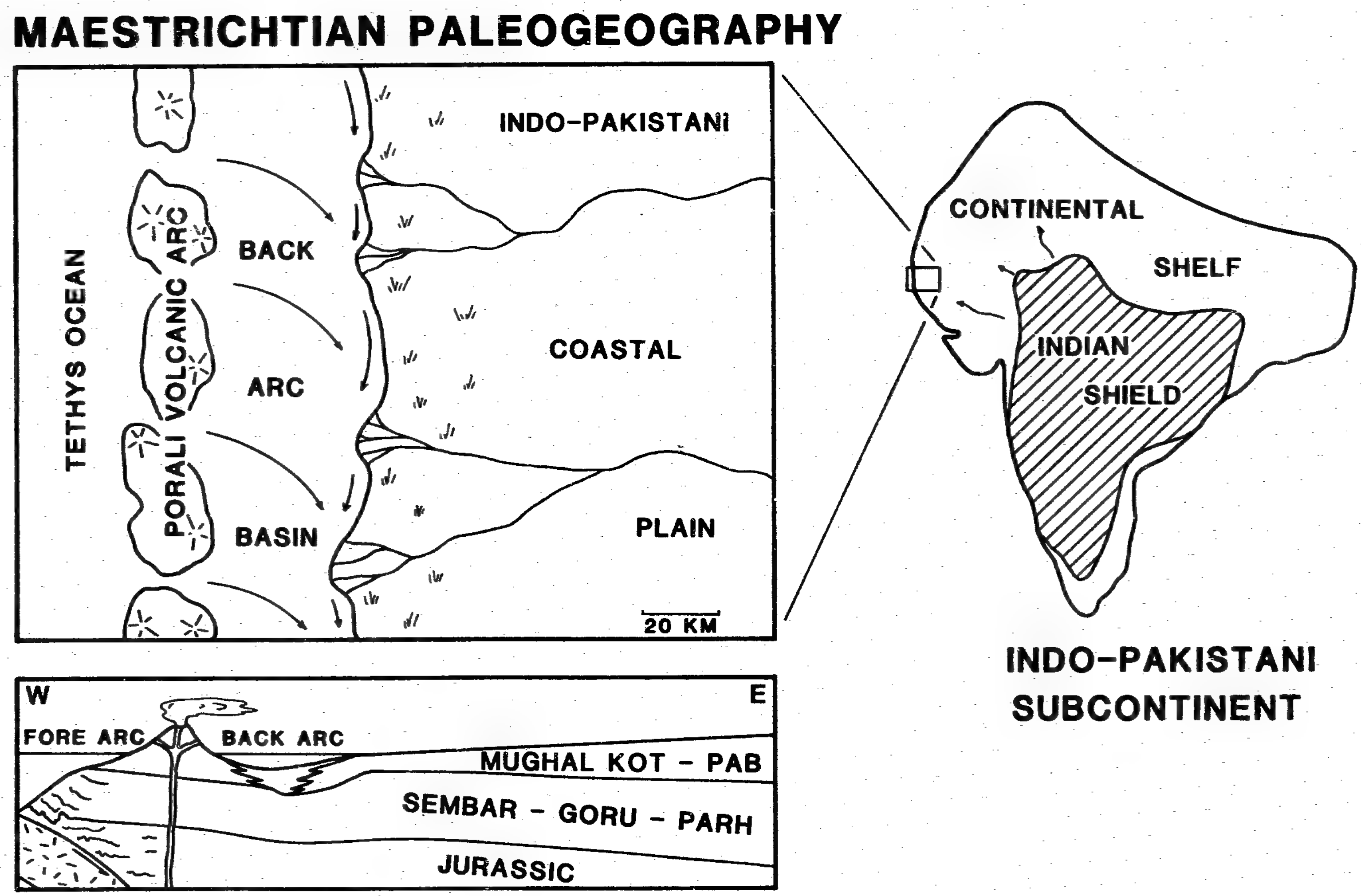

FIGURE 27. Maestrichtian paleogeography of the western Indo-Pakistani continental shelf

can Traps concurs with this magnitude of northward movement (Klootwijk, 1979). Turbidite deposition dominated conditions in the Makran and Oman; tectonic melange was emplaced east of the Lut Block (central Iran).

The 40 my BP configuration (Late Eocene, figure 28b) marks the initial rotation of the Indo-Pakistani Subcontinent. The rotation of the Subcontinent is represented by the bending of several spreading centers and their corresponding marine magnetic anomaly patterns in the Indian Ocean (e.g. the resurrected Chagos-Mascarene Plateau) (Powell, 1979). The rotation resulted from the massive continent-continent collision. Tectonic syntaxes as seen in present day Baluchistan (Sarwar and DeJong, 1979) resulted from this bending. As collision intensified, major transform faults (Chaman and Ornach-Nal faults) developed. Virtually all the Tethyan Ocean crust had been consumed by this time. Submarine volcanism and rapid facies changes typified conditions in the Zagros area; the subduction zone had begun to migrate southward (Falcon, 1974a). To the east, Makranian flysch basins continued to receive enormous turbidite thicknesses (Ahmed, 1969) concomitant with recurrent compressional folding. The flysch basins are inferred continuations of the Zagros-forearc basin.

The picture 20 my BP (Early Miocene, figure 28c) depicts further rotation of India that forced the Owen Fracture Zone into a major transform. This permitted another

500 to 600 km of crustal shortening to occur since the Late Eocene initiating thrusting and metamorphism in the intensely compressed collision zone. The magnetostratigraphy of the syndeformational Siwalik molasse records rapid Himalayan uplift and differential rates of foredeep sedimentation (Johnson et al., 1979). The Gulf of Oman - Makran - Axial Belt trend continued to receive turbidites and underwent more imbricate compression. Shallow-shelf to evaporitic sabkha conditions dominated the immediate Zagros vicinity as initial compressional thrusting began (Farhoudi, 1978). An increased rate of subduction occurred along the forearc of the Makran.

The last 20 million years (present configuration, figpre 28d) has received the greatest attention in the geologic literature. The tectonics of the present-day configuration are centered along the Alpine-Himalayan trend. The uplift of the Zagros Mountains began in Early Miocene and has been interpreted in two different ways. Stoneley (1974) represents the Zagros Mountains as a crush zone between Arabia and Eurasia that began in the Late Cretaceous. More recently, Farhoudi (1978) considered the zone an island arc system in various stages of development. The Makran shelf of Baluchistan represents the exposed and submerged section of an island arc-forearc basin and trench segment of oceanic crust subduction beneath Eurasia (Farhoudi and Karig, 1977; Jacob and Quittmeyer, 1979). The difference between the

Baluchistan Arc System and that of the Zagros is due to the difference in crustal types and sedimentation (dominantly carbonate vs terrigenous) (Farhoudi, 1978). Within this context the Tertiary of Makran is an accretionary prism of sediment "scraped off the descending Arabian plate" (White, 1979). The sediment is intricately thrusted toward the Gulf of Oman and folded in the uppermost two or three kilometers. The frontal folds (White and Klitgord, 1976; White, 1979) begin an average of 120 km off the Makran coastline at an abyssal depth of 3000 m, defining the present trench position.

Counterclockwise rotation about a pole in southern Arabia characterized the latest tectonic phase in India's history. The estimate of crustal shortening of Greater India beneath Tibet is 300 to 400 km and accounts for the rise in the Himalayan Range and the Tibet Plateau. The Plio-Pleistocene has, in fact, recorded the greatest elevation of the Himalayas. Tectonics are still active in the Indo-Pakistani region (e.g. see Kazmi, 1979a). The present estimate of convergence rate decreases from 5.4 cm/yr. to 3.7 cm/yr. from east to west in the Himalayas (Minister et al., 1974). The estimate of total plate convergence between Eurasia and its first collision with Greater India is in the neighborhood of 2500-3500 km in the north-south direction (Molnar and Chen, 1978; Klootwijk, 1979; Klootwijk and Bingham, 1980 Klootwijk et al., 1981).

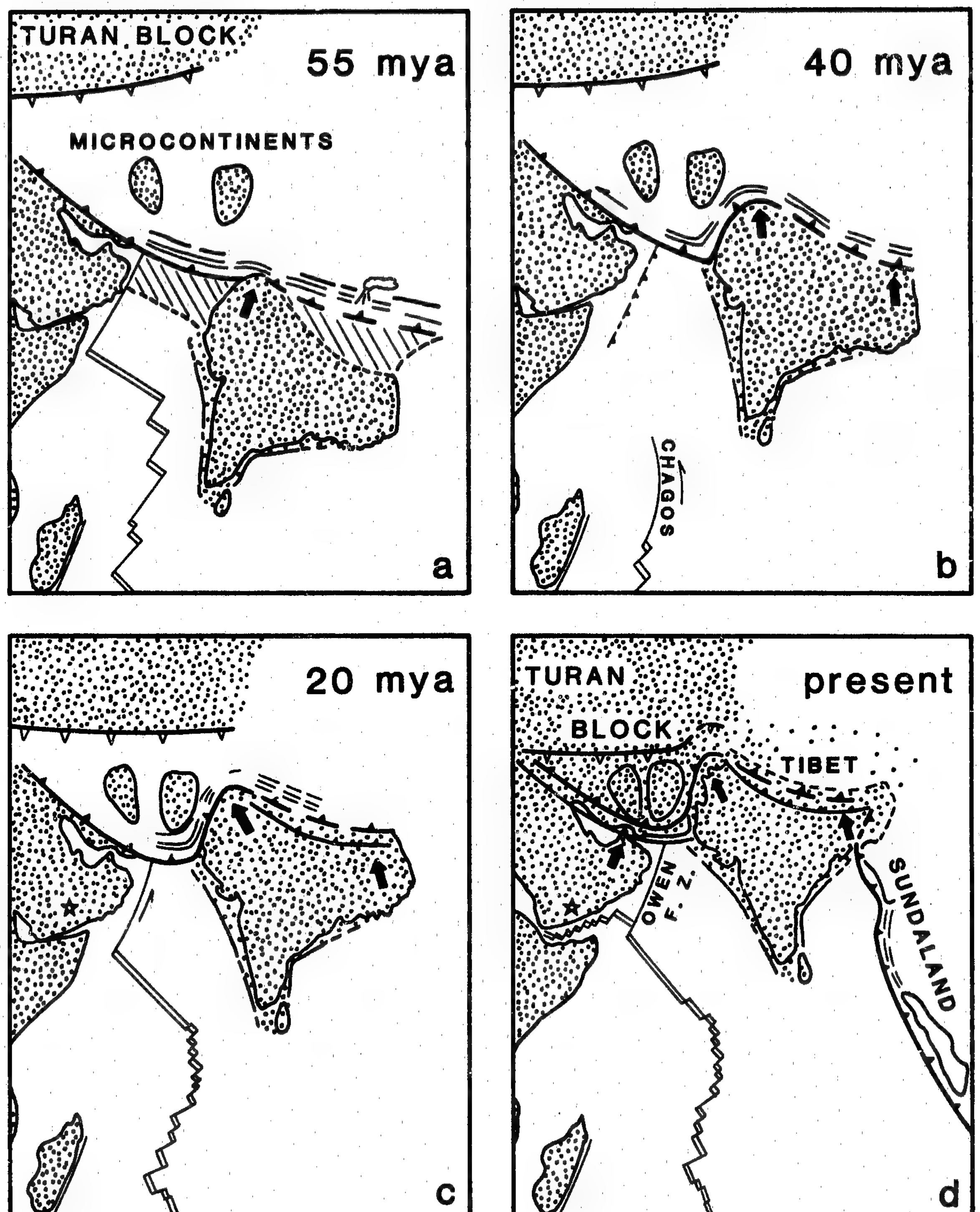

FIGURE 28. Sequential plate reconstructions during the Cenozoic (after Powell, 1979)

What this synthesis has shown is pervasive Late Cretaceous plate margin instability that culminated with the Neogene Himalayan Orogeny. Tectonically-emplaced ophiolites and melanges are known from the Oman Mountains, the Zagros Mountains, the eastern Iranian Ranges, and the Axial Belt of Pakistan. This tectonism initiated Arabian (Tethyan) oceanic crust subduction beneath continental Eurasia. The Cretaceous sediments of the northwestern Indo-Pakistani shelf were deposited during the Subcontinent's isolated northward advance. Rapid Late Cretaceous movement created unstable continental margins. The resulting tectonism on the continental margin was responsible for the narrow depositional shelf receiving Mughal Kot and Pab sediments.

PROVENANCE OF THE UPPER CRETACEOUS TETHYAN SANDSTONES OF THE MUGHAL KOT AND PAB FORMATIONS

Quartz and volcanic rock fragments comprise the principal detrital components of these Tethyan shoreline sandstones. The sands in the lower and middle Mughal Kot strata contain only plutonic quartz detritus. The significant, though subordinate, volcanic admixture first appears in the upper Mughal Kot and persists through the Pab Sandstone. The average QFR composition for this latter association is 83:1:16 (sublitharenite; Appendix D). The quartz grains are typical in that they are single crystals or polycrystalline with straight to commonly undulose extinction, and inclusions of rutile needles plus vacuole trains. Feldspars, though highly altered, are usually twinned plagioclase varieties. The volcanic grains are uniformly fine-grained with abundant microlite feldspar laths in a pilotaxitic (trachytic) texture. Dickinson and Suczek (1979) derive plate tectonic inferences from sandstone composition. The characteristics of the petrography here, namely, 1) high quartz content coupled with extremely low feldspar percentage and 2) abundant volcaniclastic detritus match feature typical of a Foreland Uplift provenance flanking a volcanic arc or collision orogen (Dickinson and Suczek, 1979, p. 2178).

The heavy mineral suite has long been applied to provenance studies. The relatively simple suite found here con-

sists of zircon, tourmaline and rutile with trace magnetite. The percentages of each are similar in both the nonvolcanic or volcanic sandstones (Appendix F). The uniformity of the assemblage throughout the sequence indicates the dominance of the plutonic provenance over the volcanic terrane in supplying detritus to the shelf basin. Further the ultrastable suite supports an ultimate quartz provenance in igneous plutonic and metamorphic terrane. The tourmaline varieties present would be so classified by Krynine (1946).

The sandstone petrography of the samples of the Mughal Kot and Pab formations exposed in the Sulaiman Range (courtesy of Dr. W.A. Pryor, University of Cincinnati) are similar to those in the southern Pab Range except for the absence of volcanic debris. The sandstones are quartzarenites with a similar paucity of feldspar.

The reconnaissance study of the Pab Sandstone by Huntington Survey Corporation (1960, p. 229) concluded the following for the source of the sand:

> The Pab formation of the Pab Range and Northern Montane Front is marine whereas that of the Lakhi range is evidently fluviatile or marine deltaic. For the most part the formation appears to represent sedimentation that was irregular in its distribution and relatively rapid. As a result some places acquired abnormally thick deposits of sand, but others nearby acquired thin deposits or none at all.
>
> Evidence strongly suggests a common source in the Foreland craton for all occurrences of Pab Sandstone. The main regions of the Pab formation contain essentially the same type of sandstone and are linked by the thin members mapped with the Moro formation and the Dungan group. In the

> southern region, the Lakhi range appears to contain the near-shore or terrestrial counterpart of the Pab sandstone, indicating and eastern source. Lateral gradation of this type is not known in the northern region, but the fact that the greatest thickness is found in the Sulaiman Range - particplarly east of the map area near Fort Munro - suggests that the source of these rocks lies to the east also. The present survey regards the metamorphic and igneous rocks that make up the hills of Jodhpur and Chiniot (in the Rajputana district of India and southern Punjab province, respectively) as the exposed remnants of the source terrane.

Plate tectonic evidence places the Subcontinent as a totally isolated entity throughout the Cretaceous period thus limiting the Indian Shield as the only possible terrigenous provenance. The overwhelming proportion of quartz suggests previous sedimentary recycling of debris ultimately derived from an igneous plutonic and/or metamorphic terrane (White, 1981). Current directions support this easterly source.

Gupta (1975; 1977) and Sharma et al. (1980) summarize the Precambrian, Paleozoic and Mesozoic stratigraphy of the Rajasthan and Punjab provinces of northwest India (figure 6). The Archean Aravalli Supergroup, named for extensive exposures in the Aravalli Range in Rajasthan represents the oldest unit exposed. The complex includes metamorphic, igneous plutonic and volcanic rocks overlain by metamorphosed sediments. Few sedimentary rocks are not metamorphosed to some degree. The Bundelkhand and Berach granites intrude the Archean basement. Unconformably overlying the

Archean are the Rialo, the Delhi and the Vindhyan supergroups, respectively. These supergroups are all Proterozoic in age. A major orogenic event is responsible for each supergroup (Sharma, et al. 1980). Each consists of a variety of high-grade metamorphic rock types as well as clastic sediments. The Proterozoic strata are preserved in large synclinoria that are strongly deformed. Intrusive granites and pegmatites are also common in the Delhi Supergroup. The Vindhyan underlies the northern Deccan Traps and outcrops extensively in Rajasthan Province of India. It consists of thick calcareous marine strata in the lower portion and arenaceous strata in the upper portion. Late Proterozoic (700 my BP) Malani Rhyolites also occur in the northwest shield area.

Triassic through Cretaceous strata outcrop on the flanks of northwest Indian Shield. The strata are stated to be coastal marine to fluvial in origin (Gupta, 1975). Local sedimentary basins within the shield contain continental deposits from Late Carboniferous to Early Cretaceous in age. The successions represent the Upper and Lower Gondwana sequences. It is not known what, if any, detritus may have been derived from the erosion of older sediments flanking the Indian Shield.

The dominant quartz component along with an ultrastable heavy mineral suite require a mature sediment source. This condition might have been satisfied by recycling of previous

sedimentary (possibly metamorphosed) units and/or paleoclimates in the Indian Shield area causing intensive weathering (disintegration and decomposition). A warm humid climate supporting thick vegetation and acid soil development would have provided the quartz-dominated detritus. Such a climate is inferred during the Late Cretaceous because the Subcontinent was crossing through subtropical to tropical paleolatitudes (Klootwijk, 1979). Frakes (1979) summarizes oxygen isotope studies on Cretaceous sediments that interpret warm and humid climates during the Middle to Late Cretaceous. The lack of abundant feldspar and plutonic/metamorphic rock fragments is attributed more to source-area weathering than transport abrasion.

Mention has also been made in previous sections of the Deccan Traps as a possible source of the volcanic fragments in the Upper Cretaceous of the Pab Range. The Traps cover several hundred thousand square kilometers in west-central India. Gupta (1975) sites the distinction of 48 basalt flows of between 7 and 27 m thick. The age of the Deccan Traps has been radiometrically determined at 60 to 65 my BP (Kaneoka and Haramura, 1973; Wensink and Hebeda, 1977). This interval comprises a much narrower time span than the latest Cretaceous to Eocene span delimited on stratigraphic and paleontologic evidence (Gupta, 1976). Reasons were given in the previous section discrediting a Deccan source for the volcanic debris in the study area. However, the

presence or absence of volcanic rock fragments in the fluvial Pab sandstones of the Laki Range has not been tested. Given a westward transport direction and a source in the Deccan basalts, equivalent strata in the Laki Range should contain a significant volcanic admixture. Unfortunately, no samples of the Pab Sandstone from the Laki Range were available to the writer during this study. The consistently larger average diameter of the volcanics with respect to quartz detritus suggest a nearby source terrane. Until further data is reported, the author favors the previously stated provenance within the postulated Porali Volcanic Arc.

DIAGENETIC HISTORY AND ECONOMIC POTENTIAL OF THE CRETACEOUS STRATA IN THE STUDY AREA

The diagenetic history of the Cretaceous strata is a simple one dominated by calcite cementation. Diagenetic features observed in carbonate thin section include limited pressure solution along compacted grain boundaries, micritic submarine cementation, and neomorphic recrystallization of calcite cement. Void-fillings and replacement minerals observed in sandstones are silica overgrowths, pervasive calcite pore fillings, clay minerals (kaolinite, chlorite and illite), zeolite formation (analcime), and trace pyrite. The results of a modified staining technique for carbonates in thin section (Dickson, 1965) reveal colors for calcite and ferroan calcite. No unstained carbonate (indicative of dolomite) remained. Similarly no dolomite rhombs were observed in thin section.

The Parh Limestone exhibits very little compaction in thin section. The limestone varies from a tightly packed to scattered foram construction (photo 8e). Boundary replacements do occur in packstones but show no stylolitic development. The major proportion of the individual tests contain a finer-grained (micritic) cement within the cellular structure. Bathurst (1975) attributes this micrite to pre-lithification, submarine floor cementation. The micritic carbonate supporting the "floating" tests may also be primary.

Patches of recrystallization yield coarser grained pore fillings. These same characteristics apply to the micstones of the overlying Mughal Kot Formation.

Early diagenesis in sandstones is typically dominated by porosity-reducing processes, namely, chemical (cementation, replacement and recrystallization) and mechanical (compaction by plastic deformation and detrital grain fracture) (Hayes, 1979). The prominent quartzarenite in the basal Mughal Kot shows appreciable grain to grain compaction features (figure 12a). Microstylolites can be seen to be weakly developed alcng grain sutures. Calcite is the only secondary mineral found in this quartz sand (figure 29a). The coarse-grained mosaic fills nearly every pore and frequently exhibits patches of poikilotopic (single crystal) calcite enclosing several quartz grains.

The volcanic admixture of the upper Mughal Kot and Pab formations produces interesting alteration characteristics. X-ray analysis of these strata, particularly the upper Mughal Kot where the percentage is greatest, records significant increases in chlorite and illite clay minerals plus the presence of analcime, a zeolite mineral commonly associated with volcaniclastic diagenesis (Pettijohn, Potter and Siever, 1973; Fuchtbauer, 1974) (figure 29b, c and d). The authigenic analcime likely formed from decomposition of interstitial glass within the volcanic fragments though few volcanic-rich sandstones displayed analcime peaks (Appendix

E). No glass was observed in thin section. Volcanic rock fragments show a wide range of chemical and mechanical alteration. The smaller grains display greater decomposition. These grains exhibit a peripheral coating of Fe-oxides/clay minerals. The thickness of this coating increases with apparent alteration within the individual grain. It is not known whether the mineralogy of the clays within the fragments matches that filling pores and coating grains. Microlite feldspars within the volcanics generally display less alteration than the groundmass (possibly consisting of glass originally). Calcite is also a common cementing agent and seems to have followed early alteration (including zeolitization) of the volcanic fragments.

Silica overgrowths locally exceed calcite cementation in upper strata of the Pab Sandstone (figure 16f). Original grain boundaries are distinguished by surrounding "dust" rims (Scholle, 1979) and distinguished from quartz overgrowths via cathode luminescence (Sippel, 1968). Calcite, however, is the dominant secondary mineral throughout the Pab, frequently showing a poikilotopic fabric. A single pyrite crystal was found during SEM observations of pore fillings.

Primary porosity in sandstones may be 35 to 40 percent (Hayes, 1979). The pervasive secondary calcite cementation occurring after initial alteration of volcanic debris and quartz overgrowth may occlude the sand during early diagene-

FIGURE 29. Diagenetic features of the Mughal Kot Formation and the Pab Sandstone

a. SEM photo of calcite pore-filling in the lower Mughal Kot quartzarenite. Bar scale is 20 microns.

SEM photos of pore-fillings in Pab Sandstone

b. Calcite, clay minerals and analcime filling pores of sublitharenites. Bar scale is 10 microns.
c. Clay mineral dominating matrix cements of volcanic arenites. Scale is 10 microns.
d. High magnification photo of clay minerals coating detrital sand grains seen in photo c. Bar scale is 1 micron.

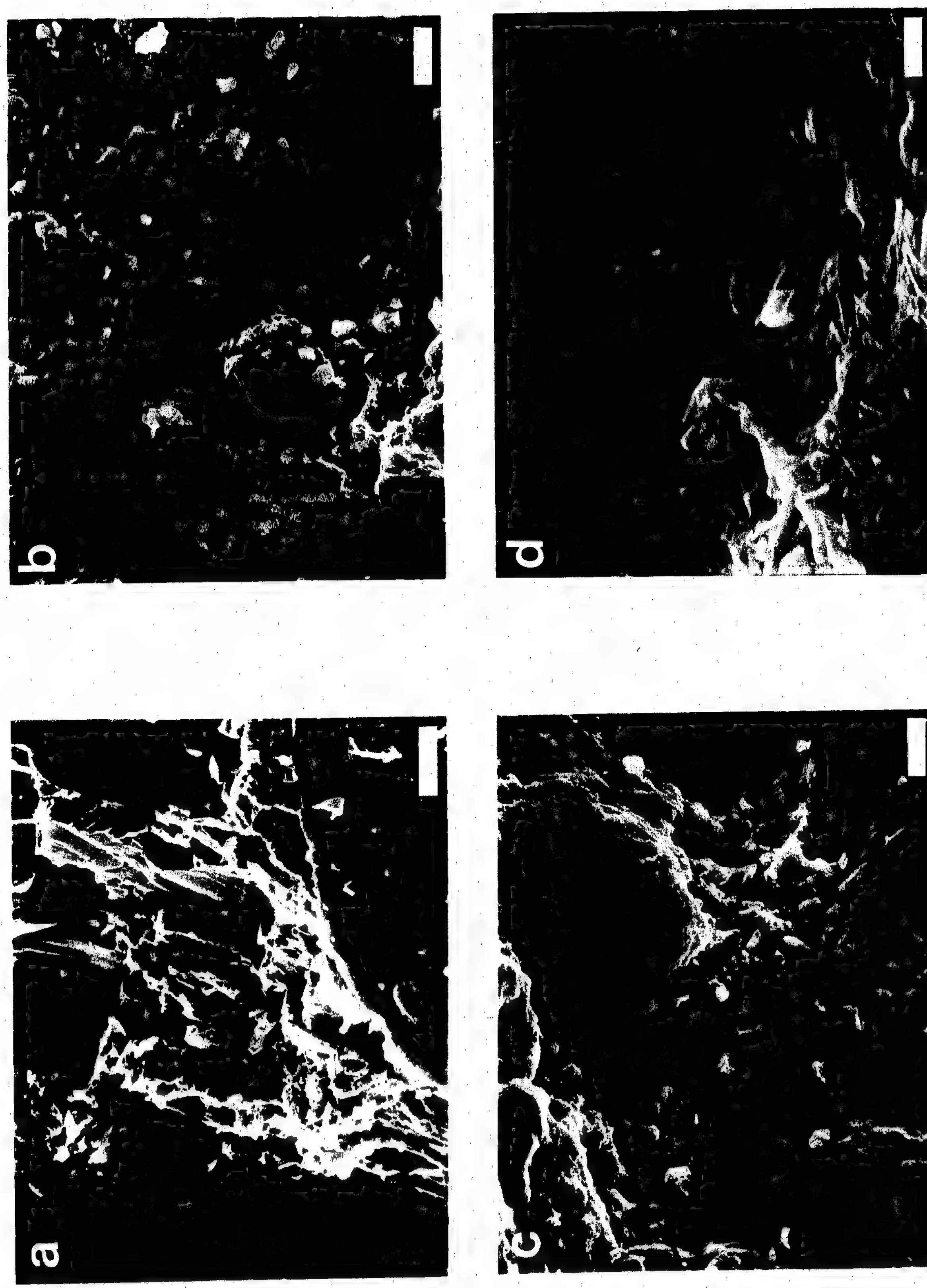
a
b
c
d

sis. The dominance of calcite and quartz cements in sandstone has been attributed by Blatt (1979) to most preserved sandstones being of shallow marine origin and thus filled with carbonate-rich pore water and to the abundance of quartz effectively buffering natural water with silica. Hayes (1979) emphasizes the importance of provenance, tectonic setting of the basin, and depositional environment, in controlling the detrital mineralogy and fluid flow so important for diagenesis. By determining what chemical constituents are transported in the hydrodynamic regime, the diagenetic history can be better understood. The sandstones of the study area reflect the influence of immature volcanic detritus locally controlling the early diagenetic history.

The responsibility that secondary solution porosity plays in petroleum reservoir porosity and permeability has been appreciated only in the last decade (Hayes, 1979; Blatt, 1979). The petrographic criteria characteristic of secondary porosity (summarized by Hayes, 1979) were not observed in the petrography of the Mughal Kot and Pab sandstones. It is thought that sufficient burial depth for pore regeneration was not achieved.

The petroleum potential constitutes the principal economic concern of the Cretaceous strata. Pakistan has traditionally been oil-poor while having found sufficient natural gas for its needs (Rahman, 1963). Oil production comes mostly from carbonate reservoirs in the Potwar Basin north

of the Salt Range. Natural gas is produced from Eocene limestones mainly in the Sui field southeast of Quetta. Production averages in 1979 were 10,100 b/d (oil) and 636,434 MCFGD (gas) (Fletcher, 1980). The total number of exploration and development wells drilled during 1979 were 8 and 5 respectively. Foreign participants are being encouraged by the Pakistani government to explore potential trends throughout the country.

At first glance the northwest Indo-Pakistani shelf seems a natural habitat for oil generation and accumulation. This stems, in part, from its geologic similarity with the northern Arabian shelf setting of Saudi Arabia, Iran and Iraq. Several explanations may be advanced to explain the lack of petroleum reserves, namely, (1) the conclusion that the northwestern shelf area is in a structurally post-matpration state, meaning that at some time in the Cenozoic the area may have been as productive as the Arabian Gulf is today, (2) the caprock overlying unconformities was not sufficiently impermeable to prevent the escape of petroleum from inclined resevoir rocks below the unconformity, and (3) the region has not yet been sufficiently prospected for an accurate evaluation of its petroleum potential.

The presence of stratigraphic traps amidst the structural complexity of the Karachi and Sulaiman arcs has yet to be established. In this regard, strata of the Parh, Mughal Kot and Pab formations have noteworthy implications. Car-

bonate facies of the Parh Limestone should be explored for promising reef and fore-reef zones. Sandstones of the Mughal Kot Formation and the Pab Sandstone may likewise contain favorable lateral facies toward the east, e.g. delta front sheet sands and distributary and fluvial channels. Certainly the reservoir potential of buried shoreface sandstones must be considered excellent.

Conditions of sufficient time and burial depth must be met for significant hydrocarbon generation and accumulation (Tissot and Welte, 1978). The potential of the shales present as source beds also remains untested. The generation, migration and storage of petroleum in the Tethyan shelf sequence depends on many depositional and diagenetic factors but hinges on the structural influence superimposed by continent-continent collision on pre-orgogenic stratigraphic and structural reservoirs.

CONCLUSIONS

The stratigraphy of the upper Cretaceous strata deposited on the Tethyan shelf of the Indo-Pakistani Subcontinent has been the focus of this report. The lithofacies and depositional environments of the Upper Cretaceous Mugahl Kot and Pab formations have been detailed from outcrops of these units in the southern Pab Range, southeast Baluchistan. The conclusions drawn from the field and laboratory work interpret the local depositional history within the regional tectonostratigraphic framework.

(1) Depositional Environments. The general stratigraphy of the continental shelf has been known since the first geological traverses of Blanford and Vredenberg. Strata of Cretaceous age were investigated for physical characteristics indicative of specific lithofacies and their respective depositional environments. The depositional environments inferred for the successive Sembar, Goru and Parh formations represent increasingly shallower water marine continental slope to open shelf environments.

The bulk of the field work was directed toward the clastic-dominated lithofacies of the Upper Cretaceous (Maestrichtian) Mughal Kot and Pab formations. The sequence of lithofacies record an initial westward progradation of a marine delta (distributary system) followed by open marine shelf conditions isolated from major influxes of sand. The

upper Mughal Kot strata contain sands from a second deltaic system. Chaotically slumped sandstones are interpreted to have slid down an oversteepened delta front face under the influence of gravity. Shoreface sedimentation dominates the Pab Sandstone. The cycles consist of offshore, transition and shoreface sequences. No lagoonal or fluvial lithofacies were observed. Also conspicuously absent are erosional ravinements resulting from tidal channel activity. The Khadro Formation marks a return to shale-dominated, shelf sedimentation.

(2) Petrography. Thin section analysis of sandstones in the Mughal Kot and Pab identify a dominant quartz fraction accompanied, beginning in the upper Mughal Kot, by a volcanic admixture. The volcanics are erosional detritus of nearby andesitic and/or basaltic flows. The volcanic provenance, most likely, was the Porali Volcanic Arc positioned on the edge of the continental margin farther to the west. The dominant quartzose fraction plus the ultramature heavy mineral suite were ultimately derived from Precambrian rocks of the northwest Indian Shield. The paucity of detrital feldspar may be attributed to decomposition resulting from tropical climatic conditions in the source area, lengthy sediment abrasion, and/or sediment recycling prior to final transport.

(3) Depositional History. The strata were deposited near

the western edge of continental shelf. The Sembar - Goru - Parh formations represent a depositional continuum from slope and outer shelf conditions through a very shallow, platform regime. The buildup of the Porali Volcanic Arc did not significantly control sedimentation patterns until Late Cretaceous time. Subsequently, Maestrichtian shoreline sedimentation kept pace with the narrow, rapidly subsiding continental shelf developed east of the volcanic arc. The Mughal Kot and Pab constitute a depositional shelf to shoreline sequence similar to the older Cretaceous strata.

(4) <u>Tectonostratigraphic Framework</u>. The Indo-Pakistani Subcontinent migrated the farthest of all the Gondwana fragments. Plate movement caused subduction of Tethyan oceanic crust along the Sinjrani Subduction Zone and generation of new Indian oceanic crust in its wake. The Maestrichtian, in particular, spanned a time of rapid Subcontinent plate movement with discontinuous volcanic arc development on the leading edge of the continental margin. Volcanic arc formation is believed responsible for back-arc basin development in the study area. This back-arc basin provided the setting for mixing of the major detrital sand influx from the Indian Shield with the limited erosional products from the exposed islands of the Porali Volcanic Arc. Throughout the region isolated tectonism, though all related to plate movements, and widespread sedimentation characterized plate margins

until the Neogene Alpine - Himalayan Orogeny which signified major continent-continent collision of the Laurasian and Gondwana fragments. Passive continental shelf sedimentation was gradually replaced by restricted synorogenic molasse deposition as collision progressed.

(5) Diagenesis. Secondary calcite prevades interstitial sandstone voids. Chlorite, illite, kaolinite and analcime help to cement detritus within strata of high volcanic content. The early diagenetic history consisted of calcite cementation following that of volcanic alteration and silica overgrowths. Features attributable to generation of secondary solution porosity, critical for hydrocarbon reservoirs, were not observed.

(6) Petroleum Potential. The Cretaceous strata of the study area include shales that may have served as petroleum source beds as well as carbonate and sandstone capable of potential reservoir capacity. The depositional environments recognized in the strata, it is hoped, will be used to project depositional trends into the subsurface for future petroleum exploration.

LITERATURE CITED

Abbas, S. G., and Z. Ahmad. 1979. The Muslimbagh Ophiolites. p. 243-249. In A. Farah and K. A. DeJong (eds.) Geodynamics of Pakistan. Geol. Surv. Pakistan, Quetta, Pakistan.

Ahmed, S.S. 1969. Tertiary geology of part of south Makran, Baluchistan, west Pakistan. Amer. Assoc. Petroleum Geologists Bull. 53:1480-1499.

Allemann, F. 1979. Time of emplacement of the Zhob Valley Ophiolites and Bela Ophiolites. p. 215-242. In A. Farah and K. A. DeJong (eds.) Geodynamics of Pakistan. Geol. Surv. Pakistan, Quetta, Pakistan.

Arthurton, R. S., G. S. Alam, A. Ahmad, and S. Iqbal. 1979. Geological history of the Alamreg-Mashki Chah area, Chagai District, Baluchistan. p. 325-331. In A. Farah and K. A. DeJong (eds.) Geodynamics of Pakistan. Geol. Surv. Pakistan, Quetta, Pakistan.

Asquith, D. O. 1970. Depositional topography and major marine environments, Late Cretaceous, Wyoming. Amer. Assoc. Petroleum Geologists Bull. 54:1184-1224.

Asquith, D. O. 1974. Sedimentary models, cycles, and deltas, Upper Cretaceous, Wyoming. Amer. Assoc. Petroleum Geologists Bull. 58:2274-2283.

Barker, P. F., I. W. B. Dalziel, D. H. Alliot, C. C. von der Borch, R. W. Thompson, G. Tlasker, R. C. Tjalsma, S. W. Wise, G. Dinkelman, A. M. Gombos, A. Lonardi, and J. Tarney. 1974. Southwestern Atlantic, Leg 36. Geotimes. 19:16-18.

Bathurst, R. G. C. 1975. Sediments and their Diagenesis. Developments in Sedimentology Vol. 12, Elsevier, New York.

Blanford, W. T. 1876. On the geology of Sind. India Geol. Surv. Mem. 9:8-22.

Blanford, W. T. 1877. Geological notes on the great Indian desert between Sind and Rajputana. Geol. Surv. India Recs. 10:10-20.

Blanford, W. T. 1878. On the geology of Sind. India Geol. Surv. Recs. 11:161-173.

Blanford, W. T. 1879. The geology of western Sind. India Geol. Surv. Mem. 17:1-196.

Blatt, H. 1979. Diagenetic processes in sandstones. p. 141-157. In P. A. Scholle and P. R. Schluger (eds.) Aspects of Diagenesis. Soc. Econ. Paleon. Mineral. Spec. Publ. No. 26.

Boulin, J. 1981. Afghanistan structure, Greater India concept and eastern Tethys evolution. Tectonophysics 72:261-287.

Byers, C. W. 1974. Shale fissility. relation to bioturbation. Sedimentology 21:479-484.

Carter, H. J. 1853. Description of some of the larger forms of fossilized Foraminifera in Sind, with observations on their internal structure. Jour. Bombay Branch of the Royal Asiatic Society 5:124-141.

Carter, H. J. 1854. Summary on the Geology of India, between the Ganges, Indus, and Cape Comorin. Jour. Bombay Branch of the Royal Asiatic Society 5:179-334.

Clifton, H. E., R. E. Hunter, and R. L. Phillips. 1971. Depositional structures and processes in the nonbarred high-energy nearshore. Jour. Sed. Petrol. 41:651-670.

D'Archiac, and Haime. 1853. Description des animaux fossils du groups nummilitique de l'Inde. Paris.

Darracott, B. W. 1974. On the crustal structure and evolution of southeastern Africa and the adjacent Indian Ocean. Earth and Planet. Sci. Lett. 24:282-290.

Davies, T. A., and R. B. Kidd. 1977. Sedimentation in the Indian Ocean through time (chapter 3). p. 61-85. In Heirtzler, J. R. et al. (eds.) Indian Ocean Geology and Biostratigraphy. American Geophysical Union, Washington D. C.

DeJong, K. A., and A. M. Subhani. 1979. Note on the Bela Ophiolites, with special reference to the Kanar area. p. 263-269. In A. Farah and K. A. DeJong (eds.) Geodynamics of Pakistan. Geol. Surv. Pakistan, Quetta, Pakistan.

Dickinson, W. R., and C. A. Suczek. 1979. Plate tectonics and sandstone composition. Amer. Assoc. Petroleum Geologists Bull. 63:2164-2182.

Dickson, J. D. 1965. A modified staining technique for carbonates in thin section. Nature 205:587.

Dietz, R. S., and J. C. Holden. 1970. Reconstruction of Pangaea: break-up and dispersion of continents, Permian to Recent. Jour. Geophys. Res. 75:4939-4956.

Dingle, R. V., and R. A. Scurtton. 1974. Continental breakup and the development of Post-Paleozoic sedimentary basins around Southern Africa. Geol. Soc. Amer. Bull. 85:1467-1474.

Embleton, B. J. J., J. J. Veevers, B. O. Johnson, and C. McA. Powell. 1980. Paleomagnetic comparison of a new fit of East and West Gondwanaland with the Smith and Hallam fit. Tectonophysics 61:381-390.

Falcon, N. L. 1974a. Southern Iran. Zagros Mountains. p. 199-211. In Spenser, A. M. (ed.) Mesozoic - Cenozoic orogenic belts, data for orogenic studies. Geol. Soc. London Spec. Publ. 4.

Falcon, N. L. 1974b. An outline of the geology of the Iranian Makran. Geog. Jour. 140:284-291.

Farah, A., and K. A. DeJong. 1979. Geodynamics of Pakistan. Geological Survey of Pakistan, Quetta, Pakistan.

Farhoudi, G. 1978. A comparison of Zagros geology to island arcs. Jour. Geol. 86:323-334.

Farhoudi, G., and D. E. Karig. 1977. Makran of Iran and Pakistan as an active arc system. Geology 5:664-668.

Fletcher, G. L. 1980. Petroleum development in Far East 1979. Amer. Assoc. Petroleum Geologists Bull. 64:1880-1960.

Flores, R. M. 1978. Barrier and back-barrier environments of deposition of the Upper Cretaceous Almond Formation, Rock Springs Uplift, Wyoming. Mountain Geologist 15:57-71.

Folk, R. L., P. B. Andrews, and D. W. Lewis. 1970. Detrital sedimentary rock classification and nomenclature for use in New Zealand. New Zealand Jour. Geol. Geophys. 13:937-968.

Folk, R. L. 1974. Petrology of sedimentary rocks. Hemphill's, Austin, Texas.

Frakes, L. A. 1979. Climates throughout geologic time. Elsevier, New York.

Friedman, G. M. 1958. Determination of sieve-size distribution from thin-section data for sedimentary petrological studies. Jour. Geol. 66:394-416.

Fuchtbauer, H. 1974. Sediments and Sedimentary Rocks, I. Halsted Press, New York.

Gansser, A. 1979. Reconnaissance visit to the ophiolites in Baluchistan and the Himalaya. p. 193-213. In A. Farah and K. A. DeJong (eds.) Geodynamics of Pakistan. Geol. Surv. Pakistan, Quetta, Pakistan.

Gealey, W. K. 1977. Ophiolite obduction and geologic evolution of the Oman Mountains and adjacent areas. Geol. Soc. Amer. Bull. 88:1183-1191.

Gigon, W. O. 1962. Upper Cretaceous stratigraphy of the well Giandari I and its correlation with the Sulaiman and Kirthar ranges, West Pakistan. p. 282-284. ECAFE Symp. Dev. Petroleum Res. Asia and Far East, Teheran.

Glennie, K. W., M. G. Boeuff, C. Hughes, M. Moddy-Stuart, W. H. F. Pilaar, and B. M. Reinhardt. 1973. Late Cretaceous nappes in Oman Mountains and their geologic evolution. Amer. Assoc. Petroleum Geologists Bull. 57:5-27.

Goldring, R., and P. Bridges. 1973. Sublittoral sheet sandstones. Jour. Sed. Petrol. 43:736-747.

Gupta, V. J. 1975. Indian Mesozoic stratigraphy. Hindustan Publ. Corp., Delhi.

Gupta, V. J. 1976. Indian Cenozoic stratigraphy. Hindustan Publ. Corp., Delhi.

Gupta, V. J. 1977. Indian Precambrian stratigraphy. Hindustan Publ. Corp., Delhi.

Harms, J. C., J. Southland, D. R. Spearing, R. G. Walker. 1975. Depositional environments as interpreted from primary sedimentary structures and stratification sequences. Soc. Econ. Paleon. Mineral. Short Course 2.

Hayes, J. B. 1979. Sandstone diagenesis - the hole truth. p. 127-139. In P. A. Scholle and P. R. Schluger (eds.) Aspects of Diageneis. Soc. Econ. Paleon. Mineral. Spec. Publ. No 26.

Helwig, J. 1970. Slump folds and early structures, northeastern Newfoundland Appalachians. Jour. Geol. 78:172-187.

Howard, J. D. 1972. Trace fossils as criteria for recognizing shorelines in stratigraphic record. p. 215-225. In J. K. Rigby and W. K. Hamblin (eds.) Recognition of Ancient sedimentary environments. Soc. Econ. Paleon. Mineral. Spec. Publ. 16.

Howard, J. D., and H. E. Reineck. 1972. Georgia coastal region, Sapelo Island, USA. Sedimentology and biology. IV, Physical and biogenic sedimentary structures of the nearshore shelf. Senckenbergiana Maritina 4:81-123.

Hunting Survey Corporation. 1960. Reconnaissance geology of part of West Pakistan (Columbo Plan Cooperative Project). Govt. Canada, Toronto.

Jacob, K. H., and R. C. Quittmeyer. 1979. The Makran region of Pakistan and Iran. trench-arc system with active plate subduction. p. 305-318. In A. Farah and K. A. DeJong (eds.) Geodynamics of Pakistan. Geol. Surv. Pakistan, Quetta, Pakistan.

Jeletzky, J. A. 1974. Cretaceous transgressions and regressions in western and Arctic Canada - Tectonic causes and general implications. Geol. Soc. Amer. Abs. w/Prog. 6:810.

Johnson, B. D., C. McA. Powell, and J. J. Veevers. 1976. Spreading history of the eastern Indian Ocean and Greater India's northward flight from Antarctica and Australia. Geol. Soc. Amer. Bull. 87:1560-1566.

Johnson, G. D., N. M. Johnson, N. D. Opdyke, and R. A. K. Tahirkheli. 1979. Magnetic reversal stratigraphy and sedimentary tectonic history of the Upper Siwalik Group, Eastern Salt Range and Southwestern Kashmir. p. 149-165. In A. Farah and K. A. DeJong (eds.) Geodynamics of Pakistan. Geol. Surv. Pakistan, Quetta, Pakistan.

Kaneoka, I., and H. Haramura. 1973. K/Ar ages of successive lava flows from the Deccan Traps, India. Earth and Planet. Sci. Lett. 18:229-236.

Kauffman, E. G. 1973. Stratigraphic evidence of Cretaceous eustatic changes. Geol. Soc. Amer. Abs. w/Prog. 5:687.

Kauffman, E. G. 1977. Feild Guide. Cretaceous Facies, Fauna, and Paleoenvironments - Western Interior Basin. Mountain Geologist 14:No. 3 and 4.

Kazmi, A. H. 1979a. Active fault systems in Pakistan. p. 285-294. In A. Farah and K. A. DeJong (eds.) Geodynamics of Pakistan. Geol. Surv. Pakistan, Quetta, Pakistan.

Kazmi, A. H. 1979b. The Bibai and Gogai nappes in the Kach-Ziarat area of northeastern Baluchistan. p. 333-339. In A. Farah and K. A. DeJong (eds.) Geodynamics of Pakistan. Geol. Surv. Pakistan, Quetta, Pakistan.

Kleist, J. R. 1974. Deformation by soft-sediment extension in the Coastal Belt, Franciscan Complex. Geology 2:501-504.

Klootwijk, C. T. 1979. A review of paleomagnetic data from the Indo-Pakistani fragment of Gondwanaland. p. 41-80. In A. Farah and K. A. DeJong (eds.) Geodynamics of Pakistan. Geol. Surv. Pakistan, Quetta, Pakistan.

Klootwijk, C. T., and D. K. Bingham. 1980. The extent of Greater India, III. Paleomagnetic data from the Tibetan sedimentary series, Thakkhola region, Nepal Himalaya. Earth and Planet. Sci. Lett. 51:381:405.

Klootwijk, C. T., R. Nazirullah, K. A. DeJong, and H. Ahmed. 1981. A paleomagnetic reconnaissance of northeastern Baluchistan, Pakistan. Jour. Geophys. Res. 86:289-306.

Krynine, P. D. 1946. The tourmaline group in sediments. Jour. Geol. 54:65-87.

Kureshy, A. A. 1980a. Foraminifera of Belemnite Formation (early Cretaceous) of Pakistan. p. 101-108. In T. Kobayashi, R. Toriyama, W. Hashimoto, and S. Kanno (eds.) Geology and Paleontology of Southeast Asia. Univ. of Tokyo Press, Tokyo.

Kureshy, A. A. 1980b. Larger foraminiferal biostratigraphy of the Kirthar Formation of Pakistan. p. 235-247. In T. Kobayashi, R. Toriyama, W. Hashimoto, and S. Kanno (eds.) Geology and Paleontology of Southeast Asia. Univ. of Tokyo Press, Tokyo.

Larson, R. L. 1977. Early Cretaceous breakup of Gondwanaland off western Australia. Geology 5:57-60.

Markl, R. G. 1974. Evidence for the breakup of Eastern Gondwanaland by the Early Cretaceous. Nature 251:196-200.

Matthews, R. K. 1966. Genesis of Recent lime mud in southern British Honduras. Jour. Sed. Petrol. 36:428-454.

McElhinney, M. W., B. J. J. Embleton, L. Daly, and J. P. Pozzi. 1976. Paleomagnetism evidence for the location of Madagascar in Gondwanaland. Geology 4:455-457.

McKenzie, D. P., and J. G. Sclater. 1971. The evolution of the Indian Ocean since the Late Cretaceous. Royal Astron. Soc. Geophys. Jour. 25:437-528.

Medlin, J. H., N. H. Suhr, and J. B. Bodkin. 1969. Atomic absorption analysis of silicates employing LiBO fusion. Atomic Absorption Newsletter 8:25-29.

Minster, J. B., T. H. Jordan, P. Molnar, and E. Haines. 1974. Numerical modelling of instantaneous plate tectonics. Royal Astron. Soc. Geophys. Jour. 36:541-576.

Molnar, P., and W. P. Chen. 1978. Evidence of large Cainozoic crustal shortening of Asia. Nature 273:218-220.

Pamic, J., G. Sestini, and D. Adib. 1979. Alpine magmatic and metamorphic processes and plate tectonics in the Zagros Range, Iran. Geol. Soc. Amer. Bull. 90:569-576.

Pascoe, E. H. 1950. Manual of the geology of India and Burma. Calcutta.

Pettijohn, F. J., P. E. Potter, and R. Siever. 1973. Sand and sandstone. Springer-Verlag, New York.

Pierce, J. W. 1978. The northward motion of India since the Late Cretaceous. Royal Astron. Soc. Geophys. Jour. 52:277-311.

Potter, P. E., J. B. Maynard, and W. A. Pryor. 1980. Sedimentology of shale. Springer-Verlag, New York.

Powell, C. McA. 1979. A speculative tectonic history of Pakistan and surroundings. Some constraints from the Indian Ocean. p. 5-24. In A. Farah and K. A. DeJong (eds.) Geodynamics of Pakistan. Geol. Surv. Pakistan, Quetta, Pakistan.

Powell, C. McA., B. D. Johnson, and J. J. Veevers. 1980. A revised fit of East and West Gondwanaland. Tectonophysics 63:13-29.

Pryor, W. A. 1978. Cretaceous marine sedimentation in West Pakistan. Geol. Soc. Amer. Abs. w/Prog. 10:474.

Pryor, W. A., M. N. Qazi, K. A. R. Ghori, and S. M. Shuaib. 1979. Cyclic sedimentation of Cretaceous-Paleocene reservoir sandstones in west-central Pakistan. Amer. Assoc. Petroleum Geologists Bull. 63:512.

Quittmeyer, R. C., A. Farah, and K. H. Jacob. 1979. The seismicity of Pakistan and its relation to surface faults. p. 271-284. In A. Farah and K. A. DeJong (eds.) Geodynamics of Pakistan. Geol. Surv. Pakistan, Quetta, Pakistan.

Rahman, H. 1963. Geology of Petroleum in Pakistan. 5th World Petroleum Congress, Frankfurt. 1:659-683.

Roberts, D. G. 1972. Slumping on the eastern margin of the Rockall Bank, North Atlantic Ocean. Marine Geol. 13:225-237.

Rupke, N. A. 1978. Deep clastic seas. Chapter 12. In H. G. Reading (ed.) Sedimentary environments and facies. Elsevier, New York.

Ryer, T. A. 1977. Patterns of Cretaceous shallow-marine sedimentation, Coalville and Rockport areas, Utah. Geol. Soc. Amer. Bull. 88:177-188.

Sarwar, G., and K. A. DeJong. 1979. Arcs, Oroclines, Syntaxes. the curvatures of mountain belts in Pakistan. p. 341-349. In A. Farah and K. A. DeJong (eds.) Geodynamics of Pakistan. Geol. Surv. Pakistan, Quetta, Pakistan.

Schlich, R. 1975. Structure et age de l'ocean Indian Occidental. Soc. Geol. Fr., Mem, hors-serie no. 6.

Scholle, P. A. 1979. Constituents, Textures, Cements, and Porosities of Sandstone and Associated Rocks. Amer. Assoc. Petroleum Geologists Memoir 28.

Sclater, J. G., and R. C. Fisher. 1974. Evolution of the east central Indian Ocean with emphasis on the tectonic setting of the Ninety east Ridge. Geol. Soc. Amer. Bull. 85:683-702.

Shah, S. M. I. (ed.) 1977. Stratigraphy of Pakistan. Geological Survey of Pakistan Mem. 12. Quetta, Pakistan.

Shapiro, L. 1975. Rapid silicate, carbonate and phosphate rocks -- revised edition. U. S. Geol. Surv. Bull. 1401.

Sharma, K. K., K. D. Bal, Rajinda Parshad, Nand Lol, K. K. Nagpaul. 1980. Paleo-uplift and cooling rates from various orogenic belts of India as revealed by radiometric ages. Tectonophysics 70:135-158.

Sippel, R. F. 1968. Sandstone petrography, evidence from luminescence petrography. Jour. Sed. Petrol. 38:530-554.

Smith, A. G., and A. Hallam. 1970. The fit of the southern continents. Nature 225:139-144.

Stocklin, J. 1974. Possible ancient continental margins in Iran. p. 873-887. In C. A. Burke and C. L. Drake (eds.) The geology of continental margins. New York, Springer.

Stoneley, R. 1974. Evolution of the continental margins bounding a former southern Tethys. p. 889-903. In C. A. Burke and C. L. Drake (eds.) The geology of continental margins. New York, Springer.

Tapponnier, P., M. Mattauer, F. Provst, and C. Cassaigneau. 1981. Mesozoic ophiolites, sutures, and large-scale tectonic movements in Afghanistan. Earth and Planet. Sci. Lett. 52:355-371.

Tissot, B. P., and D. H. Welte. 1978. Petroleum formation and occurrence. a new approach to oil and gas exploration. Springer-Verlag, New York.

Vallier, T. L., and R. B. Kidd. 1977. Volcanogenic sediments in the Indian Ocean. p. 84-118. In J. R. Heirtzler, H. M. Bolli, T. A. Davies, J. B. Saunders, and J. G. Sclater (eds.) Indian Ocean Geology and Biostratigraphy. American Geophysical Union, Washington, D. C.

Veevers, J. J., C. McA. Powell, and B. D. Johnson. 1975. Greater India's place in Gondwanaland and in Asia. Earth and Planet. Sci. Lett. 27:383:387.

Verma, K. K. 1980. Paleogeography of Peninsular India during the Cretaceous based on invertebrate and vertebrate fauna. p. 91-93. In T. Kobayashi, R. Toriyama, W. Hashimoto, and S. Kanno (eds.) Geology and Paleontology of Southeast Asia. Univ. of Tokyo Press, Tokyo.

Vicary, N. 1846. Geological report on a portion of the Beloochistan hills. Quart. Jour. Geol. Soc. 2:260.

Vicary, N. 1847. Note on the geological structure of parts of Sind. Quart. Jour. Geol. Soc. 3:334-349.

Vredenburg, E. W. 1901. A geological sketch of the Baluchistan desert and part of Eastern Persia. India Geol. Surv. Mem. 31:179-302.

Vredenburg, E. W. 1906. The classification of the Tertiary system in Sind with reference to the zonal distribution of the Eocene Echinoidea described by Duncan and Sladen. India Geol. Surv. Recs. 34:172-198.

Vredenburg, E. W. 1908. The Cretaceous Orbitoides of India. India Geol. Surv. Recs. 36:171-213.

Vredenburg, E. W. 1909a. Mollusca of the Ranikot series, introductory note on the stratigraphy of the Ranikot series. India Geol. Surv. Mem., Paleont. Indica, New Series. 3:5-19.

Vredenburg, E. W. 1909b. Report on the geology of Sarawan, Jhalawan, Makran and the State of Lasbela. India Geol. Surv. Recs. 38:189-215.

Weimer, R. J. 1973. A guide to Uppermost Cretaceous stratigraphy Central Front Range, Colorado; deltaic sedimentation, growth faulting and early Laramide crustal movement. Mountain Geologist 10:53-97.

Weimer, R. J. 1975. Deltaic and shallow marine sandstones. Sedimentation, tectonics and petroleum occurrences. Amer. Assoc. Petroleum Geologist. Continuing education course note series No. 2.

Weimer, R. J., and C. B. Land. 1975. Maestrichtian deltaic and interdeltaic sedimentation in the Rocky Mountain region of the United States. p. 633-666. In W. G. E. Caldwell (ed.) The Cretaceous System in the Western Interior of North America. Geol. Assoc. Canada Spec. Paper No. 13.

Weimer, R. J., and R. W. Tillman. 1980. Tectonic influence on deltaic shoreline facies Fox Hills Sandstone, West-central Denver Basin. Colorado School of Mines. Prof. Contrib. No. 10.

Welland, M. J. P., and A. H. G. Mitchell. 1977. Emplacement of the Oman ophiolite. A mechanism related to subduction and collision. Geol. Soc. Amer. Bull. 88:1081-1088.

Wensink, H., and E. H. Hebeda. 1977. Paleomagnetism and radiometric age determination of the Deccan Traps, India. p. 89. 4th Int. Gondwana Symp., Calcutta.

White, H. J. 1981. Petrography and provenance of Tethyan shoreline sandstones, southern Pab Range, Pakistan. In Geol. Soc. Amer. Abs. w/Prog. North-central section.

White, H. J., and C. F. Vondra. 1980. Stratigraphy of the southern Pab Range, southeast Baluchistan, Pakistan. Geol. Soc. Amer. Abs. w/Prog. 12:547.

White, R. S. 1979. Deformation of the Makran continental margin. p. 295-304. In A. Farah and K. A. DeJong (eds.) Geodynamics of Pakistan. Geol. Surv. Pakistan, Quetta, Pakistan.

White, R. S., and K. D. Klitgord. 1976. Sediment deformation and plate tectonics in the Gulf of Oman. Earth and Planet. Sci. Lett. 32:199-209.

Williams, M. Dean. 1959. Stratigraphy of the lower Indus basin, West Pakistan. p. 377-390. Proc. 5th World Petroleum Cong, New York.

Wilson, J. L. 1975. Carbonate facies in geologic history. Springer-Verlag, New York. 471 p.

Woodcock, N. H. 1976. Structural style in slump sheets. Ludlow series, Powys, Wales. Jour. Geol. Soc. London. 132:399-415.

Woodcock, N. H. 1979. The use of slump structures as palaeslope orientation estimators. Sedimentology 26:83-100.

ACKNOWLEDGMENTS

The field research in Pakistan was funded by the Geodynamics of Pakistan Program, under NSF grants INT-76-22304 end EAR-76-13682. The writer wishes to thank the co-principal investigators of the program, Dr. Kees A. DeJong, University of Cincinnati, USA, and Mr. Abul Farah, Deputy Director General of the Geological Survey of Pakistan. Dr. Wayne Pryor, University of Cincinnati, proposed the project in the Pab Range; his suggestions are gratefully acknowledged. Members of the Geological Survey of Pakistan who provided assistance include Messrs. Waheeduddin Ahmed, M. W. A. Iqbal, M. I. Durrazi and M. J. Quershi. Special thanks are also extended to Dr. Mushtaq Rahman, Iowa State University.

Laboratory facilities were provied by the Department of Earth Sciences, Iowa State University. Laboratory costs were partially funded by a Geological Society of America Research Grant to the writer. Appreciation is given to the members of the graduate committee: Drs. Carl Vondra, advisor, Robert Cody, Robert Palmquist, Tom Fenton and M. A. Tabatabai. Valuable counsel was received from Messrs. Dan Burggraf and Scott Thieben and Dr. Donald Biggs. Finally to my wife, Elaine, I extend a very special thanks for her assistance in typing this document and for her support.

APPENDIX A MECHANICAL (PIPETTE) ANALYSIS OF SELECTED SHALES

Sample	Median[1] (phi)	Mean (phi)	Sorting (phi)	Skewness	Kurtosis[2]
Sembar					
S-1	7.75	8.15	2.77	0.18	0.58
Goru					
G-1	8.70	8.73	4.00	0.003	0.44
Mughal Kot					
MK-DP-66	7.60	6.47	4.11	-0.30	0.38
MK-DP-21	8.20	8.08	2.82	-0.08	0.44
MK-DP-34	10.10	9.97	2.02	-0.14	0.48
MK-DP-36	9.50	9.57	2.07	-0.01	0.49
MK-DP-38	9.05	8.73	2.77	-0.19	0.39
MK-DP-39a	7.80	7.93	3.03	0.30	0.40
MK-DP-42	8.10	8.25	3.19	0.01	0.42
Pab					
Pb-DP-6	9.90	9.65	2.33	-0.19	0.46
Pb-DP-27	9.60	9.43	2.85	-0.14	0.45
Pb-DP-36-2	8.15	8.57	2.91	0.16	0.42
Pb-DP-38-7b	8.05	8.30	2.97	0.07	0.42
Pb-DP-38-7c	8.20	8.33	2.17	0.08	0.44
Pb-DP-38-7g	8.50	8.60	2.57	0.02	0.42
Pb-DP-38-7h	7.70	7.85	2.76	0.04	0.44
Pb-DP-40-9	9.00	8.93	2.67	-0.05	0.42
Pb-DP-87	9.55	9.25	2.49	-0.08	0.44
Khadro					
Kh-DP-1	9.10	8.77	2.78	-0.17	0.43
Kh-DP-4	9.30	9.17	2.51	-0.29	0.45

---

[1] Median, mean and sorting are expressed in phi units; skewness and kurtosis are dimensionless numbers.

[2] The following verbal limits have been suggested by Folk (1974) for values of sorting, skewness and kurtosis.

Sorting	< 0.35	phi	very well-sorted
	0.35 - 0.50	phi	well-sorted
	0.50 - 0.71	phi	moderately well-sorted
	0.71 - 1.0	phi	moderately sorted
	1.0 - 2.0	phi	poorly sorted
	2.0 - 4.0	phi	very poorly sorted

	> 4.0 phi	extremely poorly sorted
Skewness	+1.00 to +0.30	strongly fine-skewed
	+0.30 to 0.10	fine-skewed
	+0.10 to -0.10	near-symmetrical
	-0.10 to -0.30	coarse-skewed
	-0.30 to -1.00	strongly coarse-skewed
Kurtosis (normalized)	< 0.40	very platykurtic
	0.40 - 0.47	platykurtic
	0.47 - 0.53	mesokurtic
	0.53 - 0.60	leptokurtic
	0.60 - 0.75	very leptokurtic
	> 0.75	extremely leptokurtic

APPENDIX B SIEVE-CORRECTED TEXTURAL ANALYSIS OF MUGHAL AND PAB SANDSTONES IN THIN SECTION

Sample	Component[1]	Median (phi)	Mean (phi)	Sorting[2] (phi)
Mughal Kot				
MK-DP-7	Quartz	1.20	1.14	1.02
MK-DP-11	Quartz	1.05	1.10	0.77
MK-DP-11	Fossil	1.32	1.21	0.51
MK-DP-13	Total	1.10	1.11	0.73
MK-DP-16	Quartz	1.55	1.64	0.96
MK-DP-16	Fossil	1.36	1.38	0.46
MK-DP-16	Total	1.50	1.58	0.83
MK-DP-19b	Quartz	1.96	2.06	0.96
MK-DP-26a	Quartz	2.65	2.67	0.76
MK-DP-39b	Quartz	1.47	1.55	0.75
MK-DP-39b	Volcanic	1.42	1.43	0.62
MK-DP-39b	Total	1.48	1.51	0.70
MK-DP-45b	Quartz	1.90	1.85	0.99
MK-DP-45b	Volcanic	1.80	1.88	0.77
MK-DP-45b	Total	1.88	1.88	0.91
Pab				
Pb-DP-9	Quartz	1.64	1.63	0.71
Pb-DP-9	Volcanic	1.85	1.90	0.63
Pb-DP-9	Total	1.70	1.70	0.69
Pb-DP-36-1	Quartz	1.50	1.53	0.61
Pb-DP-36-1	Volcanic	1.44	1.54	0.38
Pb-DP-36-1	Total	1.50	1.55	0.59
Pb-DP-36-2	Quartz	4.54	4.36	0.54
Pb-DP-36-2	Volcanic	4.30	4.22	0.49
Pb-DP-36-2	Total	4.35	4.25	0.51

[1] Total point counts of all components exceeded 300 counts per thin section. The relative percentages of each component are averaged in the total for each sample.

[2] Sorting parameters follow the verbal limits given in Appendix A.

Sample	Component	Median (phi)	Mean (phi)	Sorting (phi)
Pb-DP-36-3	Quartz	1.92	1.98	Ø.95
Pb-DP-36-3	Volcanic	1.83	1.83	Ø.63
Pb-DP-36-3	Total	1.87	1.92	Ø.86
Pb-DP-36-4	Quartz	1.37	1.46	1.11
Pb-DP-36-4	Volcanic	1.35	1.42	Ø.69
Pb-DP-36-4	Total	1.37	1.47	1.Ø3
Pb-DP-37-5	Quartz	2.15	2.16	Ø.67
Pb-DP-37-5	Volcanic	2.Ø9	2.Ø9	Ø.45
Pb-DP-37-5	Total	2.15	2.18	Ø.59
Pb-DP-38-6a	Quartz	1.8Ø	1.82	Ø.89
Pb-DP-38-6a	Volcanic	1.71	1.77	Ø.53
Pb-DP-38-6a	Total	1.75	1.83	Ø.8Ø
Pb-DP-38-6b	Quartz	4.3Ø	4.27	Ø.64
Pb-DP-38-6c	Quartz	2.8Ø	2.84	Ø.97
Pb-DP-38-6c	Volcanic	2.42	2.35	Ø.6Ø
Pb-DP-38-6c	Total	2.67	2.71	Ø.79
Pb-DP-38-6d	Quartz	3.63	3.69	Ø.71
Pb-DP-38-6d	Volcanic	3.46	3.51	Ø.55
Pb-DP-38-6d	Total	3.6Ø	3.64	Ø.66
Pb-DP-38-6e	Quartz	2.1Ø	2.22	Ø.94
Pb-DP-38-6e	Volcanic	1.86	1.93	Ø.56
Pb-DP-38-6e	Total	1.95	2.Ø6	Ø.8Ø
Pb-DP-38-6f	Quartz	2.76	2.99	1.23
Pb-DP-38-6f	Volcanic	2.4Ø	2.37	Ø.79
Pb-DP-38-6f	Total	2.65	2.75	1.12
Pb-DP-38-7a	Quartz	1.64	1.91	1.Ø6
Pb-DP-38-7a	Volcanic	1.43	1.42	Ø.65
Pb-DP-38-7a	Total	1.58	1.8Ø	1.Ø1
Pb-DP-38-7d	Quartz	2.37	2.41	Ø.7Ø
Pb-DP-38-7d	Volcanic	2.Ø7	2.Ø8	Ø.47
Pb-DP-38-7d	Total	2.24	2.29	Ø.65
Pb-DP-38-7e	Quartz	2.ØØ	2.Ø9	Ø.77
Pb-DP-38-7e	Volcanic	1.97	2.ØØ	Ø.55
Pb-DP-38-7e	Total	1.98	2.Ø6	Ø.74
Pb-DP-39-8a	Quartz	2.72	2.79	Ø.89
Pb-DP-39-8a	Volcanic	2.72	2.69	Ø.65

Sample	Component	Median (phi)	Mean (phi)	Sorting (phi)
Pb-DP-39-8a	Total	2.71	2.75	1.Ø1
Pb-DP-39-8b	Quartz	1.81	1.9Ø	Ø.93
Pb-DP-39-8b	Volcanic	1.84	1.89	Ø.65
Pb-DP-39-8b	Total	1.85	1.91	Ø.82
Pb-DP-39-8c	Quartz	1.86	1.87	Ø.99
Pb-DP-39-8c	Volcanic	2.1Ø	2.12	Ø.8Ø
Pb-DP-39-8c	Total	1.98	1.94	Ø.91
Pb-DP-39-8d	Quartz	1.59	1.59	Ø.61
Pb-DP-39-8d	Volcanic	1.85	1.89	Ø.55
Pb-DP-39-8d	Total	1.7Ø	1.71	Ø.59

APPENDIX C SANDSTONE PETROGRAPHY

Sample	Q[1]	F[2]	Rock Frag[3] VRF	SRF	Heavy[4] Min.	Matrix[5] Cal.	Clay	Q:F:R[6]
Mughal Kot (Drabber Pass)								
MK-DP-7	71[7]	-	-	-	-	28	-	100:0:0
MK-DP-11	78	-	-	5	T	17	-	100:0:0
MK-DP-16	59	-	-	6	-	35	T	100:0:0
MK-DP-18	63	-	-	6	T	31	T	100:0:0
MK-DP-19b	47	-	-	1	-	51	-	100:0:0
MK-DP-23	47	-	-	2	T	49	1	100:0:0
MK-DP-26a	40	-	T	17	T	43	-	70:0:30
MK-DP-29	51	-	-	-	1	43	5	100:0:0
MK-DP-39b	44	-	17	1	-	36	1	72:0:28
MK-DP-40	46	-	9	2	T	11	32	84:0:16
MK-DP-41	34	-	14	1	1	22	27	71:0:29
MK-DP-45b	49	T	8	1	T	14	28	84:0:16
MK-DP-47	66	T	15	1	-	29	9	81:1:18
Mughal Kot (Jakkher Pass)								
MK-JP-6	90	-	-	-	1	3	6	100:0:0
MK-JP-11a	33	-	-	-	T	42	15	100:0:0
MK-JP-11b	69	-	-	T	T	29	2	100:0:0
MK-JP-12d	62	-	-	1	1	36	-	99:0:1
MK-JP-14b	84	-	-	1	T	14	-	99:0:1

[1] Quartz detritus is dominantly single crystal, planar to undulose extinction. Polycrystalline quartz grains are included.

[2] All varieties of feldspar (orthoclase, microcline and plagi clase) are included.

[3] Volcanic and sedimentary rock fragments are tallied separately. Shale clast fragments, chert and detrital glauconite comprise the sedimentary fraction. No igneous plutonic/metamorphic fragments were observed.

[4] The heavy mineral content includes both opaque and nonopaque grains.

[5] Calcite and clay minerals comprise the principal sandstone cement. Fe-oxides and silica cement are tallied with the clay percentage.

[6] The allogenic grain ratio of quartz, feldspar and rock fragments forms the basis for the compositional classification of Folk (1974), used in this report.

[7] Number percent relative to 100. At least 300 point counts per thin section were tabulated.

Sample	Q	F	Rock Frag		Heavy Min.	Matrix		Q:F:R
			VRF	SRF		Cal.	Clay	
MK-JP-15	62	-	-	T	1	36	T	100:0:0
MK-JP-16	52	-	-	T	-	45	2	100:0:0
MK-JP-17a	64	-	-	1	T	33	1	99:0:1
MK-JP-18	68	-	-	T	T	31	-	100:0:0
MK-JP-21	59	-	-	T	1	39	-	100:0:0
MK-JP-33	44	1	20	1	T	30	3	67:1:32
MK-JP-34	39	1	32	-	T	23	4	55:1:45
MK-JP-40	44	-	29	-	T	26	-	60:0:40
MK-JP-43b	46	-	36	T	T	6	11	56:0:44
MK-JP-47a	73	-	15	-	T	10	1	83:0:17
MK-JP-52a	57	1	26	-	-	16	-	68:1:31
Mughal Kot (average)	57	T	8	1	1	28	3	88:0:12
Pab Sandstone (Drabber Pass)								
Pb-DP-3	35	T	28	-	-	5	31	56:0:44
Pb-DP-4	39	-	20	2	-	6	33	66:0:34
Pb-DP-9	57	-	14	T	T	28	T	80:0:20
Pb-DP-36-1	60	1	11	T	-	21	6	83:1:16
Pb-DP-36-3	33	-	9	12	T	43	3	62:0:38
Pb-DP-36-4	46	T	14	T	T	36	4	77:1:22
Pb-DP-37-5	51	T	6	T	-	39	3	89:1:10
Pb-DP-38-6a	43	T	12	T	1	37	7	77:1:22
Pb-DP-38-6b	46	T	16	2	-	24	12	74:1:25
Pb-DP-38-6c	50	T	17	-	T	25	7	75:0:25
Pb-DP-38-6d	26	T	2	2	3	51	14	93:0:7
Pb-DP-38-6e	44	T	14	1	T	34	6	76:1:23
Pb-DP-38-6f	35	T	12	8	1	29	15	65:1:34
Pb-DP-38-7a	43	T	10	-	T	41	5	81:1:18
Pb-DP-38-7d	50	T	6	-	T	40	3	89:1:10
Pb-DP-38-7e	46	T	6	T	T	37	11	88:1:11
Pb-DP-39-8a	51	T	5	-	2	31	10	91:1:8
Pb-DP-39-8b	58	-	6	-	-	34	2	91:0:9
Pb-DP-39-8c	74	T	10	T	1	13	2	88:1:11
Pb-DP-39-8d	74	T	10	T	T	13	2	88:1:11
Pb-DP-59	68	T	5	1	-	23	3	93:0:7
Pb-DP-72	53	T	1	T	1	44	T	98:0:2
Pb-DP-95	63	-	3	T	-	34	T	95:0:5
Pab Sandstone (Jakkher Pass)								
Pb-JP-4b	57	T	16	T	T	25	1	78:0:22
Pb-JP-13	69	T	9	-	T	21	-	88:0:12
Pb-JP-17	63	1	14	T	T	21	T	81:1:18
Pb-JP-22	60	1	12	T	-	26	-	82:1:17

Sample	Q	F	Rock Frag VRF	Rock Frag SRF	Heavy Min.	Matrix Cal.	Matrix Clay	Q:F:R
Pb-JP-26	64	4	20	1	T	-	10	72:5:23
Pb-JP-30	65	T	23	T	T	11	T	74:0:26
Pb-JP-40	61	T	17	T	T	21	T	78:0:22
Pb-JP-48	64	1	9	T	T	25	-	87:1:12
Pb-JP-55	69	1	9	T	T	20	T	87:1:12
Pb-JP-64	72	-	6	-	T	21	-	92:0:8
Pb-JP-69	67	1	13	-	T	18	T	83:1:16
Pb-JP-72	64	T	7	1	T	27	-	89:0:11
Pb-JP-87	66	-	10	T	T	23	-	87:0:13
Pb-JP-89	57	-	7	4	-	31	T	89:0:11
Pb-JP-94c	91	-	5	T	T	3	-	95:0:5
Pb-JP-99	68	-	6	-	T	23	2	92:0:8
Pb-JP-100	72	-	3	-	T	20	4	96:0:4
Pab Sandstone (average)	58	T	11	T	T	26	4	83:1:16
Khadro Fm.								
Kh-DP-2	62	-	3	T	T	27	7	95:0:5
Kh-JP-1c	70	-	6	T	T	20	3	92:0:8
Kh-JP-2	55	-	9	-	1	34	T	86:0:14
Kh-JP-3	38	-	5	19	T	34	3	63:0:37
Khadro Fm. (average)	56	-	6	4	T	29	4	84:0:16

APPENDIX D X-RAY DIFFRACTION ANALYSIS OF WHOLE ROCK SAMPLES

SAMPLE	Lithology[2]	Mineralogy[1] Q	C	F	Chl./Kao.	I
Sembar Fm.						
S-KH-1	Sh	X	M	M	X	T
Goru Fm.						
G-DP-1	Marl	X	X	T	X	T
G-DP-2	Marl	X	X	T	X	T
G-DP-3	Lm	X	X	-	T	T
Parh Lm.						
P-DP-1	Lm	M	X	-	-	T
Mughal Kot Fm. (Drabber Pass)						
MK-DP-2	marl	X	X	-	X	M
MK-DP-6a	Sh	X	X	-	X	M
MK-DP-6b	Sh	X	X	-	X	M
MK-DP-19a	S.Sh	X	X	-	X	T
MK-DP-21	S.Sh	X	X	T	X	M
MK-DP-25	Sh	M	X	-	X	M
MK-DP-31a	marl	X	X	-	X	M
MK-DP-33	marl	X	X	T	X	M
MK-DP-34	Sh	X	X	-	X	T
MK-DP-35	marl	X	X	-	X	T
MK-DP-36	Sh	X	X	M	M	T
MK-DP-38	Sh	X	X	M	T	M

[1] Mineralogical notes: Q = Quartz; C = Calcite; F = Feldspar; Chl = Chlorite; Kao = Kaolinite; I = Illite; X = major component; M = minor component; T = trace component; The feldspar composition is plagioclase, ranging from oligocene to bytownite. Clorite and kaolinite are not easily distinguished in the x-ray patterns. The two are thus combined and may be interlayered in some samples. Additional minerals detected include analcime in samples MK-JP-33a, MK-JP-34, MK-JP-52b, and Pb-DP-38-7e. Glauconite is present in the Sembar sample.

[2] Lithology: Sh = shale; S.Sh = sandy shale; Ss = Sandstone; marl = marl; Lm = limestone.

SAMPLE	Lithology	Mineralogy Q	C	F	Chl./Kao.	I
MK-DP-39a	Ss	X	M	X	X	T
MK-DP-39b	Ss	X	X	M	X	-
MK-DP-40	Ss	X	M	X	X	-
MK-DP-41	Ss	X	X	X	X	-
MK-DP-42	Sh	X	M	X	X	-
MK-DP-45a	Ss	X	M	X	T	-
Mughal Kot Fm. (Jakkher Pass)						
MK-JP-5a	marl	X	X	-	X	-
MK-JP-9	marl	X	X	T	X	T
MK-JP-11a	Ss	X	X	T	X	T
MK-JP-31	Sh	M	X	-	M	T
MK-JP-33a	Ss	X	M	M	X	T
MK-JP-34	Ss	X	M	M	X	T
MK-JP-38	Sh	X	X	M	X	M
MK-JP-44	Sh	X	M	T	M	T
MK-JP-52a	Ss	X	M	X	X	T
MK-JP-52b	Ss	X	M	M	X	T
Pab Sandstone (Drabber Pass)						
Pb-DP-6	Sh	X	M	M	T	T
Pb-DP-27	Sh	X	X	M	X	T
Pb-DP-36-2	Sh	X	T	X	X	T
Pb-DP-37-5	Ss	X	X	X	M	T
Pb-DP-38-7b	Sh	X	M	X	X	T
Pb-DP-38-7c	Sh	M	X	X	X	M
Pb-DP-38-7e	Ss	X	M	M	T	-
Pb-DP-38-7f	Lm	M	X	X	T	-
Pb-DP-38-7g	Sh	M	X	X	X	T
Pb-DP-38-7h	Sh	X	M	X	X	T
Pb-DP-40-9	Sh	X	X	X	X	T
Pb-DP-72	Ss	X	X	-	T	-
Pb-DP-87	Sh	X	X	T	X	-
Pab Sandstone (Jakkher Pass)						
Pb-JP-8a	Sh	X	M	M	M	T
Pb-JP-37	Sh	X	X	X	X	T
Pb-JP-84	Sh	X	X	T	M	T
Khadro Fm						
Kh-DP-1	Sh	X	T	-	X	M

SAMPLE	Lithology	Mineralogy				
		Q	C	F	Chl./Kao.	I
Kh-DP-4	Sh	X	M	T	X	T
Kh-JP-1b	Sh	X	X	T	X	T
Kh-JP-4	Sh	X	M	M	X	T
Kh-JP-5	Sh	X	X	M	T	T
Mid-Tertiary Lm						
W-1-b	Lm	M	X	-	T	T
W-3	Lm	M	X	-	T	-

APPENDIX E HEAVY MINERAL ABUNDANCE

Sample [1]	Zircon	Tourmaline [2]	Rutile	Magnetite
Mughal Kot Fm.				
MK-DP-7	46 [3]	34	4	16
MK-DP-18	74	19	2	5
MK-DP-19b	45	51	4	T
MK-DP-39b	47	41	12	T
MK-DP-40	68	26	6	T
MK-DP-45b	59	34	7	T
Pab Sandstone				
Pb-DP-9	48	48	4	T
Pb-DP-36-1	79	17	4	T
Pb-DP-36-4	65	30	5	T
Pb-DP-38-6a	65	32	3	T
Pb-DP-38-7a	61	35	4	T
Pb-DP-38-7d(1)	78	20	2	T
Pb-DP-38-7d(2)	68	26	6	T
Pb-DP-39-8b	74	21	5	T
Pb-DP-39-8c	72	22	6	T
Pb-DP-59	83	14	3	-
Pb-DP-72	65	30	5	-
Pb-DP-95	47	44	9	-
Khadro Fm.				
Kh-DP-2	97	2	1	-
Z:T:R ratio				
Mughal Kot	08	36	6	
Pab	67	28	5	

---

[1] Opaque leucoxene or hematite coats most heavy mineral grains. Cleaning with 50% HCl removed most of these rinds but only recognizable grains were counted from grain mounts. The 2-3 phi (250 to 125 micron) fraction was used for bromoform separation except for sample Pb-DP-38-7d(2) which was a test comparison run on the 3-4 phi (125 to 62 micron) size fraction.

[2] Dravite was the only species of tourmaline found.

[3] Number percent relative to 100.

APPENDIX F ACID-INSOLUABLE RESIDUES OF SELECTED SHALES AND MARLS

Sample[1]	Carbonate	Acid-Insoluable Residue
Sembar		
S-KH-1	13.98[2]	86.Ø2
Goru		
G-DP-1	38.72	61.28
G-DP-2	42.2Ø	57.8Ø
G-DP-3	79.22	2Ø.79
Parh		
P-DP-1	85.67	14.33
Mughal Kot		
MK-DP-2	45.77	54.23
MK-DP-19a	37.Ø1	52.99
MK-DP-22	69.95	3Ø.Ø5
MK-DP-25	57.94	42.Ø6
MK-DP-26b	67.41	32.59
MK-DP-31a	56.96	43.Ø4
MK-DP-31b	75.86	24.14
MK-DP-32	64.Ø4	35.96
MK-DP-33	55.61	44.39
MK-DP-34	4Ø.Ø4	59.96
MK-DP-35	58.Ø7	41.93
MK-DP-42	19.28	8Ø.72
Pab		
Pb-DP-38-7f	76.2Ø	23.8Ø
Pb-DP-4Ø-9	3Ø.99	69.Ø1
Khadro		
Kh-DP-1	13.42	86.58
Kh-JP-5	21.28	78.72

[1] 5% HCl was used to dissolve the carbonate from the crushed samples. X-ray analysis of the insoluble residue demonstrates negligible calcite remaining.

[2] Weight percent